Mon. Not. R. Astron. Soc. **272,** 96–138 (1995)

Galactic methanol masers at 6.6 GHz

J. L. Caswell,[1] R. A. Vaile,[2] S. P. Ellingsen,[3] J. B. Whiteoak[1] and R. P. Norris[1]

[1] *Australia Telescope National Facility, CSIRO, PO Box 76, Epping, NSW 2121, Australia*
[2] *Department of Physics, Faculty of Business & Technology, University of Western Sydney, Macarthur, PO Box 555, Campbelltown, NSW 2560, Australia*
[3] *Physics Department, University of Tasmania, GPO Box 252c, Hobart, Tasmania 7001, Australia*

Accepted 1994 August 1. Received 1994 July 29; in original form 1994 May 9

ABSTRACT

We have searched for 6.6-GHz methanol maser emission from the directions of more than 200 OH masers, together with a number of other sites of star formation. We have also observed previously reported methanol masers south of declination 24°. Where we detected methanol emission, we measured its position and have found more than 40 instances of small clusters of sources. We present observations of a total of 245 methanol masers with peak intensities ranging from 0.3 to 5000 Jy.

For a typical source, the velocity range of the emission is quite large – commonly 10 km s^{-1} and, in a few instances, exceeding 20 km s^{-1}. Some of the largest velocity ranges are suggestive of emission from an outflow region as well as a central source. Our observations over several epochs show that many sources possess at least some features whose intensity varies on a time-scale of several months. Towards most of the 6.6-GHz masers we have searched for 12-GHz methanol maser emission, and have made 131 detections; the median ratio of 12- to 6.6-GHz intensity is 0.11.

We discuss the general properties of this large sample of 6.6-GHz methanol masers. They appear to be more prevalent than OH masers, with intensities typically seven times higher, and are thus excellent tracers of compact H II regions and sites of recent star formation.

Key words: masers – stars: formation – ISM: molecules – radio lines: ISM.

1 INTRODUCTION

In the vicinity of many star-forming regions, there is strong maser emission from OH and H_2O, and both species have been studied extensively over the past two decades. The masers pinpoint dusty ultracompact H II regions which are often very weak in the radio continuum, and whose embedded newly formed stars are totally obscured optically by the dust. Although there is strong emission from the dust near 60 μm, infrared studies using the *IRAS* survey are limited by confusion in the plane of our Galaxy where the star-forming regions are concentrated.

The masers often show many individual spots of high brightness which allow investigations not readily achieved by other means. These include precise measurements of the kinematics of the regions (including the systemic velocity which can be used to establish a distance) and maps of very high spatial resolution. In turn, these measurements can enhance our understanding of the early stages in the formation of massive stars. Methanol masers have now joined OH and H_2O masers as immensely valuable tools for studying these regions.

The first detection of a methanol maser occurred 20 years ago, and there are now more than 20 transitions known to exhibit maser activity. It is only recently, however, with the detection of the $5_1 \rightarrow 6_0$ A^+ transition at 6.6 GHz (Menten 1991b), that the full potential of methanol masers has been realized. Maser emission from this transition is typically stronger than that from any of the OH transitions, and is present at the majority of OH maser sites and also at many similar sites where OH emission is absent. Several other methanol transitions are often found as masers in close association with the 6.6-GHz masers, and have been categorized as class II methanol masers by Menten (1991a). We are concerned here with these class II masers, chiefly those at 6.6 GHz and, to a lesser extent, those as 12 GHz. Frequently, the individual features on these two transitions are coincident to high accuracy, and their relative intensities may yield unique estimates of the physical conditions when there is further development of current pumping theories (Cragg et al. 1992).

Ultimately, large-scale unbiased surveys for methanol masers may prove to be the most sensitive means of recognizing young star-forming regions. We do, however, already have such surveys of 1665-MHz OH masers, which locate over 200 star formation sites in the southern sky, and these provide an excellent starting point for methanol maser searches. In the present study we have searched for 6.6-GHz methanol masers in the directions of all presently known star-forming regions delineated by 1665-MHZ OH masers. We have complemented this with new high-sensitivity observations of the 12-GHz methanol transition; these supplement our earlier survey for 12-GHz masers (Caswell et al. 1993) made before the discovery of 6.6-GHz masers. We have detected 245 methanol masers at 6.6 GHz and have made several statistical investigations of the sample as a whole. These have allowed us to establish the typical properties and recognize individual sources that deviate from the norm. While an extensive study of each maser is beyond the scope of the present paper, we present detailed notes on many of the more interesting sources.

2 OBSERVATIONS

Our observations were made with the Parkes 64-m telescope in the periods 1992 February 29, March 5–9, June 1–9, September 24–29 and December 17–24, and 1993 September 27–30. Dual-channel receivers, accepting two circular polarizations, were used at both 6.6 and 12 GHz. The new Parkes correlator was configured to record a 2048-channel spectrum for each polarization, spanning 2 MHz at 6.6 GHz and 4 MHz at 12 GHz. The adopted rest frequencies were 6668.518 MHz (Menten 1991b) and 12 178.595 MHz (Gaines, Casleton & Kukolich 1974). In Section 4.7 we discuss further the choice of precise rest frequencies for these transitions. Our intensity calibration at 6.6 GHz is relative to Hydra A, with an assumed peak flux density (with our beamwidth to half-power of 3.3 arcmin) of 9.84 Jy. At 12 GHz the calibration is relative to Virgo A, with an intensity of 33.5 Jy (reduced to a peak of 31.4 Jy with our 2.0-arcmin beamwidth). The calibration of individual spectra has uncertainties of 5 per cent. The system noise was 100 Jy at 6.6 GHz and 275 Jy at 12 GHz.

The principal positions searched for 6.6-GHz methanol masers were towards OH masers emitting in the 1665-MHz transition. We have searched all those known to us that are within the declination range of the telescope and for which we have reasonably accurate positions. Most of the OH masers are close to the Galactic plane in the longitude range 270° through 360° to 50°, and were taken from Caswell & Haynes (1983a,b, 1987a) and Caswell, Haynes & Goss (1980), with more accurate positions for the northern sources taken from Forster & Caswell (1989). Integration times of 5 min were used for the search, and the detection limit was typically 0.3 Jy (5 × rms noise). Where methanol emission was detected, we derived a position for each maser by observing at a grid of points around the discovery position. In a surprisingly large number of cases, this led to the discovery of further sources in the vicinity; our results contain more than 40 small clusters of sources. When we began our survey, there were only 83 known 6.6-GHz methanol masers (reported by Menten 1991b) and, of these, we have reobserved the 73 accessible to the Parkes telescope. We have also searched at the positions of the few 12-GHz methanol masers with no known OH counterpart, at the positions of several H_2O masers without known OH masers, and at the position of a compact H II region, 321.71 + 1.17.

3 RESULTS

Spectra of a typical source from our survey are shown in Fig. 1, and exemplify several facets of the survey. The search position was the direction of the OH maser OH 345.50 + 0.35, whose 1665-MHz OH spectrum is shown in the top panel. The 6.6-GHz spectra in the next two panels show the strong methanol emission at this position, and the variability that occurred over 3 months. Although super-

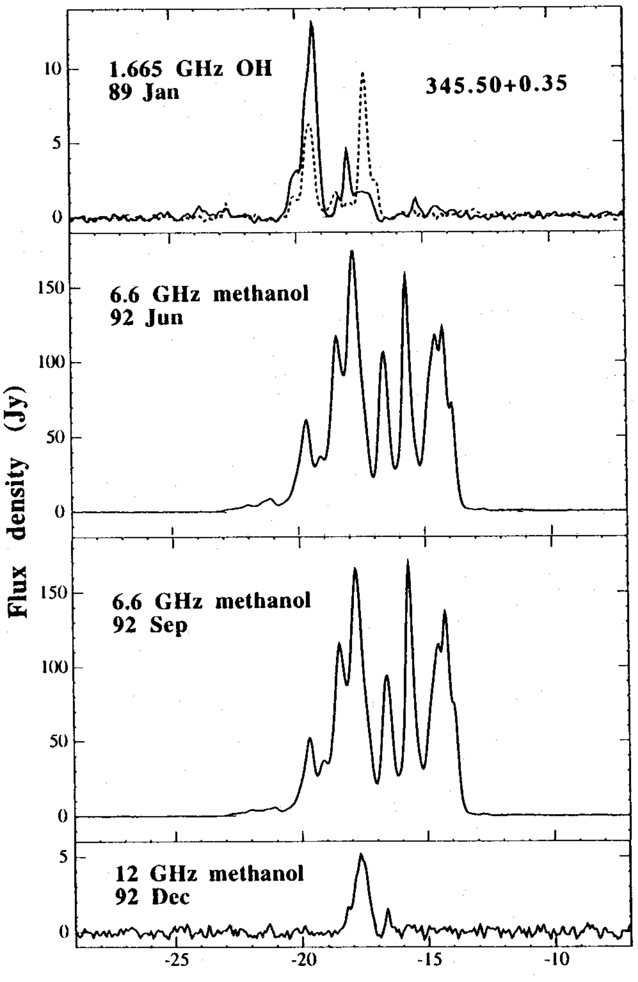

Figure 1. Spectra of 345.50 + 0.35, a typical source from our sample. The upper panel shows the 1665-MHz OH spectrum: the solid line denotes right-hand circular polarization; the broken line denotes left-hand circular polarization. The second and third panels show total intensity spectra of 6.6-GHz methanol at two different epochs. The bottom panel shows the total intensity of the 12-GHz transition of methanol. Note that the top and bottom intensity scales differ from those of the central panels.

ficially similar, the spectra on close inspection reveal *relative* changes of intensity of up to 15 per cent in individual features; most obviously, the strongest feature in September was the second strongest in June, and vice versa. The bottom panel shows the weaker emission from the 12-GHz methanol transition. This particular data set is discussed in the notes on individual sources later in this section, and also in Sections 4.1, 4.2, 4.2.1, 4.2.2, 4.5, 4.6 and 4.7.

The bulk of our results are summarized in Table 1, but the rich variety in the characteristics of the sources can be seen only in the spectra themselves, and these are shown in Fig. 2. Apart from the sample spectrum of Fig. 1, we show only the 6.6-GHz spectra in this paper, and will present detailed results from our 12-GHz measurements in a later paper.

In Table 1 we list 245 distinct methanol maser sites; they are ordered by Galactic longitude, with minor variations to ensure that closely related sources are adjacent to each other. In subsequent remarks we adopt the common convention of using the Galactic coordinates as an abbreviated name for each source, with the understanding that we refer to the 6.6-GHz methanol maser at this position unless indicated otherwise. A site is generally listed separately if it is located more than 30 arcsec from any neighbour, or emits in a totally different velocity range; some sources at smaller separations are distinguished if they possess some strong features that are not blended, as in the case of 329.03−0.21 and 329.03−0.20. Within the notes of Section 3.1 we remark on seven of the maser sites where we suspect that additional components are present.

The positions of Table 1 have been measured with the Parkes telescope and have errors of generally less than 10 arcsec ($2 \times$ rms error) in each coordinate. In a few cases we have replaced these positions with more accurate values measured with the Australia Telescope Compact Array (ATCA) as published by Norris et al. (1993); these sources are recognizable by the additional significant figure in the equatorial positions of Table 1. Throughout this paper, equatorial coordinates refer to equinox 1950.0. Most of the sources were first observed in 1992 March, and the majority were observed again on at least two subsequent occasions. The epochs of the 1992 observations are given in column 7 of Table 1, abbreviated to the first letters of the observing months. In view of the repeated observations, and the very low incidence of interference at the Parkes site, we believe that even the weakest features are reliable detections. Variations in intensity are common and are discussed in Section 4.6, with a brief summary given in Table 1. For sources observed well enough to study variability, we use groupings into the classes 'nv' (not variable), 'sv' (slightly variable, with variations generally less than about 10 per cent), and 'v' (variable, with more than 10 per cent change in at least one feature). The number of variable features and the total number of features that were suitable for assessing variability are also tabulated. In view of the intensity variations, the quoted peak intensities are representative and taken from any one of our observing epochs (for weak sources, usually measured when the signal-to-noise ratio was best).

In the figures, the spectrum shown is the total intensity, taken as the sum of two circular polarizations. The spectra of individual polarizations were inspected, but in no case was any significant circular polarization seen. A typical upper limit to any circular polarization is 1 per cent for the strong features of complex sources such as 35.20 − 1.74. For most sources the spectrum displayed is from 1992 June, except where a later observation has lower noise; for a few weak sources, a spectrum averaged over several epochs is shown. The source spectra are ordered by increasing Galactic longitude, with slight rearrangement to allow better comparison of sources that are confused.

The sources range in peak intensity from more than 3000 Jy (323.74 − 0.26, 351.42 + 0.64, 9.62 + 0.20) down to 0.3 Jy (306.33 − 0.34, 319.84 − 0.20), with features as weak as 0.1 Jy recognizable on sources observed at several epochs. Such weak features are sometimes present in the outlying velocity wings of very strong sources, and thus the dynamic range needed for an adequate portrayal is very large; to achieve this we have shown 73 of the spectral plots with superposed magnified versions of the spectra.

We have chosen 228 spectral plots to display the 245 sources since, in 15 cases, a single plot satisfactorily displays two or more sources that lie very close together. In 75 of the plots, a neighbouring source near the edge of our 3.3-arcmin beam is also seen. In these confused sources, such as 346.48 + 0.13, 346.52 + 0.12 and 346.52 + 0.08, we have deliberately displayed spectra vertically in line and bracketed together, with velocity scales aligned. This assists in recognizing which features belong to which source, and a comment is made in the notes to the sources. In some cases, further clarification is made on the figure either by identifying the emission associated with the principal source displayed, or by marking the unrelated emission with a cross. A few spectra are aligned to demonstrate where sources are nearby but *not* confused, such as 28.15 + 0.00 and 28.20 − 0.05.

The velocity spread for each source is quoted in Table 1, and is sometimes larger than apparent on the spectra, owing to the presence of weak features not readily seen but confirmed at different epochs. In other cases, the tabulated spread is smaller because a feature seen on the spectrum is actually a sidelobe of a nearby source – as remarked in the notes on sources of special interest.

In addition to the sources of Table 1, we detected methanol emission from three further sources for which we have not measured a position. These detections are towards the well-known OH maser 208.99 − 19.38 (Orion A) and two OH masers reported by Cohen, Baart & Jonas (1988): 350.01 − 1.34 and 31.40 − 0.26. We do not show spectra for these, but they are discussed in the following notes. We also remark on the OH maser 285.26 − 0.05 for which we do not detect a methanol counterpart. 24 OH masers that showed no detectable 6.6-GHz methanol maser to a limit of typically 0.3 Jy are listed in Table 2.

3.1 Individual sources of special interest

Here we draw attention to details seen in some of the spectra, to variability, to observations of associated continuum sources, and to some of our unpublished OH observations.

188.95 + 0.89. Note that on the expanded-scale plot, shown as a broken line, there are weak features (~ 1 Jy) present in the velocity range -4 to $+2$ km s^{-1}. The shoulder of emission at velocity $+11.2$ km s^{-1} decreased slightly in 1992 December.

Table 1. 6.6-GHz methanol masers located south of declination 24°.

Methanol maser (l,b)	RA (1950) (h m s)	Dec (1950) (° ′ ″)	Radial peak (km s⁻¹)	Velocity range (km s⁻¹)	6GHz Peak (Jy)	Epoch 6 GHz	12GHz Peak (Jy)	OH Peak (Jy)	Variable 6 GHz	# of features var	# of features total
188.95+0.89	06 05 53.5	+21 39 02	11	-4, +12	495	mjsd	235	0.7	sv	1	8
189.03+0.78	06 05 41.1	+21 31 35	9	+8, +10	17	mjsd	<0.4	3	nv	0	2
189.78+0.34	06 05 36.6	+20 39 30	6	+2, +6	15	jsd	<0.4	0.05	v	3	5
192.60−0.05	06 09 59.1	+18 00 10	5	+2, +6	72	mjsd	<0.4	0.7	v	3	5
196.45−1.68	06 11 47.1	+13 50 34	15	+13, +16	61	mjsd	1.35	10	sv	1	4
213.71−12.60	06 05 21.7	−06 22 28	12	+8, +13	337	mjsd	4.2	23	v	1	4
232.62+0.99	07 29 54.6	−16 51 48	23	+21, +24	162	mjsd	24	2.5	nv	0	4
264.29+1.46	08 54 36.2	−42 54 06	9	+6, +10	0.2	mjsd	<0.4	<0.2	v	2	2
269.15−1.13	09 01 50.3	−48 15 57	16	+7, +16	1.4	mjsd	<0.4	0.2	v	4	5
270.25+0.84	09 14 54.1	−47 43 13	4	+3, +5	1.2	mjsd	<0.5	<0.2	v	1	1
284.35−0.42	10 22 20.0	−57 37 25	3	+3, +11	2.1	mjsd	0.7	1	nv	0	3
287.37+0.65	10 46 06.3	−58 11 11	-2	-4, 0	82			0.9			
290.37+1.66	11 10 07.7	−58 29 59	-24	-28, -22	2.4	mjsd	<0.3	2.8	v	3	3
291.28−0.71	11 09 46.7	−61 02 06	-30	-31, -26	107	mjsd	41	<0.2	v	2	3
291.58−0.43	11 12 58.1	−60 53 40	10	+9, +20	3.4	mjsd	<0.3	8.5		0	5
294.52−1.62	11 33 15.0	−62 58 13	-10	-14, -9	18	mjsd	<0.3	33	v	3	5
298.22−0.33	12 07 16.9	−62 33 01	37	+33, +39	1.5	mjsd	<0.3	<0.2	nv	0	3
299.01+0.13	12 14 42.9	−62 12 21	18	+18, +20	8.6	mjsd	<0.4	2.4		0	2
300.51−0.18	12 27 15.9	−62 40 25	7	+5, +11	4.7	mjsd	<0.4	1.4		0	5
300.97+1.15	12 32 02.6	−61 23 06	-37	-40, -36	5.5	mjsd	0.63	15		0	3
301.14−0.23	12 32 42.6	−62 45 57	-40	-41, -38	1.5	mjsd	<0.3	31	nv	0	2
305.20+0.02	13 08 05.7	−62 29 58	-33	-44, -29	52	mjsd	10.3	6.8	sv	2	9
305.21+0.21	13 08 01.72	−62 18 45.3	-38	-42, -34	480	mjsd	5.1	20	nv	0	7
305.20+0.21	13 07 58.60	−62 18 42.3	-44	-47, -43	50	mjsd	2.3	<1		1	3
305.25+0.25	13 08 20.5	−62 16 07	-32	-32, -29	2.3	s		<1		0	2
305.36+0.15	13 09 24.2	−62 21 22	-36	-39, -34	4	mjsd	<0.3	38		0	3
305.37+0.19	13 09 26.3	−62 19 15	-34	-35, -31	1	j	0.85	<1			
305.80−0.24	13 13 30.4	−62 42 44	-39	-40, -36	1.1	mjsd	<0.3	3.4	v	1	2
306.33−0.34	13 18 07.3	−62 45 01	-24	-25, -22	0.3	sd	<0.4	0.8		0	2
308.92+0.12	13 39 35.4	−61 53 47	-55	-56, -53	54	mjsd	10	62	sv	1	5
309.39−0.14	13 43 55.9	−62 03 14	-50	-51, -48	1.2	mjsd	<0.3	1	nv	0	1
309.92+0.48	13 47 11.85	−61 20 18.8	-60	-65,-53	780	mjsd	156	34	v	4	9
311.64−0.38	14 03 01.6	−61 44 06	32	+31, +36	15	mjsd	<0.4	8	v	3	3
311.96+0.14	14 04 19.7	−61 08 34	-38		0.6	mjsd	<0.3	0.5	v	1	1
312.60+0.04	14 09 36.2	−61 02 57	-68	-69, -59	14	mjsd	<0.5	13	v	1	3
313.47+0.19	14 16 00.5	−60 38 01	-10	-16, -3	17	mjsd	4.2	2.5	sv	3	13
316.36−0.36	14 39 22.6	−60 04 32	4	+1, +8	96	mjsd	10.5	0.2	v	3	10
316.38−0.38	14 39 34.7	−60 04 57	-1	-6, +1	38	mjsd	1.8	<0.2		0	7
316.41−0.31	14 39 34.8	−60 00 17	-6	-7, -2	10	mjsd	<0.4	0.6	sv	1	3
316.64−0.09	14 40 31.6	−59 42 40	-20	-25, -14	128	mjsd	25	2.6	v	4	9
316.81−0.06	14 41 39.3	−59 36 35	-46	-49, -37	12	mjsd	1.2	14	v	4	6
318.05+0.08	14 49 54.0	−58 56 43	-52	-59, -46	4	mjsd	0.45	32	v	3	5
318.05−1.40	14 55 14.5	−60 16 24	46	+44, +47	7.5			0.4			
318.95−0.20	14 57 03.81	−58 47 01.2	-35	-39, -31	780	mjsd	180	44	nv	0	11
319.84−0.20	15 03 03.0	−58 21 35	-9	-14, -9	0.4	mjsd	<0.3	5.4		0	1
320.23−0.29	15 06 00.5	−58 14 14	-62	-71, -58	28	mjsd	<0.4	31	v	4	10
321.15−0.53	15 12 55.3	−57 58 51	-66		9.6	mjsd	0.9	2.1		0	1
321.71+1.17	15 09 58.6	−56 14 19	-44	-45, -38	1.4	mjsd	<0.5	<0.4	v	3	3
322.16+0.64	15 14 45.7	−56 27 28	-63	-66, -51	211	mjsd	17	2	v	5	13
323.46−0.08	15 25 27.7	−56 21 02	-67	-69, -66	22	mjsd	12.2	12		0	2
323.74−0.26	15 27 51.97	−56 20 39.5	-51	-59, -46	2860	mjsd	500	0.8	nv	0	15
324.72+0.34	15 31 07.2	−55 17 25	-47	-51, -45	8	mjsd	<0.5	1.5	sv	1	3
327.12+0.51	15 43 44.3	−53 43 26	-87	-92, -83	90	mjsd	5	8	nv	0	5
327.29−0.58	15 49 16.0	−54 28 14	-37	-49, -37	2.6	mjsd	0.9	36	v	2	5
327.40+0.44	15 45 30.4	−53 36 10	-83	-85, -72	93	mjsd	55	5	sv	5	12
328.24−0.55	15 54 06.11	−53 50 47.0	-45	-47, -31	400	mjsd	13	12	sv	5	10
328.25−0.53	15 54 07.58	−53 49 25.0	-37	-50, -36	430	mjsd	3.3	8	sv	3	5
328.81+0.63	15 52 00.32	−52 34 22.2	-44	-47, -42	380	mjsd	25	102	sv	1	6
329.03−0.21	15 56 42.0	−53 04 22	-37	-41, -34	200	mjsd	17.5	14	sv	3	9
329.03−0.20	15 56 40.6	−53 03 58	-42	-48, -40	30	mjsd	7.2	<1		0	4
329.18−0.31	15 57 55.5	−53 03 26	-56	-60, -51	13	mjsd	1.7	5	sv	4	6
329.41−0.46	15 59 40.8	−53 01 13	-67	-73, -63	156	mjsd	0.6	13	sv	1	9
330.88−0.37	16 06 34.0	−51 59 00	-73	-73, -56	0.8	mjsd	<0.5	265	sv	2	5
330.95−0.18	16 06 04.7	−51 47 11	-88	-91, -87	7	mjsd	<0.4	31	nv	0	4
331.13−0.24	16 07 10.8	−51 42 29	-91	-92, -81	28	mjsd	<0.4	16	v	6	7

Table 1 – *continued*

Methanol maser (l,b)	RA (1950) (h m s)	Dec (1950) (° ′ ″)	Radial peak (km s⁻¹)	Velocity range (km s⁻¹)	6GHz Peak (Jy)	Epoch 6 GHz	12GHz Peak (Jy)	OH Peak (Jy)	Variable 6 GHz	# of features var	total
331.28−0.19	16 07 38.14	−51 34 12.2	-78	-88, -77	207	mjsd	145	25	sv	2	12
331.34−0.35	16 08 37.4	−51 38 32	-65	-73, -61	92	jsd	<0.4	10	v	2	5
331.54−0.07	16 08 22.7	−51 18 10	-84	-87, -80	11	jsd	<0.5	15	v	1	3
331.56−0.12	16 08 40.6	−51 19 59	-104	-105, -94	47	mjsd	6	7	nv	0	7
332.65−0.62	16 15 54.4	−50 56 20	-50		7.1	jsd	<0.5	<1		0	1
332.72−0.62	16 16 14.2	−50 53 18	-46	-59, -45	5.4	mjsd	<0.5	1.2	v	1	4
333.07−0.45	16 17 02.4	−50 31 22	-55	-57, -51	10	jsd	1	<1	v	2	3
333.12−0.43	16 17 12.3	−50 28 40	-49	-57, -45	15	mjsd	<0.4	26	v	2	3
333.13−0.44	16 17 15.5	−50 28 47	-45	-45, -42	3.5	mjsd	<0.5	<1	sv	1	3
333.16−0.10	16 15 55.4	−50 12 41	-95	-96, -91	6.3	mjsd	3.8	<1	sv	1	3
333.20−0.08	16 16 00.1	−50 10 08	-82	-91, -81	5.8	jd	<0.5	<1		0	3
333.23−0.06	16 16 04.9	−50 08 04	-81	-93, -79	3.8	mjsd	<0.5	7	v	4	4
333.47−0.17	16 17 34.7	−50 02 45	-42	-49, -36	70	mjsd	<0.5	4	sv	1	12
335.55−0.31	16 27 11.3	−48 39 28	-116	-119, -110	23	mjsd	5	0.2	v	1	10
335.59−0.29	16 27 15.4	−48 37 20	-47	-56, -44	110	jsd	<0.4	3.4	sv	3	12
335.73+0.19	16 25 46.0	−48 11 23	-44	-55, -43	74	jsd	12.5	<0.6	nv	0	6
335.79+0.17	16 26 06.0	−48 09 22	-49	-59, -45	167	mjsd	126	0.6	sv	4	14
336.36−0.14	16 29 47.9	−47 57 28	-74	-81, -70	21	mjsd	2.3	0.9	nv	0	10
336.43−0.26	16 30 37.59	−47 59 18.9	-93	-95, -86	46	mjsd	36	<0.5	sv	2	8
336.41−0.26	16 30 30.7	−48 00 10	-85.6	-86, -85	8	jsd	<0.6	<0.5		0	1
336.83+0.02	16 31 00.6	−47 30 20	-77		16	mjsd	1.4	2	nv	0	2
336.86+0.01	16 31 11.2	−47 29 39	-76	-82, -68	34	mjsd	0.6	<1	nv	0	8
336.99−0.03	16 31 51.9	−47 25 03	-126	-127, -116	38	mjsd	<0.5	2.5	v	4	9
337.41−0.40	16 35 09.8	−47 22 07	-40	-43, -36	67	mjsd	3.5	102	sv	3	7
337.61−0.06	16 34 29.4	−46 58 57	-42	-54, -38	21	mjsd	12	2.5	nv	0	13
337.63−0.08	16 34 38.7	−46 58 53	-57	-63, -54	13	mjsd	1.5	<1	sv	1	6
337.71−0.05	16 34 49.6	−46 54 43	-55	-58, -43	145	mjsd	84	20	nv	0	10
337.92−0.46	16 37 25.0	−47 01 21	-38	-41, -36	47	mjsd	0.55	14	v	1	6
338.00+0.13	16 35 09.8	−46 34 12	-32	-36, -31	4	mjsd	<0.3	8.6	nv	0	3
338.08+0.01	16 35 58.2	−46 35 28	-53	-54, -30	18	mjsd	14.7	2	sv	4	14
338.28+0.54	16 34 29.8	−46 05 00	-57	-59, -56	5	mjsd	<0.5	10		0	2
338.46−0.25	16 38 36.1	−46 28 38	-50	-57, -49	83	mjsd	8.5	5.2	sv	4	8
338.47+0.29	16 36 18.6	−46 06 35	-30	-35, -29	0.7	mjsd	<0.5	3.6		0	2
338.87−0.08	16 39 28.7	−46 03 38	-41	-42, -38	19	mjsd	2.2	5	nv	0	4
338.93−0.06	16 39 36.5	−46 00 05	-42	-44, -42	12	jsd	3.8	<1	v	1	1
338.92+0.55	16 36 54.8	−45 36 14	-62	-68, -59	71	mjsd	<0.5	38	sv	6	12
339.62−0.12	16 42 26.5	−45 31 18	-36	-39, -30	83	mjsd	18.4	12.2	v	8	10
339.68−1.21	16 47 25.0	−46 10 59	-21	-41, -21	70	mjsd	<0.4	7.5	v	5	8
339.88−1.26	16 48 24.76	−46 03 33.9	-39	-45, -27	1820	mjsd	850	30	sv	2	12
340.05−0.24	16 44 35.2	−45 16 24	-60	-63, -46	42	mjsd	16	12	sv	1	6
340.79−0.10	16 46 38.35	−44 37 18.5	-107	-112, -88	242	mjsd	43	11.8	v	3	17
341.22−0.21	16 48 42.1	−44 21 53	-38	-50, -35	167	mjsd	5	8.7	sv	6	11
341.28+0.06	16 47 43.9	−44 08 41	-74	-77, -66	5.5	mjsd	0.85	2		0	6
343.93+0.12	16 56 38.7	−42 02 58	14	+7, +19	11	mjsd	3.9	5.4	nv	0	4
344.23−0.57	17 00 35.0	−42 14 29	-20	-33, -16	118	mjsd	2.7	2.3	v	3	10
344.42+0.05	16 58 37.1	−41 42 36	-71	-73, -63	16	mjsd	0.55	2.9	nv	0	5
344.58−0.02	16 59 26.2	−41 37 36	1	-5, +2	3.4	mjsd	<0.5	18.6	nv	0	2
345.00−0.22	17 01 38.5	−41 24 59	-22	-32, -20	448	mjsd	20	3.6	v	10	10
345.01+1.79	16 53 19.69	−40 09 46.0	-18	-24, -15	508	mjsd	310	14	sv	3	11
345.01+1.80	16 53 18.9	−40 09 29	-13	-15, -10	31	mjsd	14	<0.2		0	5
345.41−0.95	17 06 04.9	−41 32 04	-15	-19, -13	2.8	mjsd	<0.6	1	v	2	2
345.50+0.35	17 00 54.2	−40 40 18	-18	-23, -11	174	mjsd	4.7	15.6	v	9	11
346.48+0.13	17 04 55.0	−40 01 40	-11	-12, -5	2.9	mjsd	<0.5	3.3		0	3
346.52+0.12	17 05 05.5	−40 00 15	-2	-2, 0	0.9	jsd		<1		0	2
346.52+0.08	17 05 13.4	−40 01 25	6		1.8	jsd	<0.6	<1		0	1
347.58+0.21	17 07 59.5	−39 05 58	-103	-104, -95	2.7	jsd	0.7	<1	sv	1	3
347.63+0.21	17 08 09.6	−39 03 36	-92	-93, -89	11.5	jsd	<0.4	<1		0	2
347.63+0.15	17 08 24.8	−39 06 00	-97	-98, -96	18	mjsd	<0.5	8.6		0	1
347.82+0.02	17 09 32.1	−39 01 17	-25	-26, -23	3.4	jsd	<0.6	<1	sv	1	2
347.86+0.02	17 09 39.1	−38 59 16	-29	-38, -23	7.2	mjsd	0.9	6.4	sv	3	9
347.90+0.05	17 09 39.4	−38 56 02	-28	-31, -27	5.3	jsd	2	<1		0	4
348.55−0.98	17 15 53.0	−39 00 53	-13	-23, -7	74	mjsd	5.6	4.5	v	10	16
348.70−1.04	17 16 37.1	−38 55 31	-3	-17, -3	60	mjs	34.5	1.5	sv	6	14
348.72−1.04	17 16 38.9	−38 54 31	-8	-9, -6	90	mjs	11	<1		0	2
348.88+0.10	17 12 24.7	−38 06 49	-75	-77, -70	7.7	mjsd	<0.7	3.3	v	3	5

Table 1 – *continued*

Methanol maser (l,b)	RA (1950) (h m s)	Dec (1950) (° ′ ″)	Radial peak (km s⁻¹)	Velocity range (km s⁻¹)	6GHz Peak (Jy)	Epoch 6 GHz	12GHz Peak (Jy)	OH Peak (Jy)	Variable 6 GHz	# of features var	total
348.89−0.19	17 13 36.3	−38 16 30	1		2	mjs	<0.5	1.5		0	1
349.07−0.02	17 13 25.5	−38 02 07	7	+6, +16	1.9	mjsd	0.75	2.4	sv	3	6
349.09+0.11	17 13 00.5	−37 56 19	-77	-83, -74	30	mjsd	<0.5	3	sv	3	7
350.01+0.43	17 14 22.4	−37 00 18	-31	-37, -29	6	mjsd	<0.6	1.4	v	2	3
350.10+0.09	17 16 02.9	−37 07 48	-74	-76, -60	41	mjsd	5	69	sv	1	9
351.16+0.70	17 16 36.5	−35 54 49	-5	-7, -2	11	mjsd	<0.5	70	sv	2	4
351.42+0.64	17 17 32.35	−35 44 04.2	-10	-12, -7	3300	mjsd	1210	249	sv	1	8
351.44+0.66	17 17 33.58	−35 42 11.1	-3	-14, +1	16	mjsd	88	<1	sv	4	6
351.58−0.35	17 22 03.2	−36 10 09	-95	-100, -87	63	mjsd	<0.6	9.2	v	1	11
351.77−0.54	17 23 20.67	−36 06 45.4	2	-9, +3	225	mjsd	8.5	960	v	1	4
352.11+0.17	17 21 22.8	−35 26 12	-55	-60, -53	5.8	d		<0.2			
352.08+0.16	17 21 20.6	−35 27 55	-67	-70, -64	2.3			<0.2			
352.52−0.16	17 23 51.4	−35 17 06	-51	-54, -49	6.3	mjsd	<0.6	2.6	nv	0	4
353.41−0.36	17 27 06.6	−34 39 30	-20	-23, -19	90	mjsd	19.5	8.7	sv	1	6
353.46+0.56	17 23 33.2	−34 05 53	-50	-53, -50	13	mjsd	<0.4	1.3	sv	1	3
354.61+0.47	17 26 59.8	−33 11 34	-23	-27, -13	216	mjsd	28	8.2	v	7	12
355.34+0.15	17 30 12.2	−32 45 56	20	(+5, +21)	9.6	mjsd	<0.6	16.4	nv	0	5
356.66−0.27	17 35 14.2	−31 53 07	-54	-57, -45	9	mjsd	<0.5	2.9	sv	1	6
359.14+0.03	17 40 14.2	−29 38 03	-4	-7, 0	17	mjsd	<0.4	8.4	sv	1	7
359.44−0.10	17 41 29.1	−29 26 59	-52	-57, -45	27	mjsd	<0.5	8	sv	1	8
359.61−0.24	17 42 27.2	−29 22 18	20	+14, +27	48	mjsd	13.5	2.7	v	5	10
359.97−0.46	17 44 09.8	−29 10 59	23	+20, +23	1	mjsd	<0.4	15.5		0	2
0.38+0.04	17 43 11.3	−28 34 37	37	+35, +40	0.7	mjsd	<0.4	3		0	2
0.55−0.85	17 47 04.4	−28 53 39	14	+8, +20	68	mjsd	3.9	2.3	sv	6	13
0.64−0.04	17 44 08.9	−28 23 29	49	+48, +53	69	jd	<0.5	<1			
0.65−0.05	17 44 11.0	−28 23 23	48	+46, +52	33	jd	7.2	<1			
0.66−0.03	17 44 09.2	−28 21 57	70.4	+70, +73	18	jd	<0.5	<1			
0.67−0.03	17 44 10.8	−28 21 40	69.2	+57, +77	24	jd	<0.5	<1			
0.69−0.04	17 44 14.7	−28 20 52	68.6	+64, +72	32	jd	<0.5	<1			
2.14+0.01	17 47 28.1	−27 05 02	63	+53, +65	10	mjsd	<0.5	5	sv	3	7
3.91+0.00	17 51 33.1	−25 34 16	17	+17, +24	2.1	mjsd	<0.5	4.6		0	2
5.90−0.43	17 57 36.9	−24 04 22	10	-1, +13	8	mjsd	<0.5	<1	v	2	6
8.67−0.36	18 03 18.6	−21 37 45	39		5.6	mjsd	<0.5	2.4		0	1
8.68−0.37	18 03 22.6	−21 37 24	43	+41, +46	148	mjsd	14	3	sv	1	6
9.62+0.20	18 03 15.98	−20 31 52.9	1	-4, +9	5090	mjsd	180	19.2	nv	0	10
10.45−0.02	18 05 47.0	−19 55 01	73.2	+68, +79	25	jsd	7	<0.9		0	5
10.47+0.03	18 05 40.0	−19 52 24	75	+58, +77	61	mjsd	17	0.9	v	1	8
10.48+0.03	18 05 39.7	−19 51 52	65	+58, +66	16	jsd	<0.3	<0.9		0	4
10.62−0.38	18 07 31.0	−19 56 19	5	-10, +7	3.6	mjsd	1.2	30	nv	0	6
10.63−0.34	18 07 21.4	−19 54 39	-8	-13, +1	3.4	jsd	<0.5	<1	v	5	9
11.03+0.06	18 06 42.4	−19 22 03	20	+15, +21	0.7	mjs	<0.5	7.2		0	2
11.90−0.14	18 09 15.2	−18 42 21	43	+39, +44	67	mjsd	21	6.6	nv	0	7
11.91−0.11	18 09 08.0	−18 41 15	36	+33, +37	2.6	jd	<0.6	<1		0	3
11.93−0.15	18 09 20.3	−18 40 51	48	+45, +49	2.3	jd	<0.6	<1		0	3
11.94−0.62	18 11 04.1	−18 54 21	32	+30, +44	47	jsd	6.8	<0.2	sv	1	10
12.03−0.03	18 09 06.3	−18 32 43	108	+105, +113	82	mjsd	13.5	3.1	sv	1	9
12.21−0.10	18 09 44.0	−18 25 09	20	+19, +21	15	mjsd	<0.5	21		0	3
12.20−0.11	18 09 44.1	−18 25 36	17	+16, +23	3.7	jd	<0.5	<1	sv	1	3
12.20−0.12	18 09 46.4	−18 25 55	26	+26, +32	3.5	jd	<0.5	<1		0	3
12.68−0.18	18 10 59.6	−18 02 29	52	+50, +62	544	jsd	16.5	17.3	sv	4	10
12.89+0.49	18 08 56.4	−17 32 14	39	+27, +43	93	jsd	62	4	v	5	8
12.91−0.26	18 11 43.8	−17 53 04	39	+35, +47	317	mjsd	11.5	95	nv	0	6
15.03−0.68	18 17 31.6	−16 13 02	21	+21, +24	39	mjsd	17	3		0	2
16.59−0.05	18 18 18.5	−14 33 16	59	+52, +69	21	mjsd	1.1	4.1	sv	1	10
16.87−2.16	18 26 32.5	−15 17 58	15	+15, +19	32			2.6			
17.64+0.16	18 19 36.5	−13 31 38	21		25	jd	<0.5	3		0	1
18.46−0.01	18 21 48.5	−12 52 51	49	+47, +50	23	jd	<0.3	2.9		0	2
19.47+0.17	18 23 07.3	−11 54 30	18	+13, +27	6	jsd	<0.6	<1	sv	1	5
19.48+0.15	18 23 12.7	−11 54 16	21	+20, +27	19.3	mjsd	2.9	17		0	3
19.61−0.14	18 24 29.5	−11 55 39	57	+50, +61	18	mjsd	2.8	2.5		0	3
19.61−0.12	18 24 26.6	−11 55 18	53		3.6	jsd	1	<1		0	1
19.61−0.23	18 24 49.7	−11 57 52	36	+36, +43	0.4	mj	<0.6	3.8		0	3
20.08−0.14	18 25 23.3	−11 30 44	44		2.9	mjd	<0.6	11.7		0	1
20.23+0.07	18 24 56.9	−11 16 59	72	+60, +78	100	mjsd	2.7	1.7	sv	2	12
21.88+0.01	18 28 16.6	−09 51 10	21	+17, +22	15	jd	<0.5	0.4		0	2

Table 1 – *continued*

Methanol maser (l,b)	RA (1950) (h m s)	Dec (1950) (° ′ ″)	Radial peak (km s⁻¹)	Velocity range (km s⁻¹)	6GHz Peak (Jy)	Epoch 6 GHz	12GHz Peak (Jy)	OH Peak (Jy)	Variable 6 GHz	# of features var	# of features total
22.43−0.16	18 29 57.5	−09 26 41	29	+22, +40	20	mjsd	5	4.8	sv	1	12
23.01−0.41	18 31 55.6	−09 03 09	75	+69, +84	405	mjsd	28	4.9	sv	5	9
23.44−0.18	18 31 55.3	−08 34 01	103	+94, +113	77	mjsd	17	4.7	v	10	15
24.33+0.14	18 32 26.8	−07 37 25	110	+107, +116	10.8	mjsd	20	0.2	v	2	6
24.79+0.08	18 33 29.9	−07 14 45	114	+105, +115	82	mjd	<0.4	5.5	sv	2	10
24.85+0.09	18 33 35.1	−07 11 33	110	+109, +115	21	jd	<0.5	<1		0	1
27.36−0.16	18 39 11.0	−05 04 43	100	+88, +104	29	mjsd	20	1.1	sv	7	9
28.15+0.00	18 40 02.2	−04 18 26	101	+92, +105	34	sd	21	<1	nv	0	6
28.20−0.05	18 40 19.3	−04 17 02	99	+94, +102	3.3	mjd	<0.5	15	nv	0	4
28.83−0.25	18 42 13.1	−03 49 01	83	+79, +94	73	mjsd	3.1	4.2	nv	0	9
28.84−0.23	18 42 09.5	−03 47 58	100	+99, +104	1.3	mjd	<0.6	<1	nv	0	3
28.86+0.07	18 41 07.9	−03 38 36	105		1.1	mjsd	<0.4	11.3	v	1	1
29.86−0.05	18 43 22.9	−02 48 26	101	+99, +105	67	mjsd	13	3	sv	2	5
29.95−0.02	18 43 26.7	−02 42 38	96	+95, +102	206	jd	53	0.9			
29.94−0.02	18 43 25.6	−02 43 22	100.4		23	jd	<1	<0.9			
29.98−0.04	18 43 34.9	−02 42 19	104	+97, +105	14	jd	4	<0.9			
30.20−0.17	18 44 25.8	−02 33 57	108	+101, +111	18.7	mjd	10	1.5	nv	0	6
30.22−0.18	18 44 31.3	−02 32 50	113	+111, +115	11.7	jd	2.8	<0.2	v	2	4
30.59−0.04	18 44 42.5	−02 09 43	43	+36, +49	7.5	mjd	<0.7	7	nv	0	7
30.70−0.07	18 45 00.6	−02 04 12	88	+85, +90	87	mjd	<0.4	19	sv	2	5
30.76−0.05	18 45 02.8	−02 00 46	92	+88, +95	68	mjsd	1.5	<0.2	sv	1	5
30.82−0.05	18 45 10.5	−01 57 46	101	+91, +110	18	jsd	0.8	2	sv	2	8
30.78+0.23	18 44 05.7	−01 51 48	49	+47, +49	24	mjd	9	<0.2	nv	0	3
30.79+0.20	18 44 12.3	−01 52 04	86	+75, +89	23	mjd	11.5	1.5	sv	3	8
30.82+0.27	18 44 00.6	−01 48 41	105	+100, +111	8	mjd	<0.4	3.4		0	4
31.28+0.06	18 45 37.2	−01 30 00	110	+102, +114	81	mjsd	59	2.5	sv	4	8
31.41+0.31	18 44 57.9	−01 15 59	104	+90, +108	11	sd	2.1	5		0	6
32.74−0.08	18 48 47.8	−00 15 50	39	+24, +45	47	mjsd	10.5	2.5	nv	0	9
33.09−0.07	18 49 25.1	+00 02 51	96	+95, +106	30	md	0.4	<0.2	sv	2	6
33.13−0.09	18 49 33.6	+00 04 25	73	+71, +81	12.4	mjd	0.6	8.2	sv	3	6
34.24+0.13	18 50 49.0	+01 09 57	55.5	+55, +62	20	jd	0.9	<1			
34.26+0.15	18 50 46.6	+01 11 06	58	+58, +62	29	mjd	3.5	55	nv		
35.02+0.35	18 51 29.1	+01 57 26	44	+40, +47	56	mjd	<0.4	8.1	sv	2	5
35.20−0.74	18 55 41.1	+01 36 26	28	+26, +35	125	mjsd	31	2.8	nv	0	7
35.20−1.74	18 59 13.1	+01 09 07	42	+39, +47	560	mjsd	109	41	sv	3	11
40.62−0.14	19 03 34.6	+06 41 57	31	+30, +37	17	mjsd	<0.6	80	sv	1	5
43.15+0.02	19 07 47.0	+09 00 30	13		26	mjd	3.7	5.6			
43.16+0.02	19 07 48.3	+09 01 18	9	+8, +20	22	mjd	<0.8	99			
43.17+0.01	19 07 51.0	+09 01 21	20	+19, +22	12.8	mjd	1	9			
43.17−0.00	19 07 52.6	+09 01 04	-1		3.4	mjd	1.7	<1			
43.80−0.13	19 09 30.7	+09 30 42	40	+39, +44	144	mjsd	<0.4	90	nv	0	4
45.07+0.13	19 11 00.5	+10 45 41	58	+57, +60	33	mjsd	<0.5	50		1	1
45.44+0.07	19 11 56.6	+11 03 44	50		1.9	jd	<0.5	<1	v	2	2
45.47+0.05	19 12 02.5	+11 04 31	56	+55, +59	5.3	mjd	2.2	20	sv	1	3
45.47+0.13	19 11 46.2	+11 07 03	65	+59, +74	7	mjd	<0.6	25		0	5
45.49+0.13	19 11 50.0	+11 07 53	57.2		13.4	mjd	<0.5	<1	sv	1	2
49.47−0.37	19 21 20.6	+14 24 16	64	+60, +75	12	d	<0.7	0.6			
49.49−0.39	19 21 25.7	+14 24 42	59	+51, +60	850	d	<1	93			
49.49−0.37	19 21 21.8	+14 25 08	56		33	d	21	1.6			
59.78+0.06	19 41 03.6	+23 36 51	25	+14, +27	42	jsd	15.8	1.7	v	6	9

189.03 + 0.78. Note that weak emission at a velocity of $+11$ km s^{-1} is a sidelobe response to 188.95 + 0.89, as can be seen from the alignment of the two spectra.

189.78 + 0.34. OH emission (from a source designated S252) is reported by Mirabel, Rodriguez & Ruiz (1989); the OH peak flux densities of 0.1 Jy at 1667 MHz and 0.05 Jy at 1665 MHz suggest that the OH emission may be diffuse quasi-thermal emission rather than a maser.

196.45 − 1.68. Although we see only slight variations from 1992 March to 1992 December, we note that Menten (1991b) lists it (as S269) with a peak intensity of 134 Jy, approximately twice our value.

208.99 − 19.38. From this direction (an OH maser in Orion A) we detected weak (0.5 Jy) emission in 1992 December at velocity $+7$ km s^{-1}. Methanol absorption of comparable amplitude is also present in the vicinity, hindering us from measuring an accurate position for the emission, and so we have not listed it in Table 1 nor shown a spectrum.

213.71 − 12.60. The feature at velocity 10.5 km s^{-1} decreased in amplitude by 30 per cent in our observations.

Menten (1991b) lists the peak intensity as 160 Jy, about half our value, which also suggests variability in some features.

264.29 + 1.46. This source was strongest on our original 1992 March detection, with a peak of 0.7 Jy at velocity + 6.2 km s^{-1}. The broad feature shown in the spectrum (1992 June) later decayed in 1992 December to a narrow (width 0.2 km s^{-1}), weak (0.15 Jy) spike. Near this position there are two H_2O masers, but OH spectra show only absorption, at velocity + 6 km s^{-1}.

269.15 − 1.13. The weak OH emission of 0.2 Jy cited in Table 1 is at velocity + 12 km s^{-1}, at the edge of absorption, and was measured in 1992 August and 1993 July.

270.25 + 0.84. There is an H_2O maser in this direction, but no detectable OH emission.

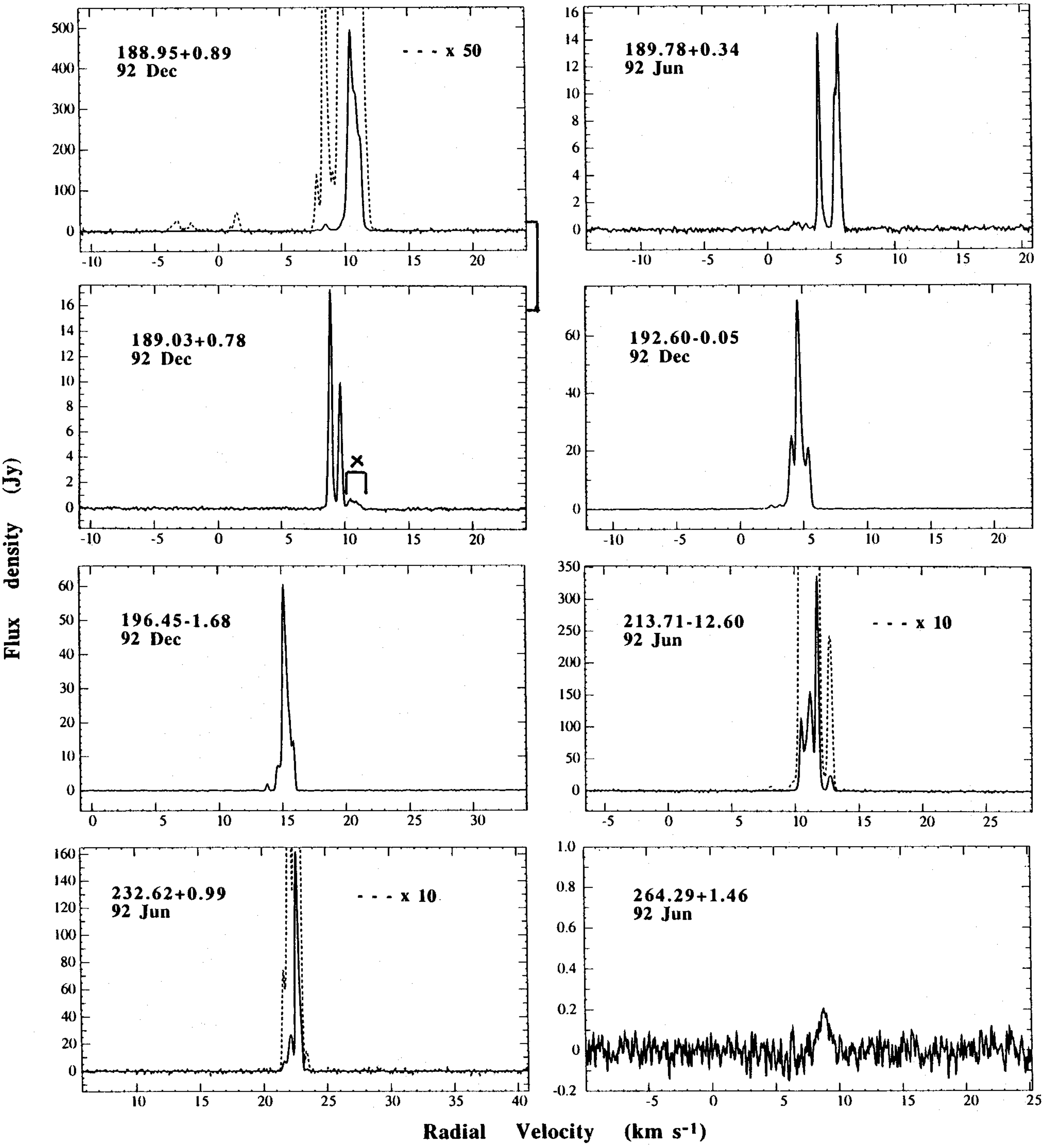

Figure 2. Spectra of 6.6-GHz methanol masers. All spectra have been Hanning-smoothed to a velocity resolution of 0.088 km s^{-1}. The date of observation is shown. The broken line shown on the spectra of many of the strong sources is an expanded scale, added to show the weak features more clearly; the magnification of this expanded intensity scale is indicated within the frame. Spectra are bracketed together in many cases to draw attention to the blending of adjacent sources.

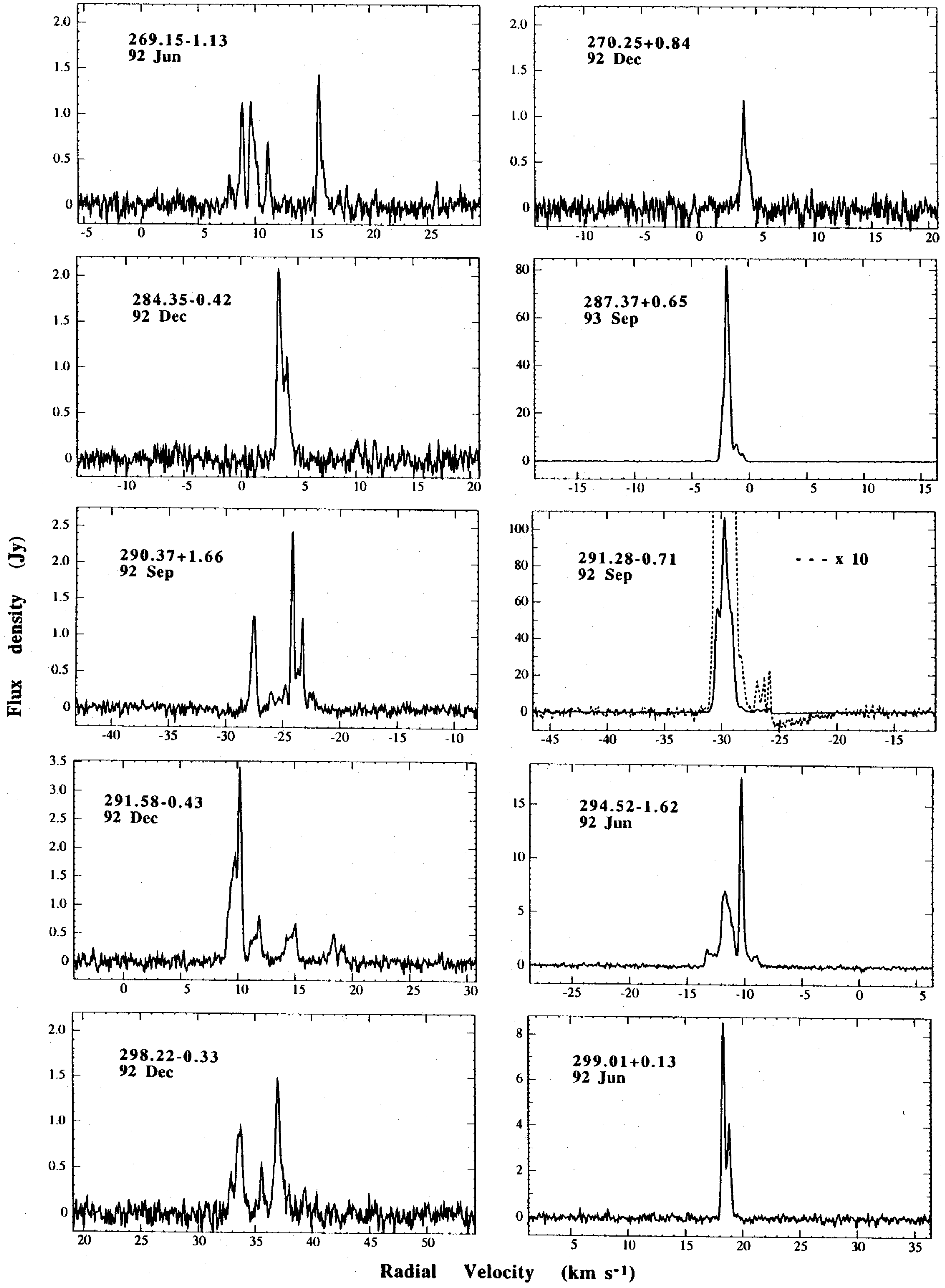

Figure 2 – *continued*

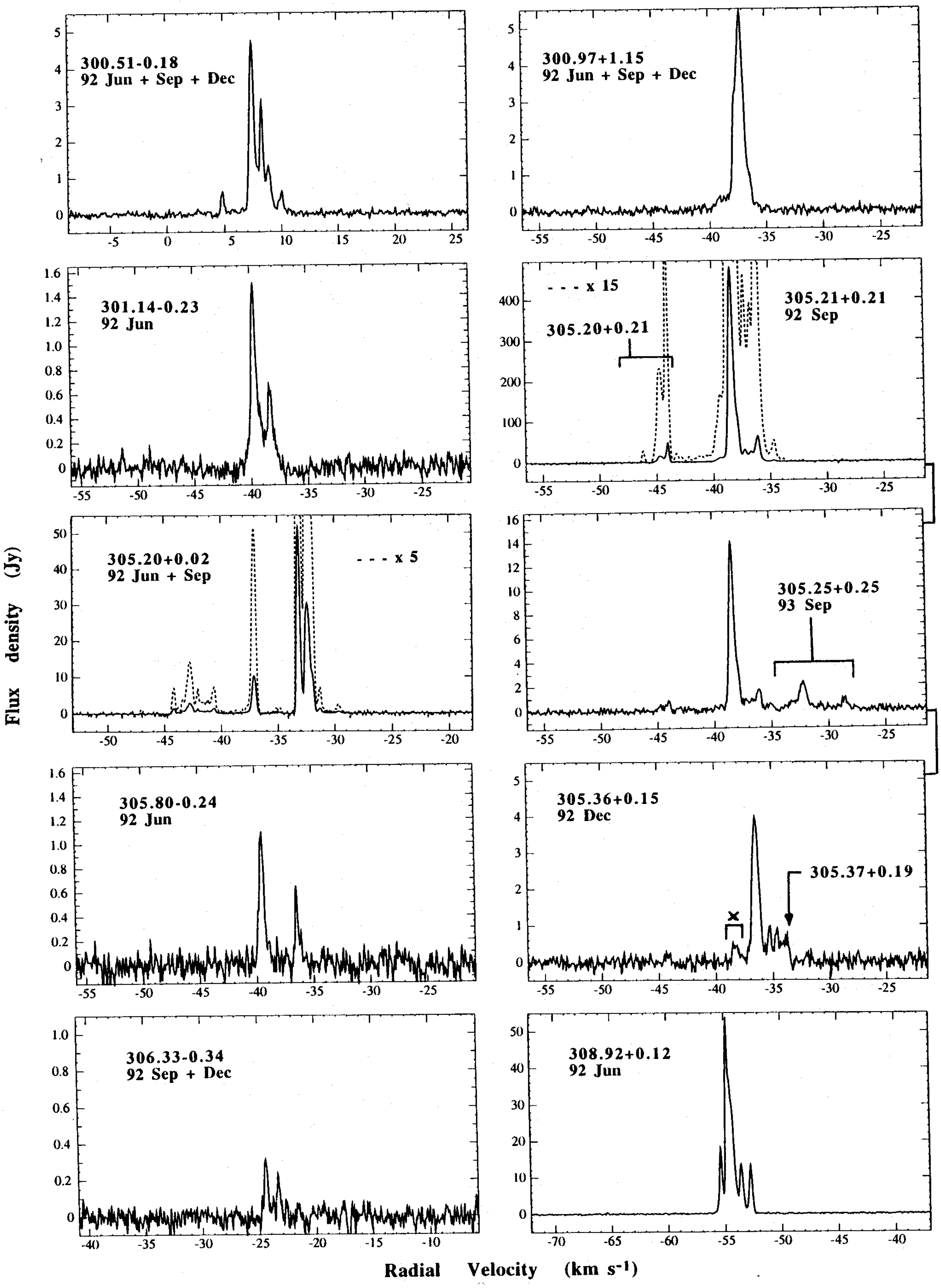

Figure 2 – *continued*

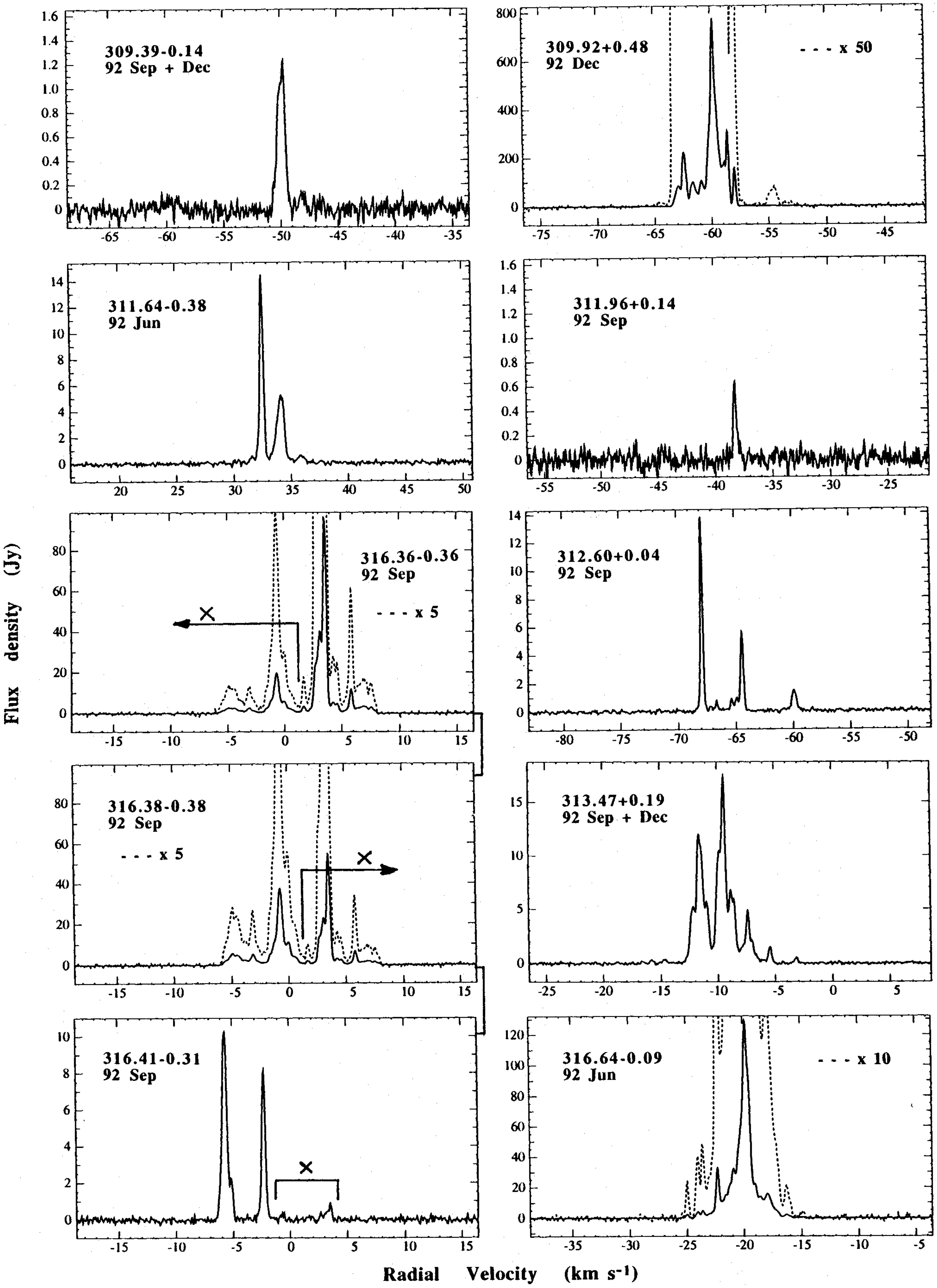

Figure 2 – *continued*

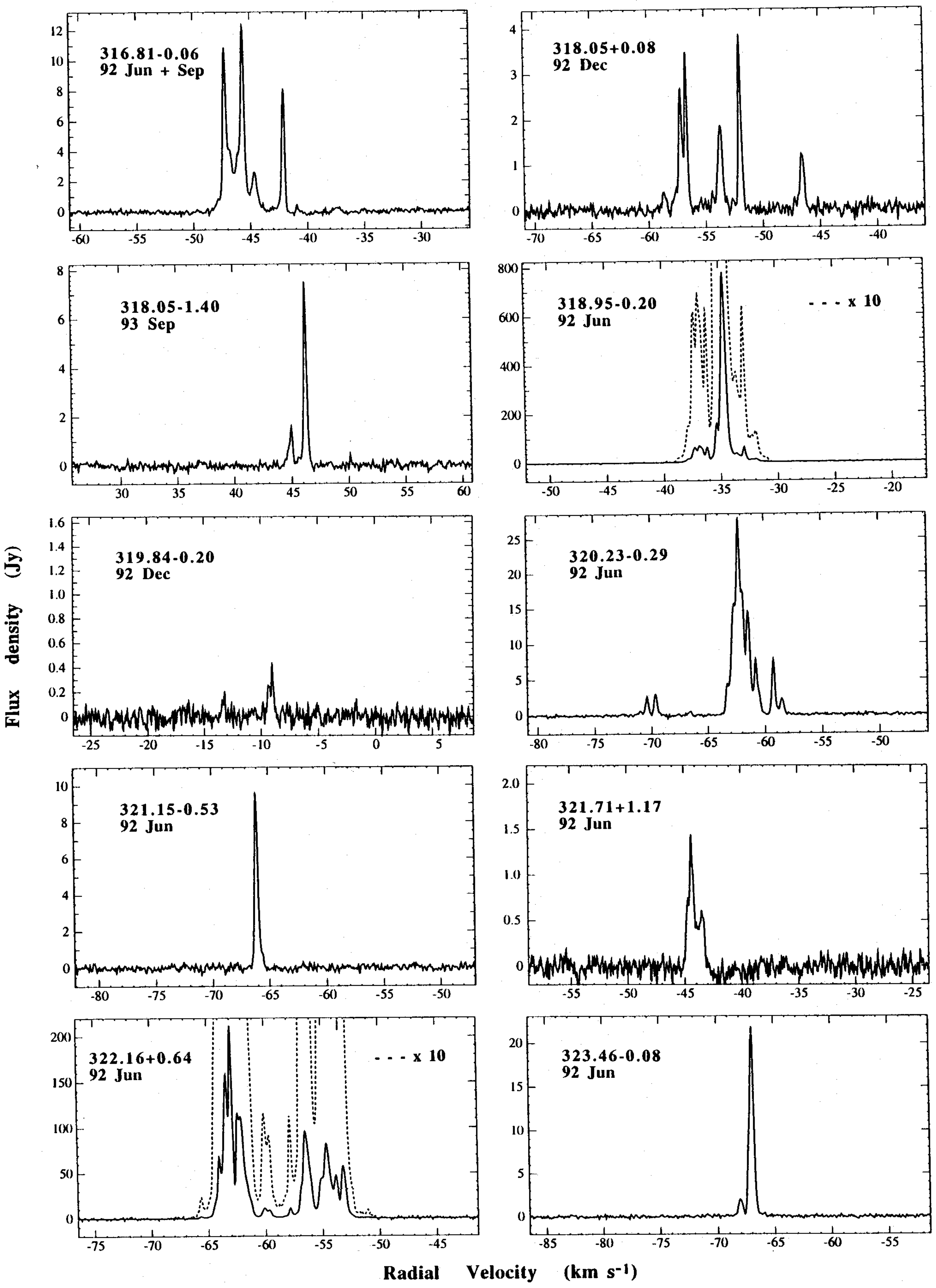

Figure 2 – *continued*

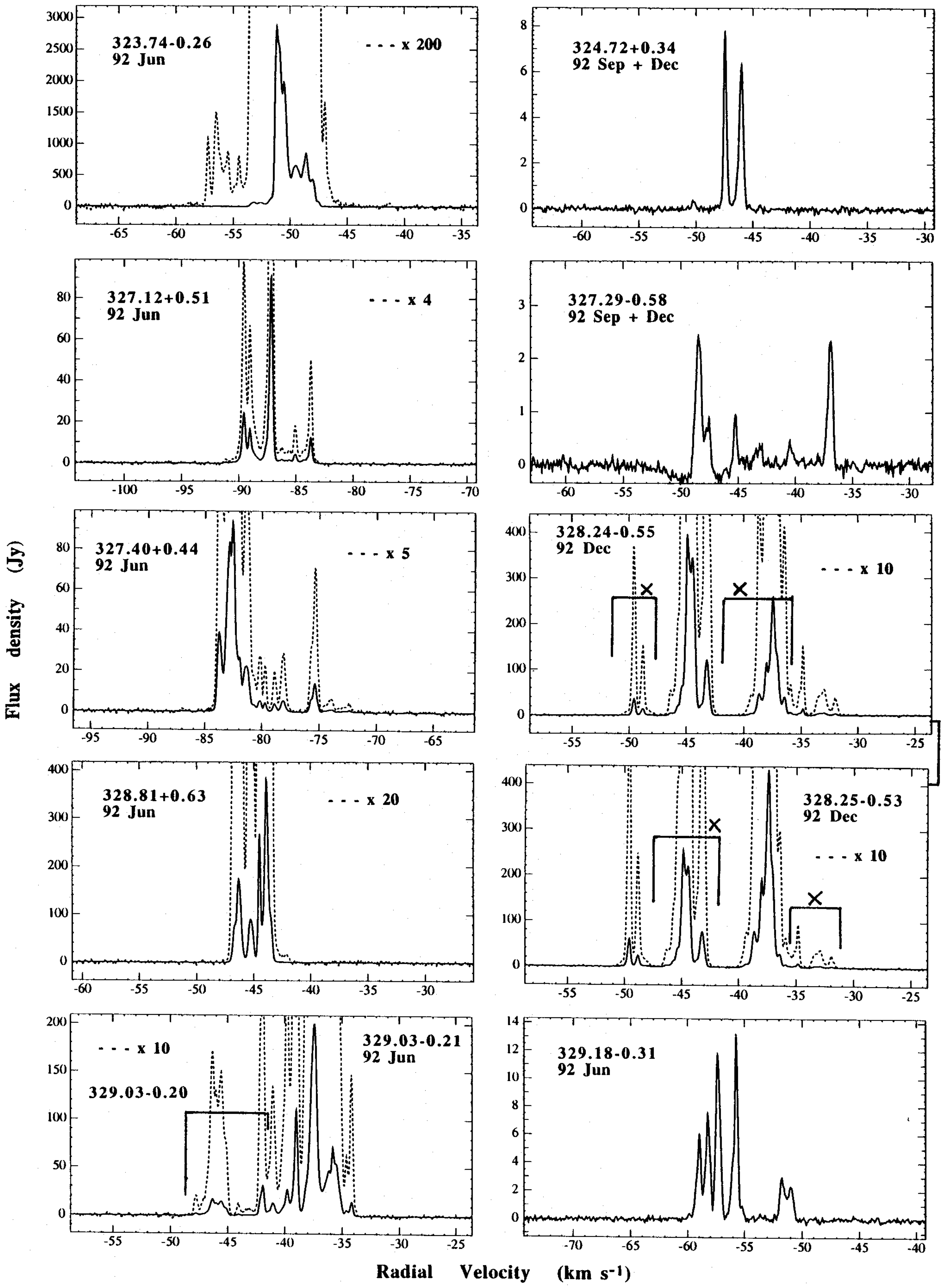

Figure 2 – *continued*

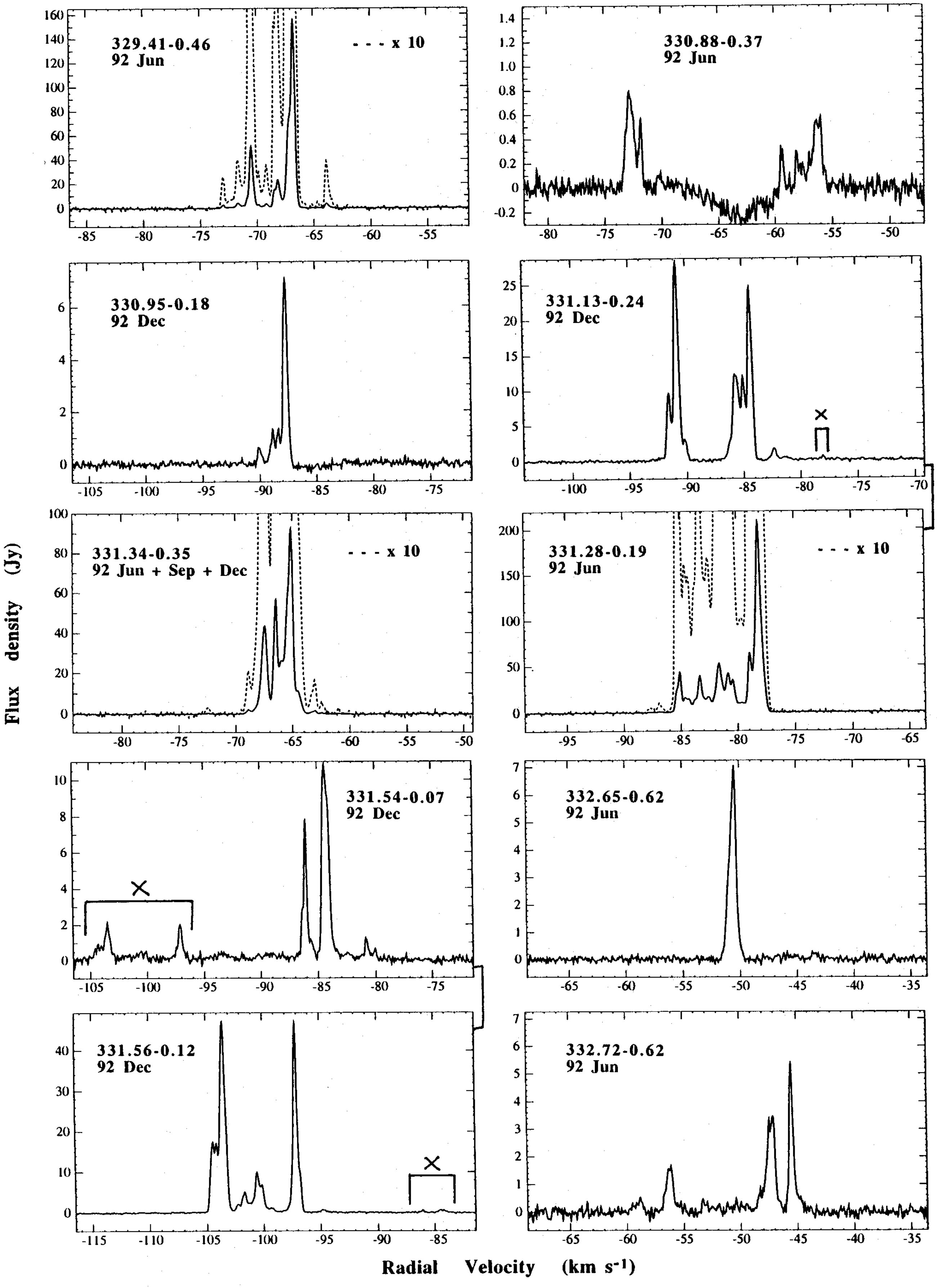

Figure 2 – *continued*

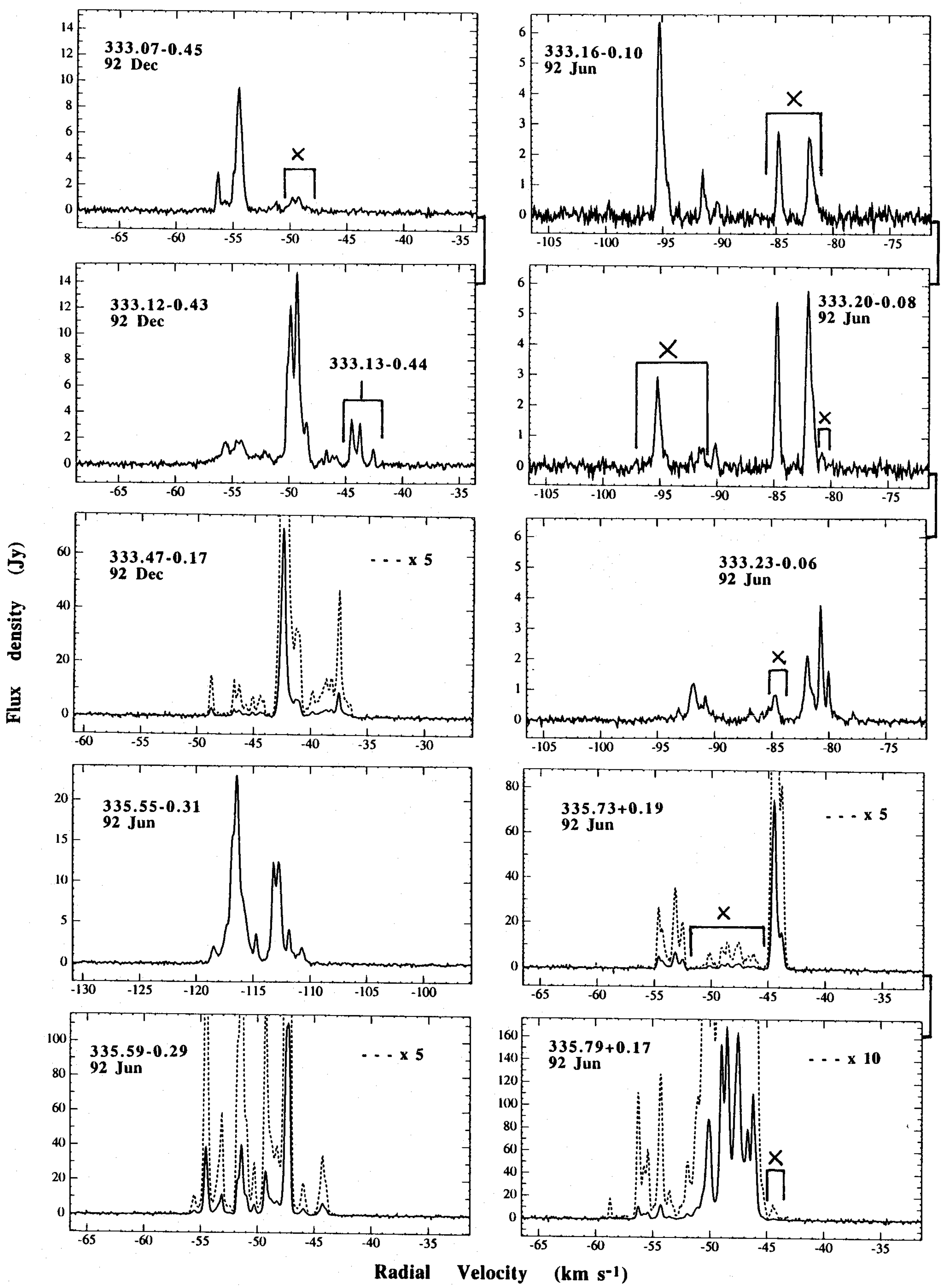

Figure 2 – *continued*

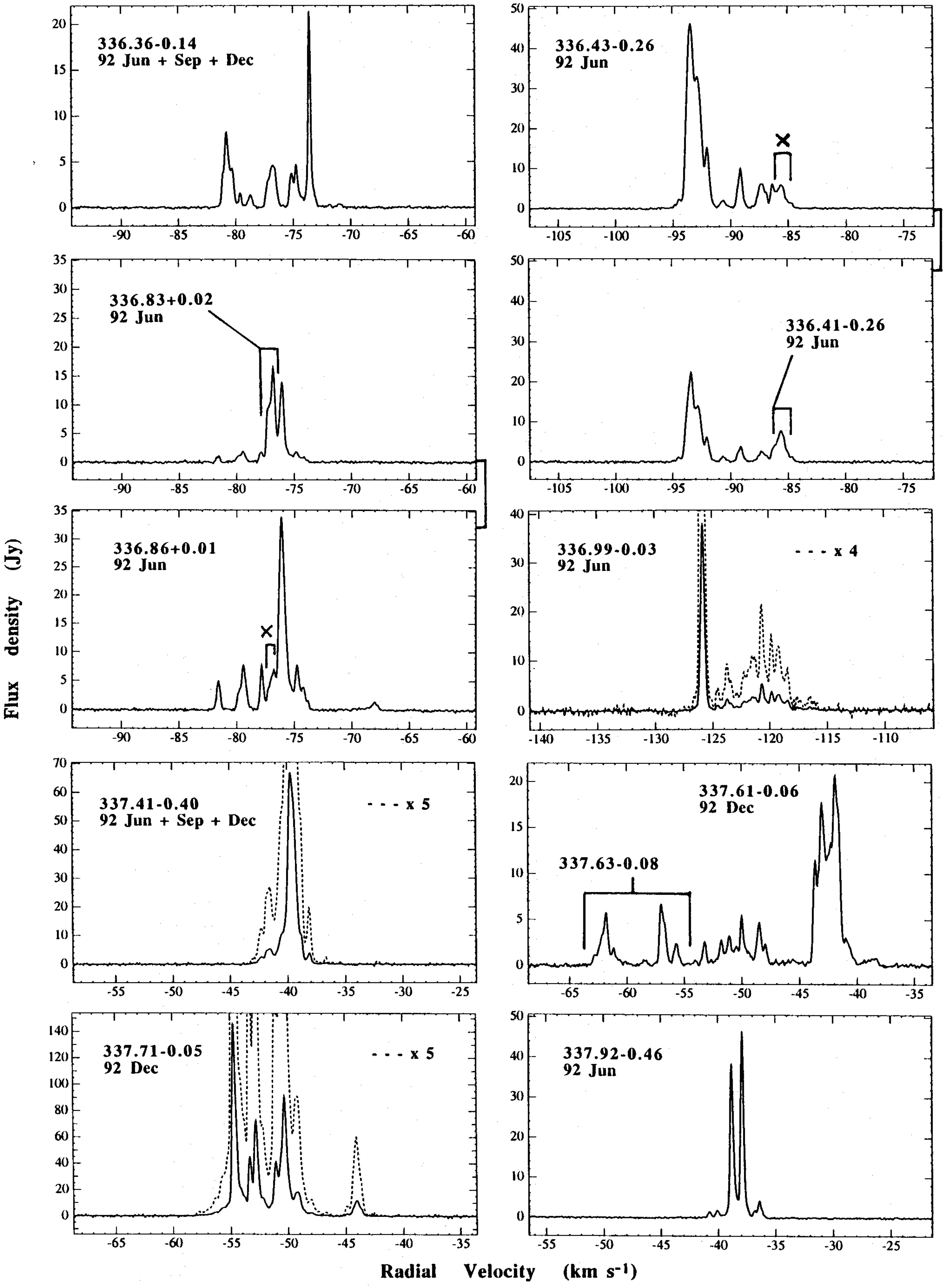

Figure 2 – *continued*

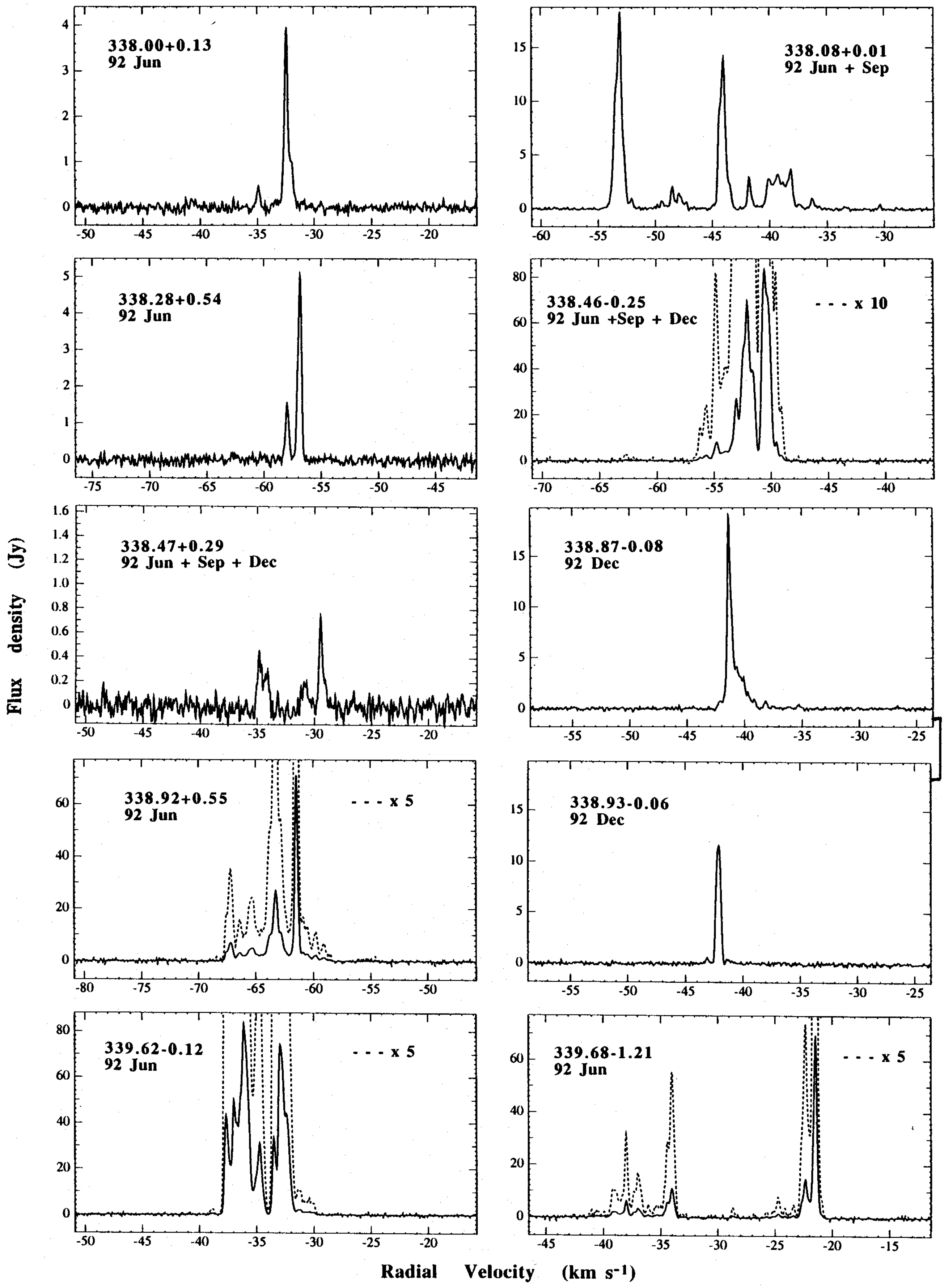

Figure 2 – *continued*

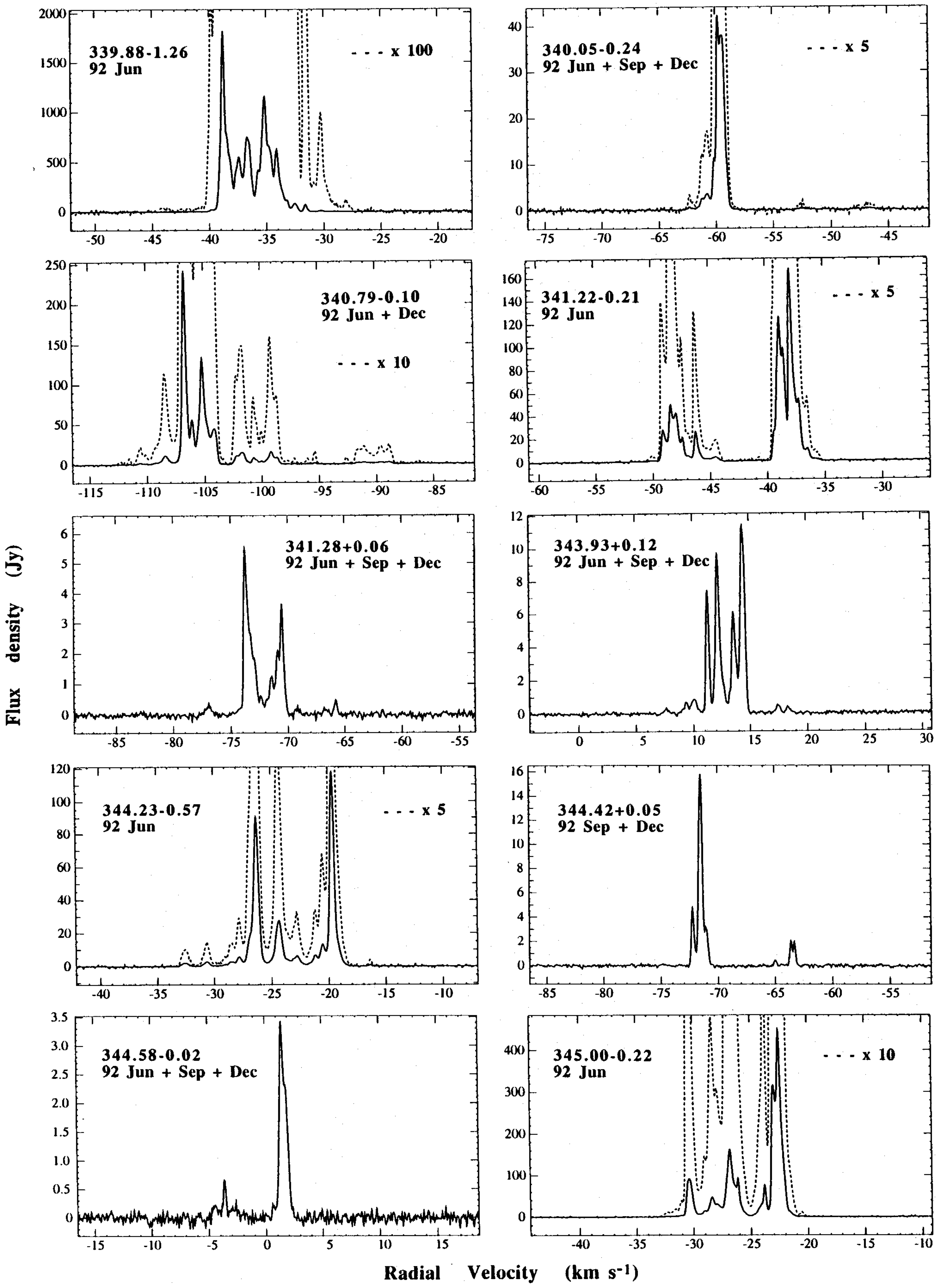

Figure 2 – *continued*

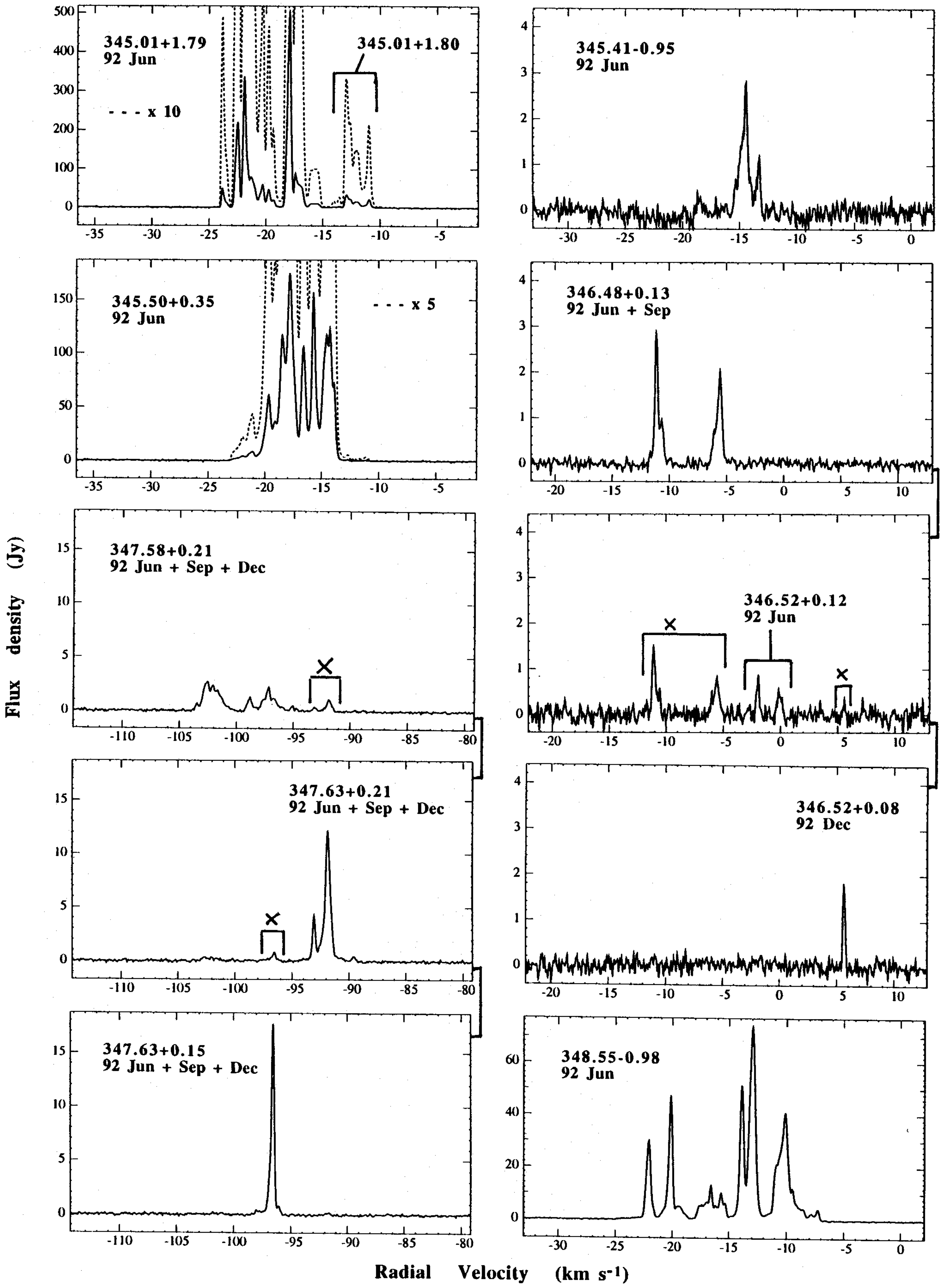

Figure 2 – *continued*

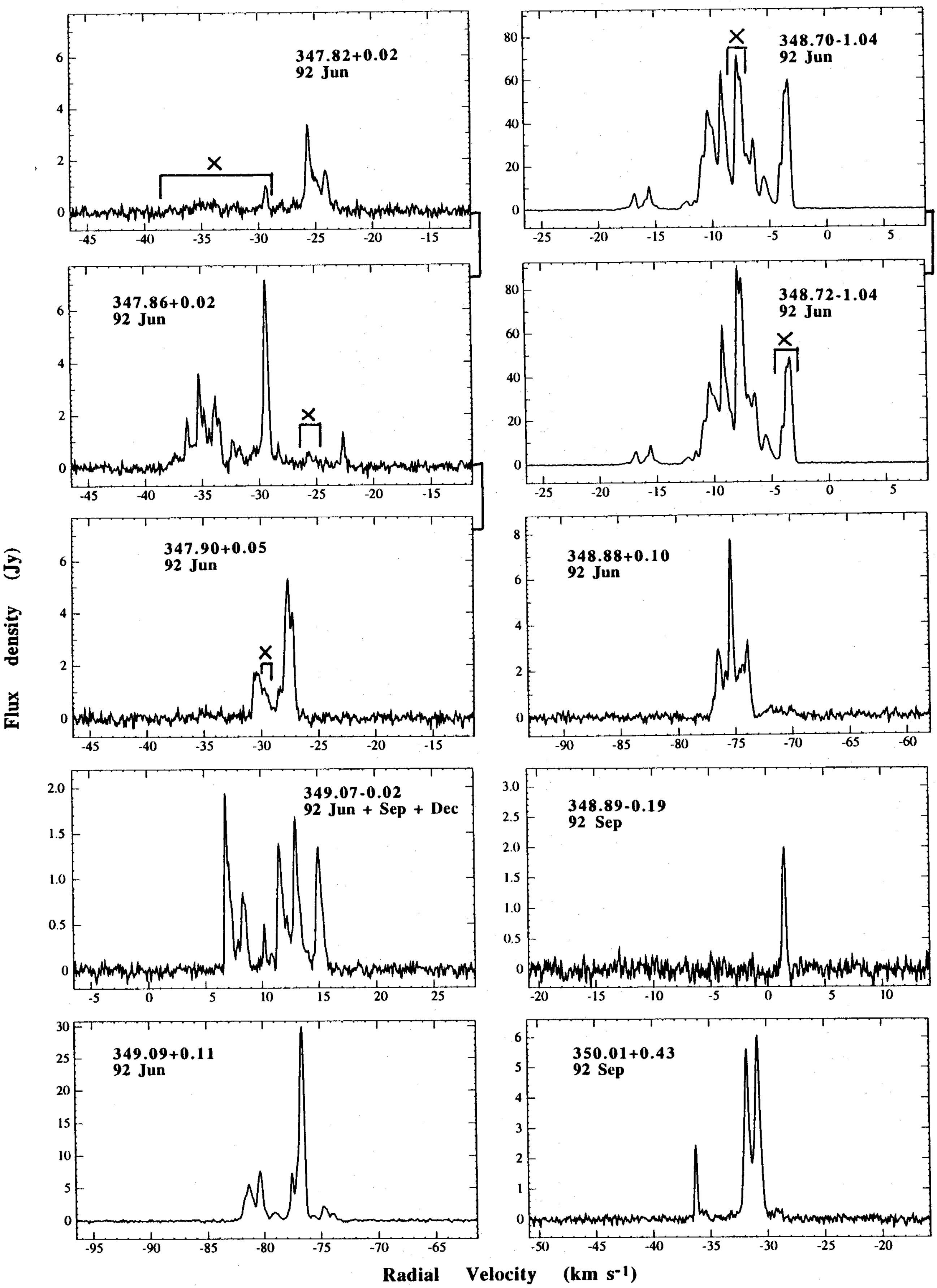

Figure 2 – *continued*

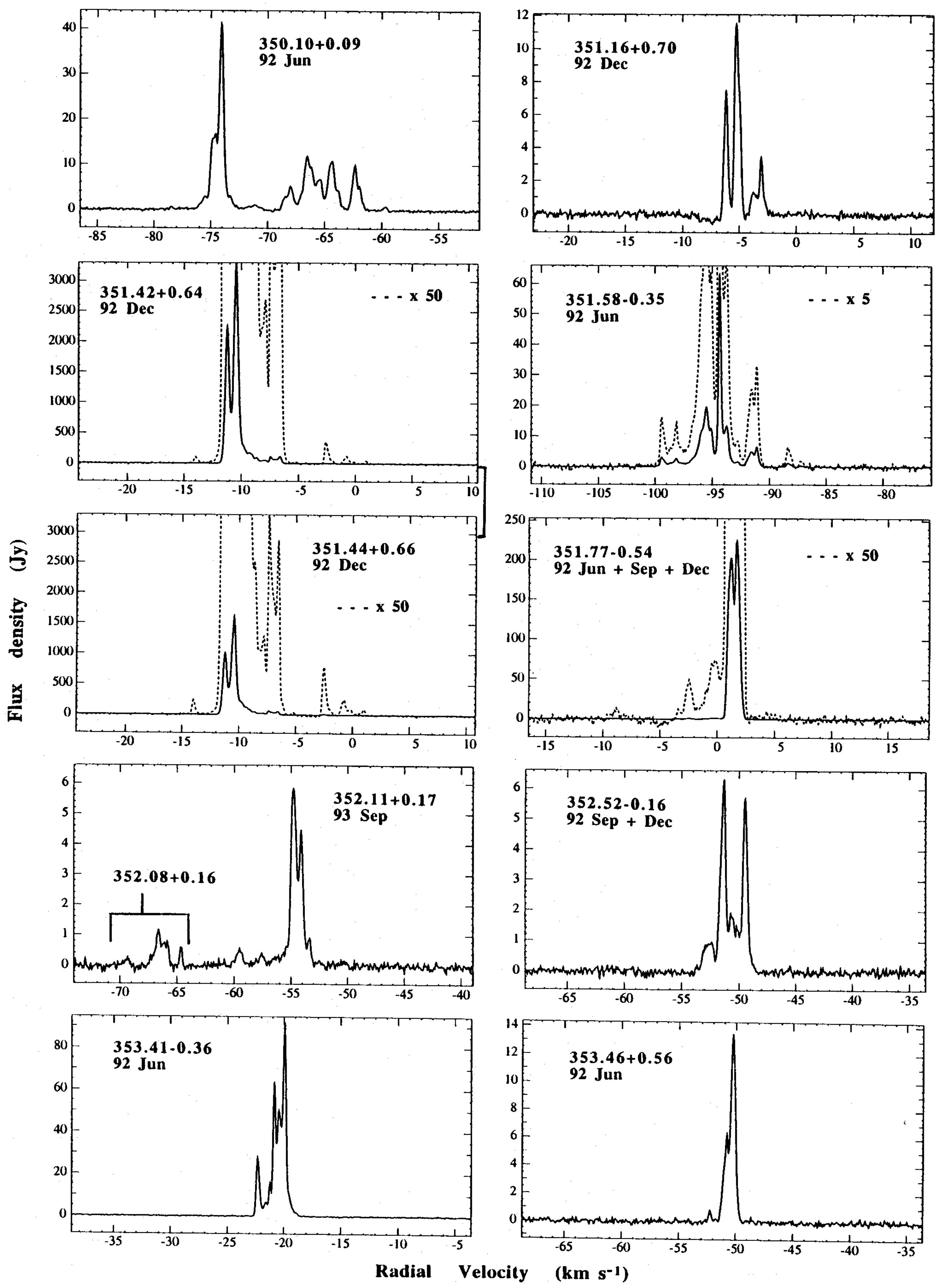

Figure 2 – *continued*

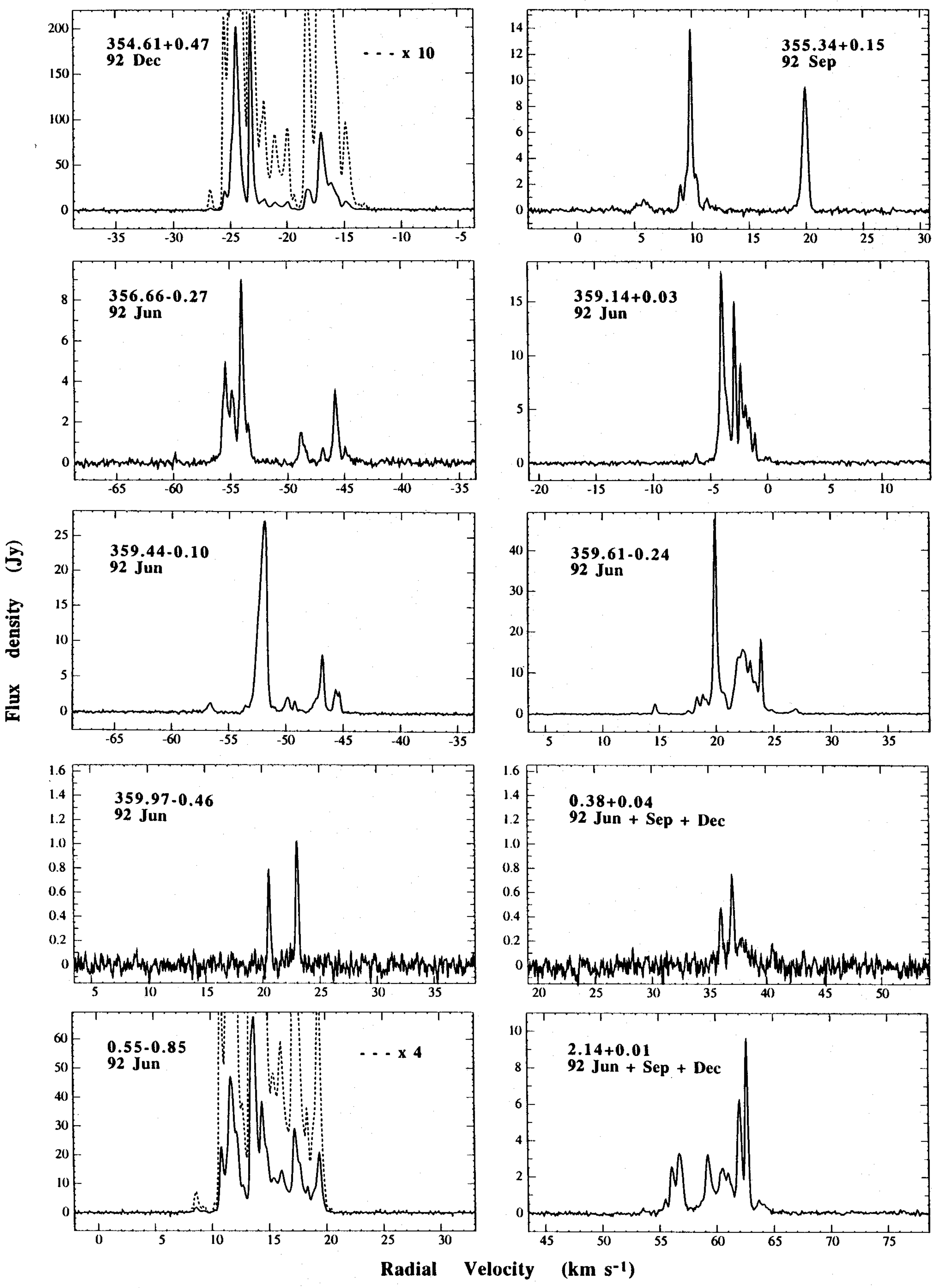

Figure 2 – *continued*

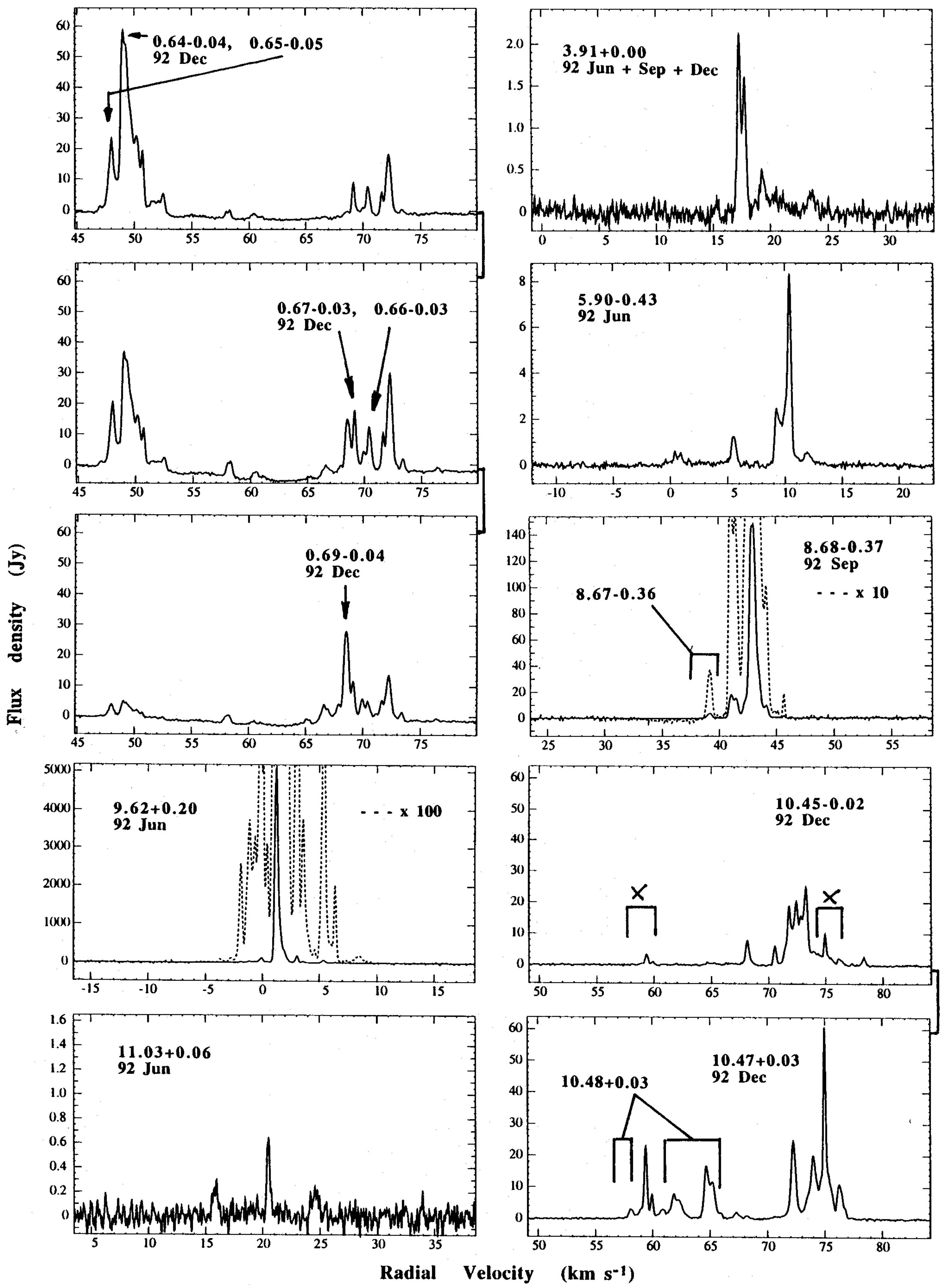

Figure 2 – *continued*

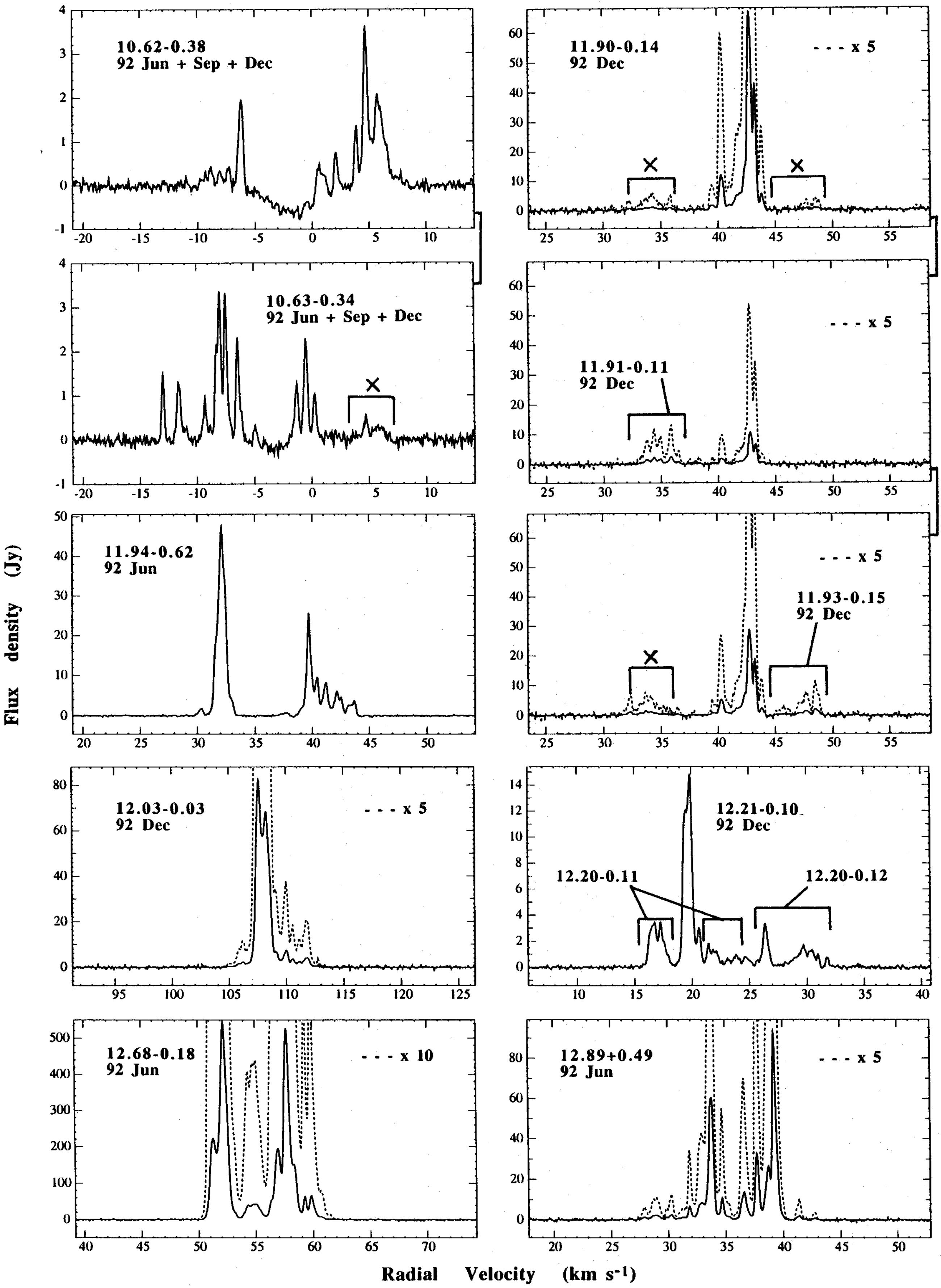

Figure 2 – *continued*

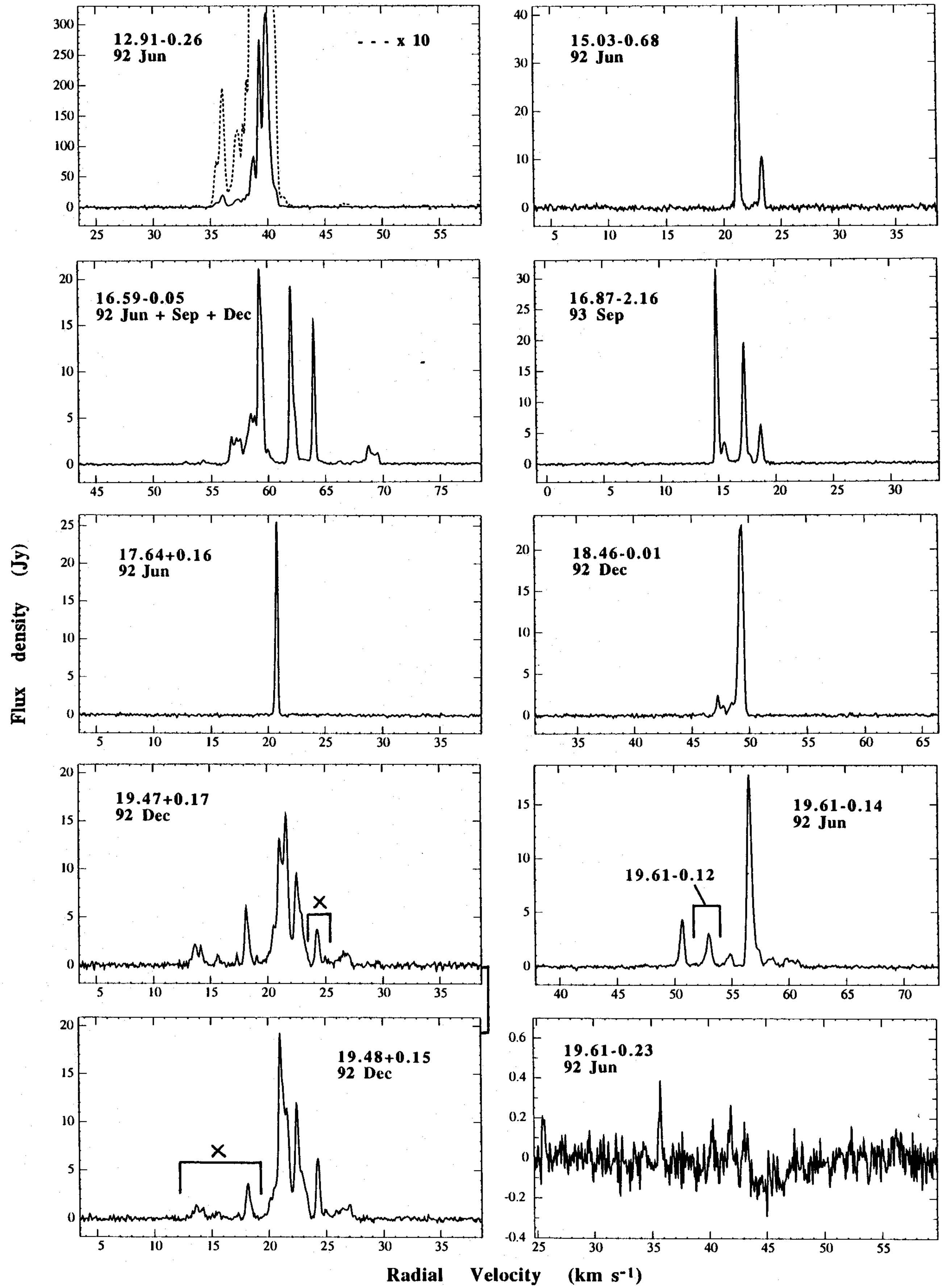

Figure 2 – *continued*

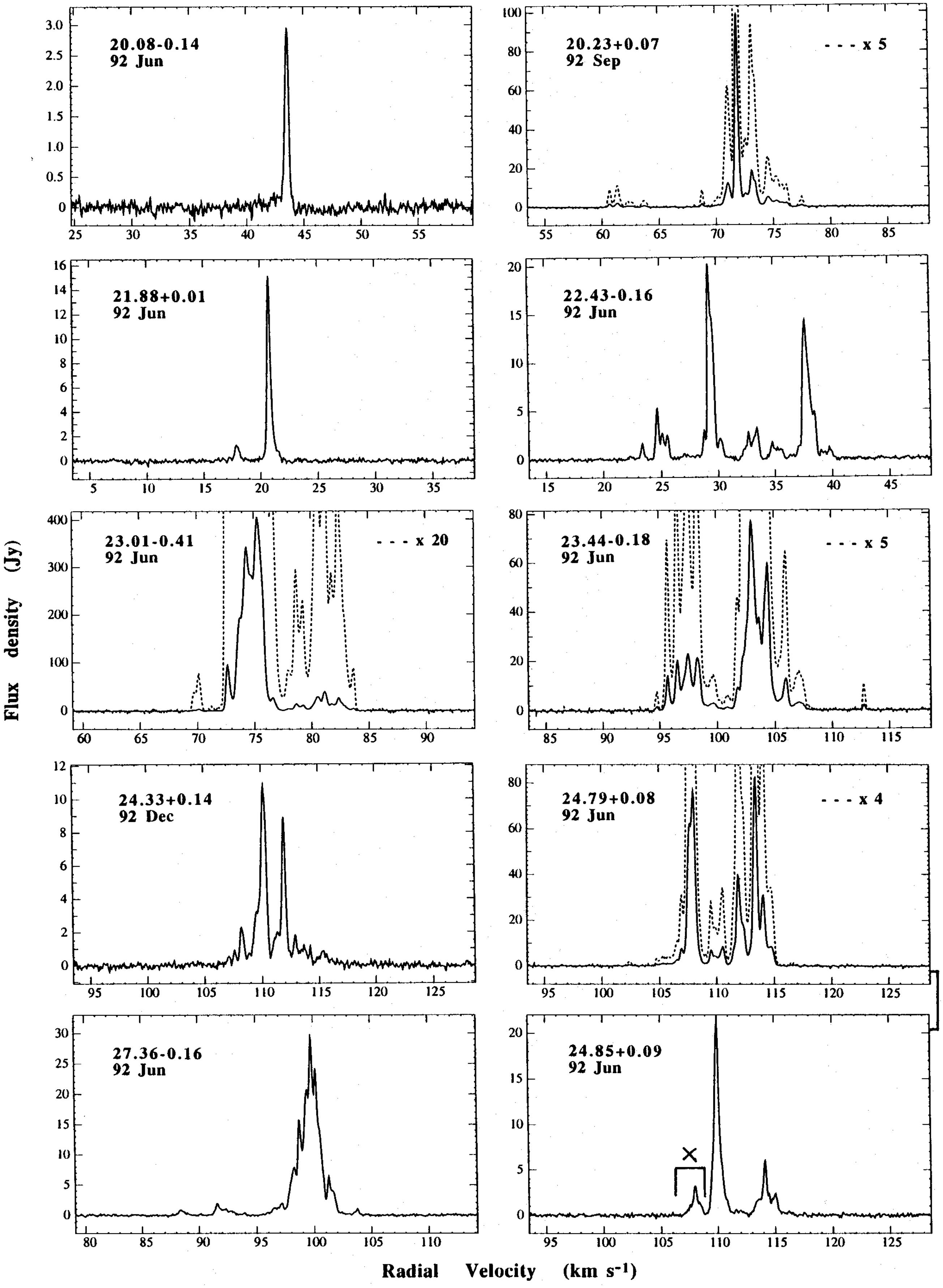

Figure 2 – *continued*

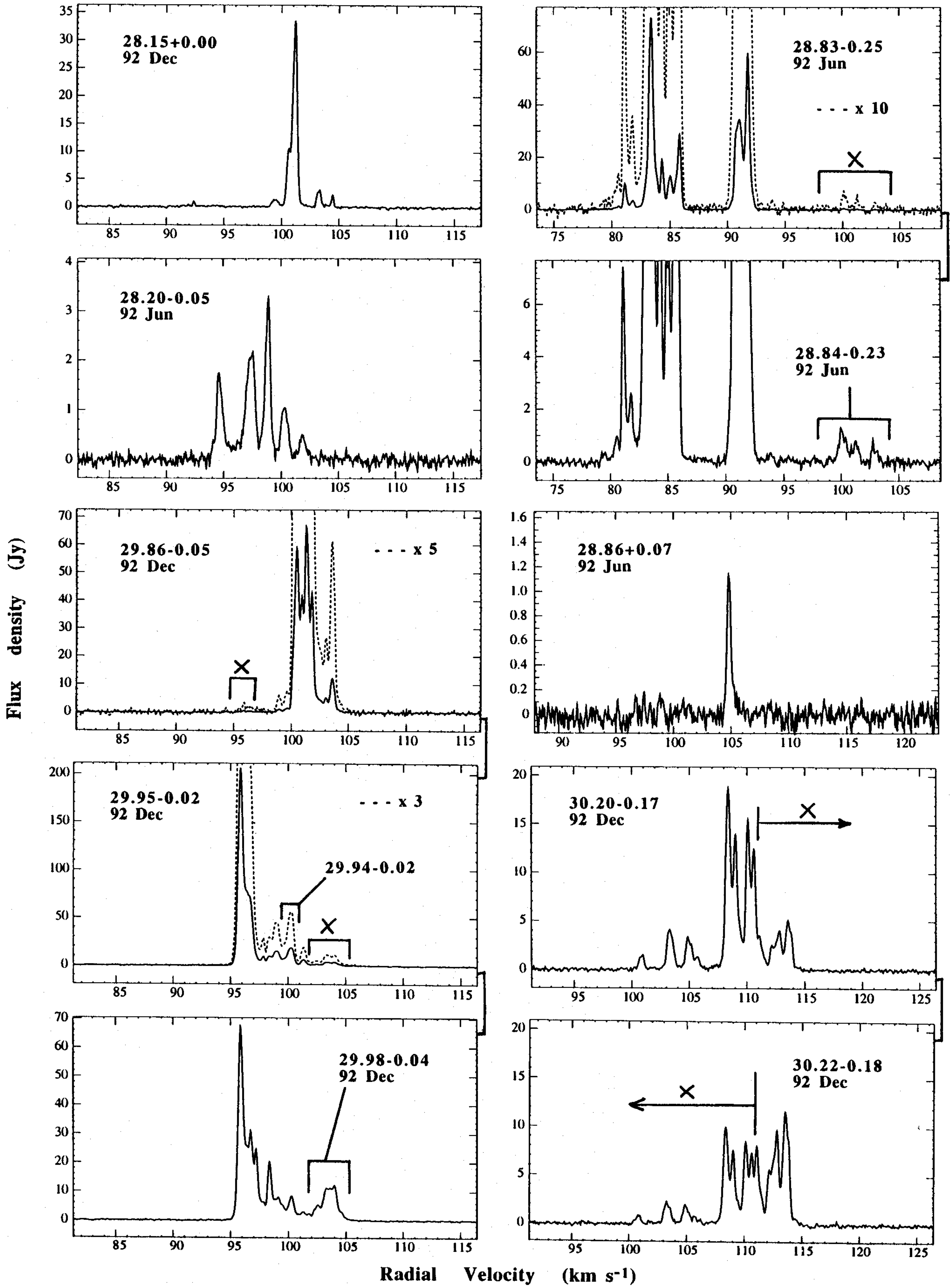

Figure 2 – *continued*

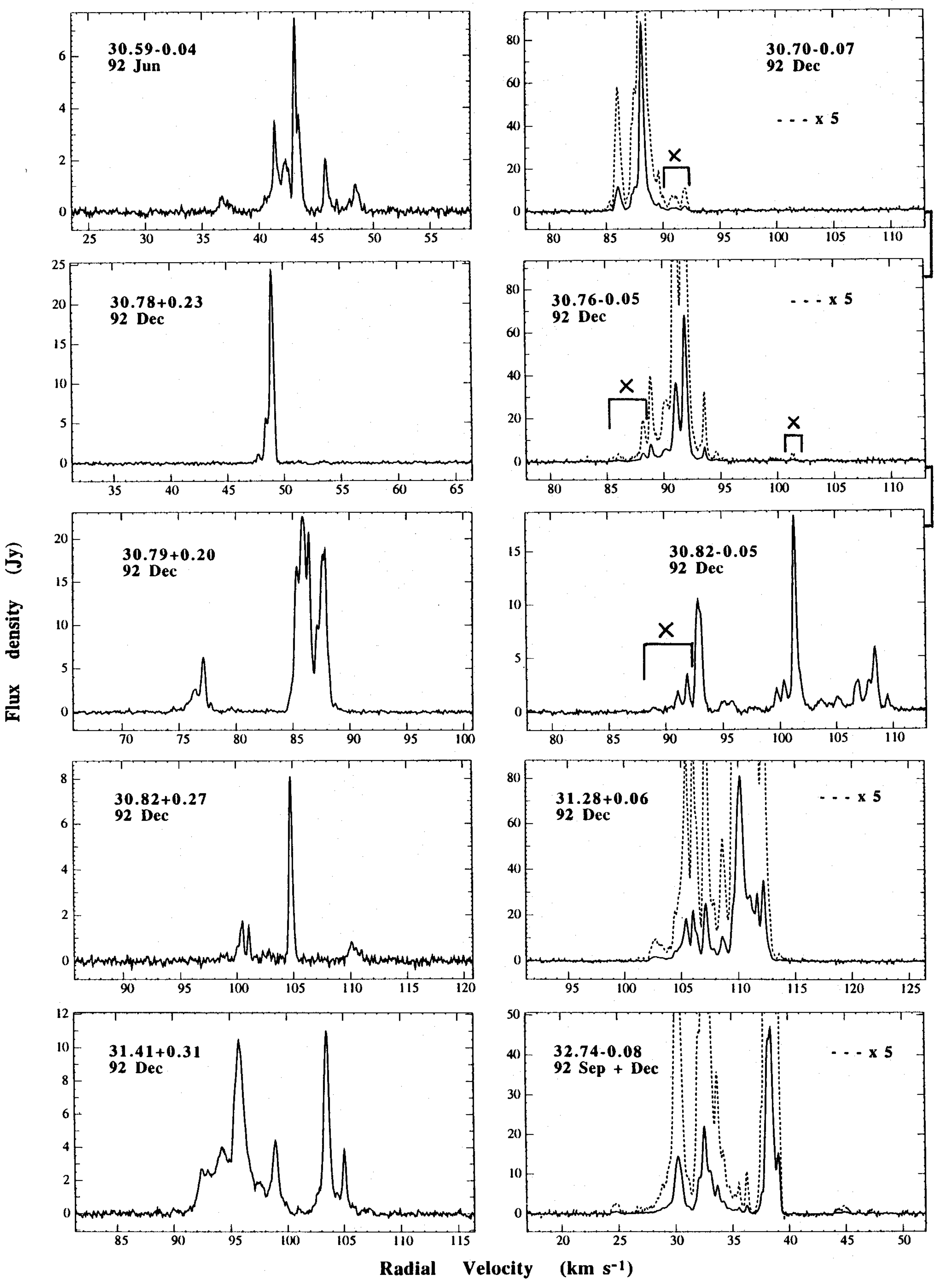

Figure 2 – *continued*

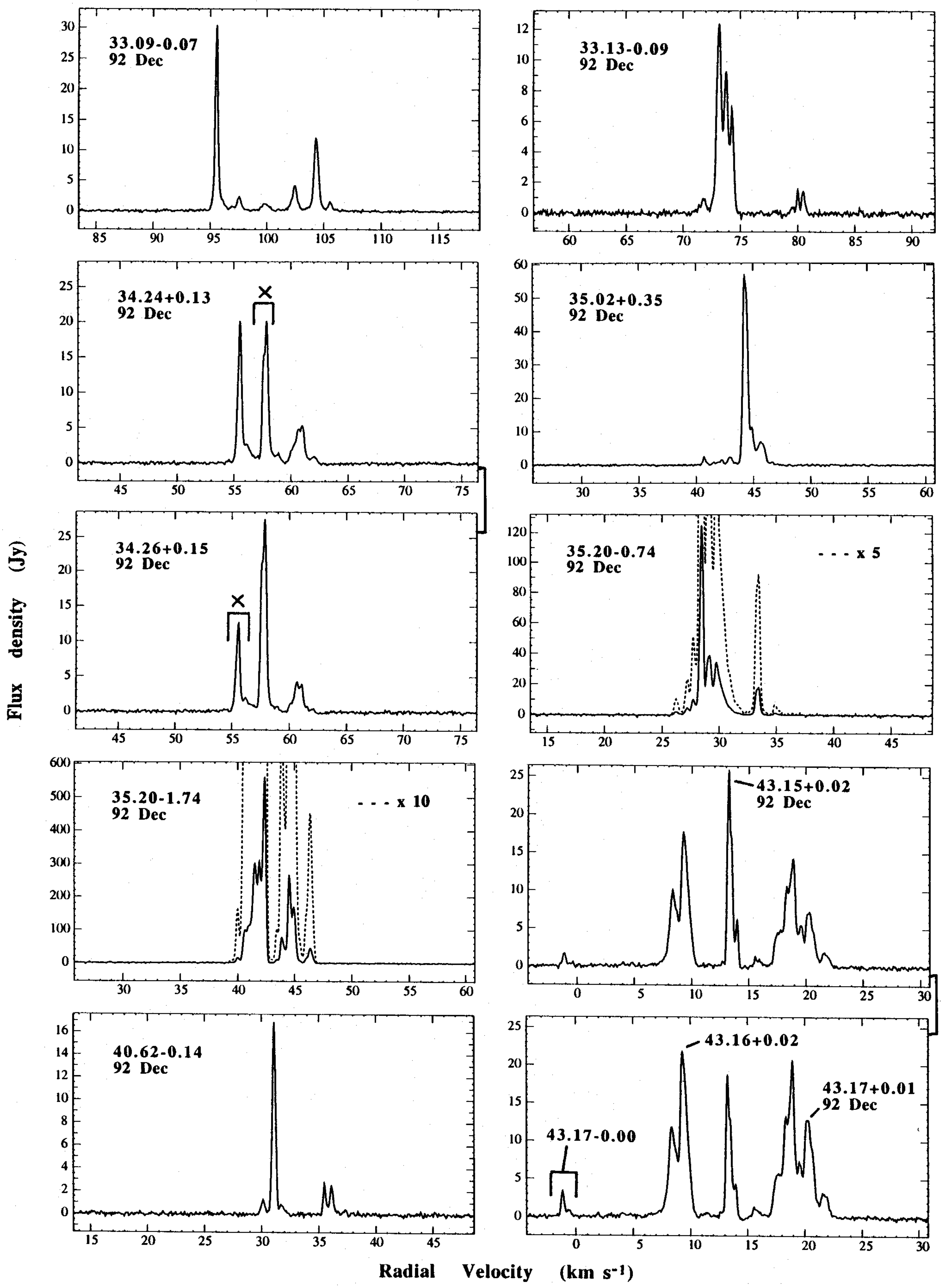

Figure 2 – *continued*

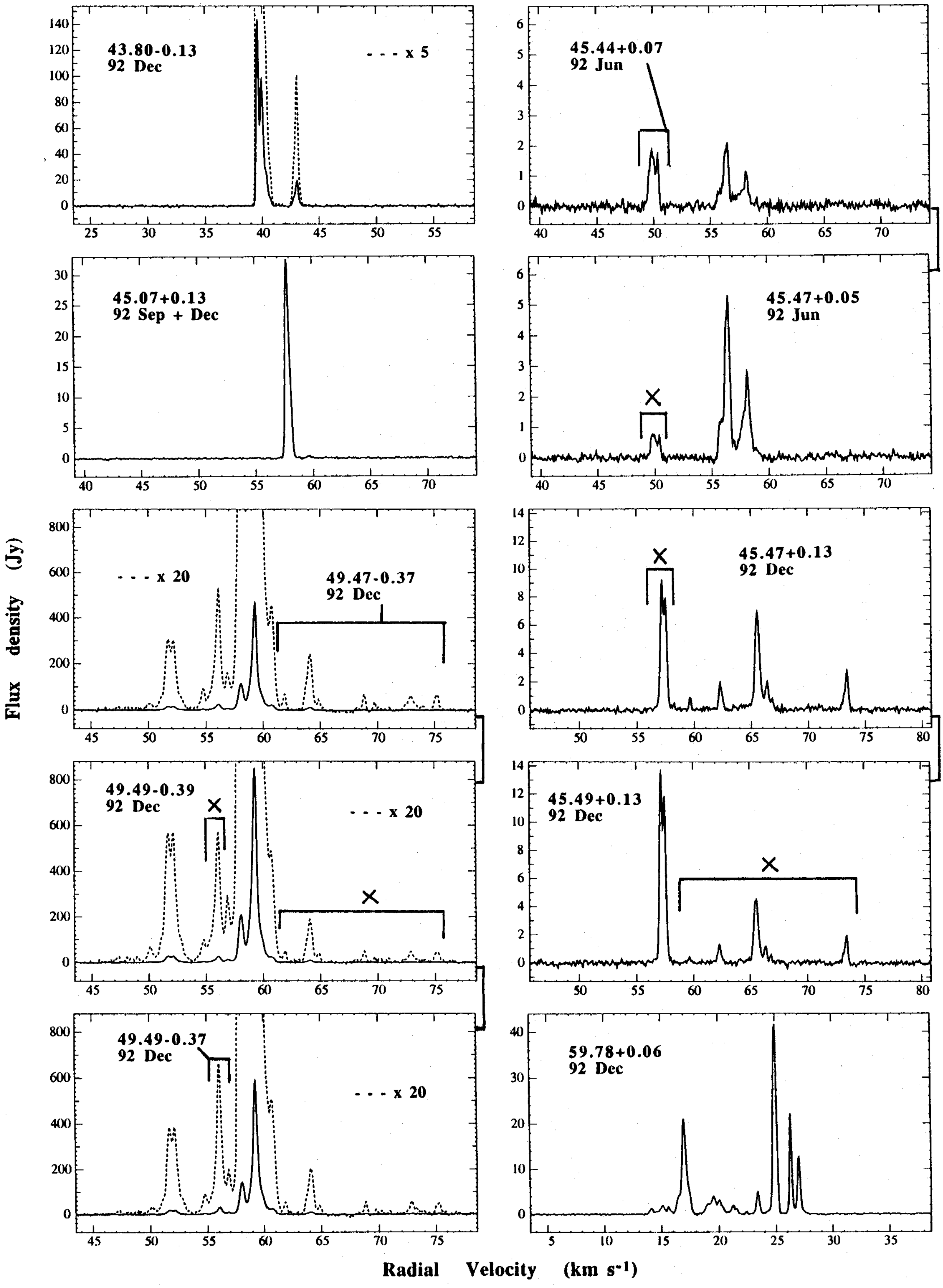

Figure 2 – *continued*

Table 2. OH masers with no detected 6.6-GHz methanol maser.

1665 MHz OH maser (l,b)	RA (1950) (h m s)	Dec (1950) (° ′ ″)	6.6 GHz methanol (Jy)
205.12–14.11	05 44 30.3	+00 20 18	<0.3
240.32+0.07	07 42 45.0	–24 00 22	<0.3
285.26–0.05	10 29 37.2	–57 46 46	<0.2
291.61–0.53	11 12 51.4	–60 59 43	<0.4
297.66–0.98	12 01 33.7	–63 05 11	<0.3
316.76–0.02	14 41 09.4	–59 35 45	<0.3
319.39–0.02	14 59 22.6	–58 25 00	<0.2
324.20+0.12	15 29 01.8	–55 45 51	<0.2
326.77–0.26	15 45 04.1	–54 32 40	<0.3
328.30+0.44	15 50 13.7	–53 02 52	<0.15
333.61–0.22	16 18 27.4	–49 59 03	<0.3
338.68–0.08	16 38 44.2	–46 12 09	<0.15
343.13–0.06	16 54 43.82	–42 47 34.7	<0.3
345.70–0.09	17 03 20.78	–40 47 03.1	<0.4
352.16+0.21	17 21 24.2	–35 22 11	<0.3
5.88–0.39	17 57 26.71	–24 03 59.6	<0.3
6.05–1.34	18 01 49.7	–24 26 56	<0.3
14.17–0.06	18 13 32.3	–16 40 53	<0.4
27.18–0.08	18 38 32.3	–05 12 00	<0.4
31.24–0.11	18 46 09.51	–01 36 39.4	<0.5
35.58–0.03	18 53 51.37	+02 16 29.4	<0.25
43.16–0.03	19 07 58.2	+08 59 58	<0.5
45.12+0.13	19 11 06.2	+10 48 26	<0.2
48.61+0.02	19 18 13.00	+13 49 45.8	<0.2

284.35 − 0.42. The weak emission visible at velocity 10 km s^{-1} was confirmed at three epochs. The OH emission cited in Table 1 lies in the velocity range 4 to 8 km s^{-1}, and was measured in 1992 August and 1993 July.

285.26 − 0.05. From the direction of this OH maser, Gaylard & MacLeod (1993) reported 6.6-GHz methanol emission with a peak of 1.7 Jy at zero velocity in 1992 May/June. At this position, we found no emission in 1992 March and September, with upper limits of 0.2 Jy. Subsequent observations in 1993 December (S. P. Ellingsen, unpublished) indicate that there is a 5.5-Jy methanol maser offset 6 arcmin from the OH maser (and thus not closely related to it) at the position of a weak infrared source, listed as IRAS 10303 − 5746 in the *IRAS* Point Source Catalog (1985), and this presumably accounts for the maser reported by Gaylard & MacLeod.

287.37 + 0.65. A search at this position was prompted by the presence of an OH maser found at an *IRAS* position (P. te Lintel Hekkert & J. M. Chapman, private communication). The methanol and OH masers coincide to within 10 arcsec.

291.28 − 0.71. At the position of the methanol maser there is also an H_2O maser, with velocity −30 km s^{-1}, near the systemic velocity of an associated H II complex. OH spectra show deep absorption but no clear emission. The H_2O maser has a highly blueshifted outflow (velocity −126 km s^{-1}), stronger than the emission from the systemic velocity, but we find no methanol counterpart to this outflow. Note that on the expanded scale of our figure there is clear methanol absorption at velocity −25 km s^{-1}. We find an indication that methanol emission at velocity −27 km s^{-1} is offset by nearly 30 arcsec, but this may be the result of confusion in the baseline due to the absorption. The maser is extremely variable in the 12-GHz methanol transition (Caswell et al. 1993), as well as at 6.6 GHz.

298.22 − 0.33. The OH spectrum in this direction shows only deep absorption (at velocity 30 km s^{-1}), but there is an H_2O maser at RA $12^h07^m19\overset{s}{.}0$, Dec. −62°32′56″. Continuum observations with the ATCA at 5 and 8 GHz (J. M. Chapman, private communication) show a source at RA $12^h07^m19\overset{s}{.}4$, Dec. −62°32′58″ which is probably a compact H II region. Both the H_2O maser and the methanol maser appear to coincide with this compact source.

300.51 − 0.18. OH emission is mainly near velocity 24 km s^{-1}, but is also present near 3 km s^{-1}; hydrogen recombination-line emission is centred at 26 km s^{-1}, and an associated H_2O maser has a large blue-shifted outflow extending to −50 km s^{-1}. The methanol maser may be part of a blue-shifted outflow from a systemic velocity of about 25 km s^{-1}.

305.21 + 0.21, 305.20 + 0.21 and 305.25 + 0.25. The first two of this cluster of three sources are separated by only 22 arcsec (as measured with the ATCA: Norris et al. 1993), and are shown on a single spectrum. The spectrum of the third source has been aligned in velocity with the first spectrum, and shows that emission from the first two sources is detected at the edge of the beam. The first source, with a peak intensity of 480 Jy, is associated with an H II region which is quite distant according to Caswell & Haynes (1978b) – probably at the far kinematic distance of 8.2 kpc rather than the near distance of 3.4 kpc – and is probably one of the most luminous methanol masers (see Section 4.4).

305.36 + 0.15 and 305.37 + 0.19. Both sources are seen in a single spectrum centred on the first source; the true intensity of the second source is 1 Jy. The weak second source has a 12-GHz methanol counterpart with intensity comparable to that of the 6.6-GHz peak. Note that the 6.6-GHz methanol feature of 0.4 Jy at velocity −38.5 km s^{-1} is a sidelobe response to 305.21 + 0.21.

305.80 − 0.24. The feature at velocity −36.5 km s^{-1} has steadily decayed from 0.6 Jy in 1992 June to 0.3 Jy in 1992 December.

306.33 − 0.34. This source is one of our weakest methanol masers. The OH maser is variable and has recently brightened, allowing us to improve its positional measurement from the value given by Caswell & Haynes (1987a), and to confirm that it coincides with the methanol maser.

309.92 + 0.48. This source has also been observed with the ATCA (Norris et al. 1993). With a velocity indicative of a well-defined kinematic distance of 6 kpc (Caswell & Haynes 1987a), this methanol maser, the sixth brightest in our sample, is one of the most luminous (see Section 4.4); a weak feature of 1 Jy at velocity −55 km s^{-1} is clearly seen on the expanded-scale plot and we find it to be variable.

311.64 − 0.38. The intensities of both features decayed simultaneously in 1992 September and 1992 December, and recovered in 1993 September. Note that the large positive velocity indicates a large unambiguous distance outside the solar circle.

312.60 + 0.04. The feature at velocity −68 km s^{-1} has increased from 8 to 16.5 Jy with no change in the other two features.

313.47 + 0.19. Weak emission extends to velocity −16 km s^{-1} (confirmed at two epochs).

316.36 − 0.36 and 316.38 − 0.38. These sources are separated by less than the telescope beamwidth but, fortunately, there is very little overlap in their velocities; as can be seen from the aligned spectra, 316.30 − 0.36 is almost wholly at velocities greater than 1.2 km s^{-1}, and there is weak OH (0.2 Jy) at velocity +5 km s^{-1} seen (1993 July) at this position. 318.38 − 0.38 is almost wholly at velocities less than 1.2 km s^{-1}.

316.41 − 0.31. Weak responses to the previous two sources are seen here, but cause no significant confusion. A catalogued OH maser is present here, distinct from the new one associated with the previous source.

316.81 − 0.06. Many features are strongly variable. Weak features at velocities −41 and −37 km s^{-1} have been confirmed at several epochs.

318.05 + 0.08. Variability is quite pronounced, exceeding 10 per cent in several features.

318.05 − 1.40. A search at this position was prompted by the presence here of an OH maser found at an *IRAS* position (P. te Lintel Hekkert & J. M. Chapman, private communication). The OH maser is weak and its positional uncertainty is ~60 arcsec; to within this accuracy, both methanol and OH masers and the *IRAS* source coincide. Note that the large positive velocity indicates a large unambiguous distance outside the solar circle.

318.95 − 0.20. This strong source has been observed with the ATCA (Norris et al. 1993) and is confined to a single position; we have not detected any variability, but its OH maser counterpart is highly variable. As one of the seven strongest methanol masers, its distance is of special interest. The radio continuum H II region in this general direction (Caswell & Haynes 1987b) has a kinematic distance of 2 or 13.1 kpc; it has no optical counterpart, which favours the larger distance. At this distance, the methanol maser would then have a luminosity of 134 000 Jy kpc^2, possibly the largest known (see Section 4.4).

320.23 − 0.29. This source shows clear variability. The H_2O maser in this direction is noteworthy in displaying a large blueshifted outflow. At first glance, the methanol spectrum suggests that emission at velocity −70 km s^{-1} may be a blueshifted outflow relative to a systemic velocity of −62 km s^{-1}. However, a nearby H II region has recombination-line emission centred at −68 km s^{-1}, OH has its strongest peak at −68 km s^{-1} and the 12-GHz methanol transition is seen with absorption centred at −67 km s^{-1}. Thus the systemic velocity may be near −70 km s^{-1}, and the stronger 6.6-GHz emission at velocity −62 km s^{-1} may be a redshifted outflow.

321.71 + 1.17. This position was selected as a likely compact H II region, detected at 5 GHz with the ATCA at RA $15^h10^m01^s.8$, Dec. −56°13′49″ (an *IRAS* counterpart is present at RA $15^h10^m01^s.2$, Dec. −56°13′42″). The methanol maser is highly variable, showing a rapid rise from 1992 March to June and then a decline; there was also weak emission at velocity −38 km s^{-1} in 1992 March. Weak absorption is also seen. The OH spectrum in this direction shows prominent absorption, with possible embedded weak emission of 0.4 Jy at velocity −41 km s^{-1}.

322.16 + 0.64. Although the 66-GHz maser emission is continuous in the velocity range −66 to −51 km s^{-1}, there is a clear intensity minimum near the middle of this range, suggesting two separate (but overlapping) centres near velocities −54 and −63 km s^{-1} respectively. The corresponding 12-GHz maser (Caswell et al. 1993) shows more clearly that emission arises from two separate velocity ranges, and absorption is also present at one of these, centred at −54 km s^{-1} (seen best on the spectrum shown by Peng & Whiteoak 1992). The latter is also the velocity of 1665-MHz OH absorption (Caswell & Haynes 1987a), formaldehyde absorption, and hydrogen recombination-line emission (Caswell & Haynes 1987b). Thus −54 km s^{-1} is the systemic velocity of a prominent molecular cloud and associated H II emission. Is the methanol emission at velocity −63 km s^{-1} a separate source? Our Parkes positional measurement shows that 6.6-GHz emissions from the two velocity centres are coincident to within 2 arcsec, supporting a view that the maser emission at −63 km s^{-1} is not a separate centre of activity but represents a blueshifted outflow, seen both in methanol at 6.6 and 12 GHz and in OH at 1665 MHz,

323.46 − 0.08. In this direction there is a weak sidelobe response to the following source, 323.74 − 0.26, but its velocity is quite distinct from that of this source.

323.74 − 0.26. This source is one of the three strongest methanol masers, and has been observed with the ATCA (Norris et al. 1993). The many strong features allow a sensitive search for variability, and none is seen over the period 1992 March to December. Note the large velocity spread seen on the expanded-scale spectrum. With a minimum kinematic distance of 3.6 kpc, its luminosity of 37 000 Jy kpc^2 ranks as one of the largest well-determined values (see Section 4.4).

327.29 − 0.58. The feature at velocity −37 km s^{-1} is stable at 2.3 Jy, but several other features are highly variable. The OH emission is also variable and covers a wide velocity range from −70 to −37 km s^{-1}. The absorption seen in both OH and methanol is near the hydrogen recombination-line velocity of −48 km s^{-1}, and this seems likely to be the systemic velocity. The OH shows some redshifted emission, and even more pronounced blueshifted emission relative to this.

328.24 − 0.55 and 328.25 − 0.53. The two blended centres of activity are close enough to cause confusion. To a good approximation, however, each emits over two separated velocity ranges, as indicated in the aligned spectra. Both sources are variable. The stronger features have been studied with the ATCA (Norris et al. 1993). There is an OH maser at both centres (1993 July measurements), with velocity ranges for 328.25 − 0.53 (left-hand circular polarization stronger) of −40 to −35 km s^{-1}, and for 328.24 − 0.55 of −45 to −40 km s^{-1}; the total velocity range is similar to that of methanol, −53 to −30 km s^{-1}, but emission at the extreme velocities is too weak for an accurate positional measurement. The near and far kinematic distances are 3.1 and 13.9 kpc, with a preference for the far value since the radio continuum H II region has no visible counterpart (Caswell & Haynes 1987b); at the far distance, both methanol masers would be amongst the most luminous known (see Section 4.4).

328.81 + 0.63. This source has been observed with the ATCA by Norris et al. (1993). As with the previous pair of sources, the slightly preferred kinematic distance is nearly 14 kpc, and this too would then rank amongst the most luminous methanol masers.

329.03 − 0.21 and 329.03 − 0.20. Both sources are displayed in a single spectrum. The second, weaker, source is offset from the first by 27 arcsec. The velocity ranges overlap between −39.5 and −41 km s^{-1}; the OH counterpart seems primarily associated with the stronger source.

330.88 − 0.37. The weak methanol emission straddles in velocity the prominent absorption. The OH counterpart is one of the strongest masers in the Galaxy, with highest emission at the centre of the velocity range and extending more weakly to velocities −72 and −59 km s^{-1}.

330.95 − 0.18. The systemic velocity of this region is probably near −87 km s^{-1}. The H_2O maser has a redshifted outflow extending from −87 to +50 km s^{-1}, and the OH velocity range is −102 to −80 km s^{-1}, with a suggestion of a weak blueshifted outflow.

331.13 − 0.24. This source is extremely variable. Note that on the spectrum we have identified a weak sidelobe response to 331.28 − 0.19 (whose spectrum is shown beneath, although not aligned in velocity).

331.28 − 0.19. This source has been observed with the ATCA by Norris et al. (1993). It is one of the few methanol masers where the intensity of 12-GHz emission rivals that at 6.6 GHz.

331.34 − 0.35. Note that weak emission extends to velocity −72.5 km s^{-1}. Several features are variable.

331.54 − 0.07. The weak feature at velocity −81 km s^{-1} is clearly variable. There is a complex of OH masers in this general direction, of which at least some, notably a left-hand circularly polarized feature of 15 Jy at velocity −85 km s^{-1}, coincide with the methanol.

331.56 − 0.12. Spectra of this source and the previous one are shown one above the other (but not aligned in velocity) to show the weak response at each position to the other source. There is OH emission at 7 Jy at velocity −107 km s^{-1}, similar to the methanol velocity, which may be related.

332.65 − 0.62 and 332.72 − 0.62. The former (with no apparent OH counterpart) was found while investigating the latter (at the position of an OH maser). The feature at velocity −45.5 km s^{-1} is highly variable.

333.07 − 0.45, 333.12 − 0.43 and 333.13 − 0.44. These sources are close together and shown in two aligned spectra. The associated OH maser seems to be at the position of 333.12 − 0.43. All three methanol masers are variable.

333.16 − 0.10, 333.20 − 0.08 and 333.23 − 0.06. These sources are close together and are shown with three spectra aligned in velocity to clarify which features belong to which source. 333.23 − 0.06 is variable at velocity −81 km s^{-1}. All three sources were discovered by searching at the position of an OH maser whose total velocity extends from −94 to −82 km s^{-1}; the OH is most closely associated with 333.23 − 0.06, but may have features corresponding to the other methanol masers.

335.55 − 0.31. This source was discovered while investigating the following source. A weak OH counterpart, 0.2 Jy at velocity −114 to −111 km s^{-1}, was discovered in 1993 July.

335.59 − 0.29. We have measured an improved position for the OH maser previously listed as 335.61 − 0.31, which now suggests that it coincides with this methanol maser.

335.73 + 0.19 and 335.79 + 0.17. Some blending of the two sources can be seen from the aligned spectra. The stronger source, 335.79 + 0.17, is variable, as is its 12-GHz counterpart (Caswell et al. 1993); it is one of the few methanol masers in which the 12-GHz intensity rivals that at 6.6 GHz.

336.43 − 0.26 and 336.41 − 0.26. The first of these has been observed with the ATCA (Norris et al. 1993) and is slightly variable. The second (and weaker) source, 336.41 − 0.26 at velocity −85.6 km s^{-1}, is clearly distinguishable from the aligned spectra, and is offset by 76 arcsec. There is no OH emission (<0.5 Jy), but absorption is present between −85 and −90 km s^{-1}.

336.83 + 0.02 and 336.86 + 0.01. These two adjacent sources are blended with our beamsize (see the aligned spectra), but neither appears variable. The weak OH emission, with velocity −88 to −78 km s^{-1}, appears to coincide best with 336.83 + 0.02.

336.99 − 0.03. The strong peak at velocity −125.8 km s^{-1} is variable, and apparently decreased monotonically from 38 Jy in 1992 June to 11 Jy in 1993 September.

337.41 − 0.40. The corresponding OH is strongest at the same velocities as the methanol; additional weaker OH emission extending to velocity −56 km s^{-1} appears to be a blueshifted outflow.

337.61 − 0.06 and 337.63 − 0.08. The spectrum shown is nearest the position of 337.61 − 0.06, and the amplitude of 337.63 − 0.08 is seen on the spectrum at only half of its true value.

337.71 − 0.05. This is a strong source with many features, notable for the absence of any detectable variability.

337.92 − 0.46. Corresponding OH emission extends from −32 to −53 km s^{-1}; methanol and hydrogen recombination-line velocities suggest that the stronger blueshifted OH emission with no methanol counterpart may be an outflow.

338.08 + 0.01. Note the especially wide spread in velocity, with weak features extending to −30 km s^{-1}. It is also one of the few methanol masers in which the 12-GHz intensity exceeds that at 6.6 GHz.

338.46 − 0.25. Note the weak feature at velocity −63 km s^{-1}.

338.87 − 0.08 and 338.93 − 0.06. There is very slight confusion of each source at the position of the other, as can be seen from the aligned spectra. 338.93 − 0.06 is variable and increased from a peak of 12 Jy in 1992 December to 17.5 Jy in 1993 September.

339.68 − 1.21. The strongest features are in the velocity range −23 to −21 km s^{-1}, corresponding well with the total OH velocity range of −20 to −27 km s^{-1}; the additional group of methanol features displaced to more negative velocity may represent a blueshifted outflow and contains some variable features.

339.88 − 1.26. This source was also observed with the ATCA (Norris et al. 1993). It is the fourth strongest source detected, and is only slightly variable.

340.05 − 0.24. Weak features are present, extending to velocity −46 km s^{-1}.

340.79 − 0.10. This is the source with widest velocity spread yet discovered; it has been observed with the ATCA (Norris et al. 1993), but more sensitive observations are needed to check whether all features emanate from the same position (as appears to be the case from the Parkes single-dish observations). The largest intensity is in the velocity range −104 to −108 km s^{-1}, and generally diminishes with shift in velocity from this value; the OH emission is similar in this respect. Features near velocity −90 km s^{-1} may be from a redshifted outflow.

341.22 − 0.21. This source has a wide velocity spread with two clearly defined ranges. OH is seen only in the range −42 to −35 km s^{-1}. Features near velocity −48 km s^{-1} may be from blueshifted outflow material. The source is variable at 6.6 GHz and also at 12 GHz (Caswell et al. 1993).

345.00 − 0.22. This source is variable in several features; note that Menten (1991b) reported a peak of 148 Jy, which we now find has increased to 448 Jy.

345.01 + 1.79 and 345.01 + 1.80. Both sources, separated by 20 arcsec, are shown on a single spectrum. The sources have also been observed with the ATCA (Norris et al. 1993). Interestingly, and surely with a significance that we do not yet appreciate, both centres have 12-GHz methanol intensity similar to the 6-GHz intensity (a rare occurrence); thus the unusual conditions are similar at both sites, despite the large spatial offset.

345.41 − 0.95. Note the weak broad absorption. OH also shows emission (at -18 km s^{-1}) and absorption (from -16 to -26 km s^{-1}).

345.50 + 0.35. This source was chosen as representative of our survey, and shown in Fig. 1 to display several aspects of our results. In the top panel of Fig. 1, the 1665-MHz OH maser spectrum (1989 January) shows emission over the velocity range -13 to -25 km s^{-1} with the stronger features confined to a 4 km s^{-1} range near the middle. In OH spectra taken in 1970 (Robinson, Caswell & Goss 1974) and 1981 (Caswell & Haynes 1983a), the same features are readily recognizable. The VLA positional measurements of OH in right-hand circular polarization (Forster & Caswell 1989) show all detected components to be confined to a region 1 arcsec in size.

The 6.6-GHz methanol spectra displayed in Fig. 1 show somewhat more than 10 peaks spread over the same velocity range as the OH, and with peak intensity approximately an order of magnitude larger. Between the two epochs of 1992 June and 1992 September (separated by 3 months), there are differences of up to 15 per cent in intensity in many features, although the peak intensity is similar to the value of 171 Jy measured by Menten (1991b) in 1991 June. Furthermore, over the 18-month period 1992 March to 1993 September, we found variations comparable to those seen in just 3 months, rather than large monotonic increases or decreases; 'flickering' of this type on a time-scale of months is typical of our findings for many sources. The spectrum of the 12-GHz methanol transition shows emission to be much weaker than at 6.6 GHz, as is common. Our recent measurements at 6.6 GHz with the ATCA (unpublished) confirm coincidence with the OH position to within the 1-arcsec spread of the OH positions. Forster & Caswell (1989) found that the H_2O position in this instance is offset by nearly 4 arcsec from the OH and methanol masers, and the upper limit to any continuum emission is 20 mJy.

346.48 + 0.13, 346.52 + 0.12 and 346.52 + 0.08. The three aligned spectra show clearly the features emanating from each position. OH shows a single spike of 2 Jy at velocity -8 km s^{-1}, agreeing with 346.48 + 0.13. Note that Gaylard & McLeod (1993) reported 6 Jy (in 1992 May/June) at a velocity of -20 km s^{-1}, where we detected nothing in 1992 June.

347.63 + 0.15, 347.63 + 0.21 and 347.58 + 0.21. The three aligned spectra reveal the features at each position. VLA data from Forster & Caswell (1989) show OH at only one position, coincident with 347.63 + 0.15.

347.86 + 0.02, 347.82 + 0.02 and 347.90 + 0.05. There is slight confusion of these sources, as can be seen from the aligned spectra. An OH maser is present at the first position.

348.55 − 0.98. This source is exceptionally variable. It is also interesting because it possesses two centres separated by 2 arcsec, as seen at Parkes and confirmed with the ATCA (our unpublished data). It seems as if the northern centre of activity (velocities -22 and -20 km s^{-1}) is not variable, but many of the southern features (velocities -10 to -13 km s^{-1}) are. OH emission covers the velocity range -22 to -10 km s^{-1}, generally matching the methanol quite well; the OH position measured with the VLA (in right-hand circular polarization, at velocity -20 km s^{-1}) is nominally south of the more southerly methanol position.

348.70 − 1.04 and 348.72 − 1.04. These sources are separated by 63 arcsec, and shown on two aligned spectra which reveal severe blending over much of the velocity range. 12-GHz methanol is also present at both positions. Forster & Caswell's (1989) data show that 348.70 − 1.04 coincides with the position of an OH maser and, 348.72 − 1.04 with an H_2O maser.

348.89 − 0.19. This source has a single feature. The OH velocity range is -15 to -10 km s^{-1} and offset from the methanol velocity; the apparent offset from the VLA OH position by 27 arcsec may be significant.

350.01 + 0.43. This source is variable; interestingly, the single, narrow feature seems stable, with the broader complex of several features steadily decreasing.

350.01 − 1.34. From this direction (an OH maser reported by Cohen et al. 1988) we detected weak (1 Jy) emission in 1993 September; we have not yet measured an accurate position and we have therefore not listed the methanol emission in Table 1, nor shown a spectrum.

350.10 + 0.09. The feature at velocity -68 km s^{-1} is offset from the other emission by $+18$ and $+26$ arcsec in right ascension and declination respectively. OH emission is present at velocities -77 to -65 km s^{-1}. Note that VLA measurements of OH and H_2O show them to be separated by 19 arcsec, and apparently offset by more than 30 arcsec from the methanol. In the *IRAS* Point Source Catalog (1985), confusion limits the listing to a single source, at a nominal position (RA $17^h16^m02\overset{s}{.}6$, Dec. $-37°07'51''$) closest to our main methanol source.

351.16 + 0.70. Note that both methanol and OH show absorption, with the methanol maser at the positive-velocity edge and the OH maser at the negative side (velocity range -16 to -3 km s^{-1}).

351.42 + 0.64 [NGC 6334A (f)] and 351.44 + 0.66. The two centres are separated by 107 arcsec and have been mapped with the ATCA (Norris et al. 1993). Both have 12-GHz counterparts. 351.42 + 0.64 is the second strongest methanol maser in our sample; it has a velocity range of -12 to -7 km s^{-1}, and coincides with both an OH counterpart and a strong H II region, NGC 6334A(f). The OH emission lies chiefly in the velocity range -13 to 16 km s^{-1}, the same as the methanol, but the H II region has hydrogen recombination-line emission centred at velocity -4 km s^{-1} (Forster et al. 1990), similar to the velocity of maximum OH absorption. The weaker methanol maser, 351.44 + 0.66, has a large velocity range, -14 to $+1$ km s^{-1}, and overlaps in the middle with the stronger one, as can be seen from the two aligned spectra; it shows clear intensity variability in the velocity range that is not confused. Its peak intensity is in the confused velocity range, and is much larger than the 16-Jy value tabulated for velocity -3 km s^{-1}. The ratio of 12- to 6.6-GHz peak flux density is thus not unusually large, contrary to the indications of Table 1 taken at face value.

351.77 − 0.54. This source has also been observed with the ATCA by Norris et al. (1993). It is highly variable at velocity $+1.2$ km s^{-1}. Corresponding OH maser emission spanning velocities -28 to $+8$ km s^{-1} has the largest peak intensity yet known, 1000 Jy. The systemic velocity is very likely to be near -3 km s^{-1}, and so the offset OH velocities (-36 to $+9$ km s^{-1}) constitute a predominantly blueshifted outflow. A weak continuum source at RA $17^h23^m20\overset{s}{.}5$, Dec. $-36°06'45\overset{''}{.}8$, with flux density ~3 mJy at 5 GHz, was reported by Fix et al. (1982) and appears to be an ultracompact H II region associated with the masers.

352.11 + 0.17 and 352.08 + 0.16. These sources were discovered in 1992 December while searching at the position of OH 352.16 + 0.21; however, the new methanol sources are offset in both position and velocity from the OH maser, and are not closely related. The spectrum displayed is at the position of 352.11 + 0.17, and so the other source is seen with reduced amplitude.

352.52 − 0.16. There is an indication that the 1-Jy emission at velocity -53 km s^{-1} may be offset to a larger right ascension and north of the main position.

354.61 + 0.47. This source is especially variable at velocity -23 km s^{-1}; the 12-GHz counterpart is also variable (Caswell et al. 1993).

355.34 + 0.15. In Table 1 we have given the position of the emission at velocity 20 km s^{-1} (velocity range 2 km s^{-1}) which has an OH counterpart in both position and velocity (Forster & Caswell 1989). The methanol near velocity 10 km s^{-1} is offset 10 arcsec north, is slightly stronger, and covers the velocity range 5 to 12 km s^{-1}.

359.61 − 0.24. This source is highly variable (e.g. at velocity $+22.5$ km s^{-1}).

0.55 − 0.85. Both methanol and OH show many overlapping features between $+8$ and $+20$ km s^{-1}; variability is present in both the 6.6-GHz and the 12-GHz methanol (Caswell et al. 1993).

Sgr B2. This well-known molecular complex contains several centres of methanol maser activity spread over nearly 3 arcmin. There is blending of spectra when observed with relatively low spatial resolution, but we can recognize at least five centres distinguishable at a range of radial velocities: as listed in Table 1 these are 0.64 − 0.04, 0.65 − 0.05, 0.66 − 0.03, 0.67 − 0.03 and 0.69 − 0.04. These features, and also broad absorption, are clearly seen on the three spectra that we show. On the spectra, we have labelled for each centre one of the less-confused features since, at many velocities, there is a blend from different positions. Sgr B2 also possesses many OH centres of activity, of which some, but not all, possibly correspond with methanol masers. For methanol observations of higher spatial resolution (but lower spectral resolution), a study based on ATCA data is in progress (S. E. Houghton & J. B. Whiteoak, private communication). No intensity variations are obvious from our data, but, in view of the confusion, we are not very sensitive to the recognition of variations.

The first two centres lie to the south of the region, where there is no reported OH counterpart or strong continuum emission; they appear to be responsible for all the emission seen in the velocity range below 55 km s^{-1}. 0.64 − 0.04 is the strongest feature, and is confined to the velocity range 48.5 to 53 km s^{-1}. It appears to coincide with the H_2CO maser commonly designated 'e' (Gardner et al. 1986). Despite overlap at some velocities with the previous centre, the region 0.65 − 0.05 is clearly separate and corresponds with the site of 12-GHz methanol emission. 0.66 − 0.03 and 0.67 − 0.03 lie well to the north, in the general vicinity of the continuum peak and some OH masers (see Benson & Johnston 1984; Gaume & Mutel 1987). 0.67 − 0.03 has features spanning the wide velocity range $+57$ to $+77$ km s^{-1}. 0.69 − 0.04 is still further north, and isolated from any previously reported OH masers or continuum emission.

5.90 − 0.43. This methanol maser, although discovered by searching at the position of the OH maser 5.88 − 0.39 (Forster & Caswell 1989), is distinctly offset from it, with the methanol at larger right ascension by 10 s (= 150 arcsec). The methanol maser is highly variable. It is likely to be part of the same complex and thus at the same distance as 5.88 − 0.39 (2.6 kpc according to Forster & Caswell, but perhaps 4 kpc according to Zijlstra et al. 1990). The region of both the methanol and OH masers has been mapped in the continuum at 1.4 GHz by Zijlstra et al., and, whereas the OH has a compact continuum counterpart, a possible counterpart to the methanol is more diffuse and has not been mapped at higher frequencies. Note that the OH maser has a corresponding class I methanol maser (on the 44.069 43-GHz transition) according to Bachiller et al. (1990).

8.67 − 0.36 and 8.68 − 0.37. These sources are separated by 60 arcsec, and shown on a single spectrum. The first is the weaker and coincides with an OH maser (Forster & Caswell 1989). A compact (3 arcsec) H II region, of flux density 600 mJy, is also present (Wood & Churchwell 1989). The second 6.6-GHz methanol maser has a 12-GHz methanol counterpart, and Forster & Caswell's data show a corresponding second OH maser (unpublished) at RA $18^h03^m23\overset{s}{.}23$, Dec. $-21°37'31\overset{''}{.}1$, with velocity range 35 to 45 km s^{-1}, and peak intensity 3.5 Jy at 40 km s^{-1}.

9.62 + 0.20. Most of the methanol emission is from the position given in Table 1, but near velocity $+5.5$ km s^{-1} there is emission with intensity 72 Jy offset $+4$ and -12 arcsec in right ascension and declination respectively. The ATCA methanol data (Norris et al. 1993) confirm the positions of the two methanol centres, but we note that a third position claimed by Norris et al. was found on reanalysis to be unreliable. The VLA data of Forster & Caswell (1989) show two centres of OH maser emission, coincident with the two methanol centres. However, the OH maser emission is present in two velocity ranges, -2 to 8 and 20 to 24 km s^{-1}; the latter appears to be due to a redshifted outflow and has no methanol counterpart.

In the continuum, Garay et al. (1993a) presented maps at 15 GHz showing a 19-mJy H II region at the position of the main methanol emission and a 110-mJy source at the offset position of the weaker emission. 9.62 + 0.20 has the highest flux density of all 6.6-GHz methanol masers and, at about 2 kpc (if we adopt the distance suggested by Forster & Caswell), its luminosity would be 20 000 Jy kpc^2. Garay et al. (1993a) suggested that the complex is at 16.1 kpc and it would then have a peak luminosity of 1 000 000 Jy kpc^2, larger than W51 by a factor of 30. The linear separation of the offset source would also then be large. As a possible resolution of the arguments for wildly discrepant distances, we suggest that the source might lie at a distance of about 6 kpc, in the '3-kpc arm' as is favoured by Caswell et al. (1975) for the nearby source 10.63 − 0.38. See Section 4.4 for further discussion.

10.47 + 0.03, 10.48 + 0.03 and 10.45 − 0.02. These sources are quite close, and are displayed on two spectra. We detect no variability in either 10.48 + 0.03 or 10.45 − 0.02. The strongest feature in 10.47 + 0.03, at + 75 km s^{-1}, is variable, with our measurements ranging from 47 to 100 Jy; Menten (1991b), who listed the source as W31(1), reported a peak value of 823 Jy on 1991 June 2, while other features have intensities similar to our values (Menten, private communication). Thus the feature decreased by an order of magnitude in nine months and is one of the most variable strong features discovered. Near 10.47 + 0.03 there is a compact H II region (Wood & Churchwell 1989) and a very bright ammonia core (Garay, Rodriguez & Moran 1993b); another ammonia core is close to 10.48 + 0.03.

10.62 − 0.38 and 10.63 − 0.34. There is very little confusion between the sources, as can be seen from the two aligned spectra. The maser emission from both positions is embedded in an extensive absorbing cloud. Within the relative positional uncertainty of 10 arcsec, 10.62 − 0.38 agrees satisfactorily with the VLA OH position of Forster & Caswell (1989), and a 3.8-Jy compact H II region studied by Wood & Churchwell (1989).

11.03 + 0.06. The strongest feature is at this position, but the weak 0.2-Jy emission at velocity 24.5 km s^{-1} probably arises from the nearby source 10.96 + 0.01 reported by Schutte et al. (1993); its true peak is 20 Jy, and we detect it in a weak sidelobe of our beam (offset 333 arcsec).

11.90 − 0.14, 11.93 − 0.15 and 11.92 − 0.11. The three spectra of these sources are aligned in velocity to indicate which features arise from which position. It can thus be seen that the feature at + 32.1 km s^{-1} seems to belong to 11.93 − 0.15, most of whose other features lie in the range + 45 to + 49 km s^{-1}.

11.94 − 0.62. Wood & Churchwell (1989) reported an ultracompact (4 arcsec) H II region of 1.4 Jy at RA $18^h11^m04\overset{s}{.}5$, Dec. − 18° 54′ 19″, with recombination-line emission at velocity + 42 km s^{-1}. OH absorption extends from 34 to 40 km s^{-1}. This source is a rare variety, in which 44-GHz methanol emission (Bachiller et al. 1990) occurs in the same direction as a 6.6-GHz methanol maser.

12.21 − 0.10, 12.20 − 0.12 and 12.20 − 0.11. We use a single spectrum to show emission from all three positions. There is some indication that the emission near velocity 30 km s^{-1} is 20 arcsec south of the main feature of 12.20 − 0.12 (at velocity 26 km s^{-1}). Note that Forster & Caswell's (1989) VLA position of H_2O emission, at RA $18^h03^m43\overset{s}{.}81$, Dec. − 18° 25′ 05″.7, approximately coincides with 12.21 − 0.10, as does a compact H II region (Wood & Churchwell 1989).

12.89 + 0.49. OH measurements in 1993 July show 3.8 Jy in the velocity range 31 to 36 km s^{-1}.

15.03 − 0.68 (part of M17). OH maser emission is present in the velocity range 20 to 25 km s^{-1}, and is embedded in absorption. Wood & Churchwell (1989) reported a 1-arcsec-diameter, 0.16-Jy ultracompact H II region at RA $18^h17^m31\overset{s}{.}7$, Dec. − 16° 12′ 58″.

16.59 − 0.05. This source is slightly variable, with the emission at velocity 59 km s^{-1} steadily decreasing. Note that there are weak features at velocities 52.8 and 54.2 km s^{-1}.

16.87 − 2.16. This source is a new maser found in 1993 September towards an *IRAS*/OH complex (MacLeod 1991).

17.64 + 0.16. Note that the emission is a single narrow feature. The appearance of the OH spectrum (our unpublished data) suggests that the systemic velocity is 21 km s^{-1}, and that there is a redshifted OH outflow at velocity 40 km s^{-1}.

19.48 + 0.15 and 19.47 + 0.17. On the two aligned spectra it can be seen that the sources are blended at some velocities, so that variability is difficult to assess. We draw attention to the major features that clearly belong to the other source, but there is blending in the middle velocity range.

19.61 − 0.14 and 19.61 − 0.12. A single spectrum is adequate to show the main source and the weaker offset source.

19.61 − 0.23. Note also the absorption. The maser is one of our weaker sources with less accurate positional measurement; an apparent 39-arcsec offset from the position of OH as measured with the VLA (Forster & Caswell 1989) may not be significant. Wood & Churchwell (1989) reported a source with intensity 21 mJy and diameter 1 arcsec, at a position very near the OH.

20.08 − 0.14. Wood & Churchwell (1989) reported a compact H II region with intensity 91 mJy and diameter 1 arcsec, at RA $18^h15^m23\overset{s}{.}0$, Dec. − 11° 30′ 44.4″, which coincides with the OH and probably the methanol also.

20.23 + 0.07. The appearance of the spectrum suggests that the emission near velocity 60 km s^{-1} is from blueshifted outflow material.

22.43 − 0.16. The large number of features over a wide velocity range are remarkably stable, with only the feature at velocity 24.5 km s^{-1} showing any perceptible variation (a temporary increase in 1992 September).

23.01 − 0.41. Although only the 15th brightest in our sample, it is probably at the large distance of 12.8 kpc (compare the OH maser as noted by Caswell & Haynes 1983b) and thus one of the most luminous methanol masers.

23.44 − 0.18. This source has many variable features and is also strongly variable at 12 GHz (Caswell et al. 1993). An OH maser appears to coincide, but the nearest continuum source (10 mJy) reported by Wood & Churchwell (1989) is significantly offset.

24.33 + 0.14. The methanol was detected while searching towards a 1667-MHz OH maser with velocity 62 to 87 km s^{-1}, but this is clearly unrelated in view of the offsets in both velocity and position. At 115 km s^{-1}, however, we recently discovered a weak new 1665-MHz maser and this is likely to be associated with the methanol. The methanol maser has highly variable features. It is one of the few methanol masers in which the 12-GHz peak intensity exceeds that at 6.6 GHz.

24.79 + 0.08 and 24.85 + 0.09. As can be seen from the two aligned spectra, there is confusion at some velocities between these two close sources.

27.36 − 0.16. Corresponding OH emission is confined to velocities 79 to 87 km s^{-1}, but OH absorption extends to 97 km s^{-1} and better matches the methanol velocity range.

28.20 − 0.05 and 28.15 + 0.00. 28.20 − 0.05 is weaker and coincides with an OH maser. 28.15 + 0.00 was found while positioning the other source, but the aligned spectra show no significant confusion between the sources. 28.15 + 0.00 has a weak feature at 92.5 km s^{-1}.

28.83 − 0.25 and 28.84 − 0.23. 28.83 − 0.25, with velocity range 79 to 94 km s^{-1}, has an OH counterpart over the same velocity range. 28.84 − 0.23 is weak and is offset not only in velocity but also in position (by 84 arcsec).

29.86 − 0.05. Note that the 1-Jy emission at velocity 96 km s^{-1} is a sidelobe from the 200-Jy peak of 29.95 − 0.02, offset 6 arcmin (see the following spectrum).

29.95 − 0.02, 29.94 − 0.02 and 29.98 − 0.04. Our single-dish observations show considerable blending of features at different positions but overlapping velocities (in the range 95 to 105 km s^{-1}). The emission is variable, but the variability is difficult to assess quantitatively because of the spatial complexity. We show two spectra and attempt to distinguish only the three most obvious centres.

29.95 − 0.02, the strongest source, has a 12-GHz counterpart and was originally thought to have no OH maser. However, we detected an OH maser here in 1993 October with an intensity of nearly 1 Jy and, clearly, more intense than when searched unsuccessfully several years ago. The masers appear to coincide with continuum emission of 2.6 Jy extending over 5 arcsec (Wood & Churchwell 1989). The other two maser sites are significantly offset but confused slightly in our single-dish spectra.

30.20 − 0.17 and 30.22 − 0.18. To a good approximation, the sources as seen in the two aligned spectra emit over different velocity ranges and are not confused. A corresponding OH maser with velocity range 101 to 109 km s^{-1} agrees in position and velocity with 30.20 − 0.17; the methanol maser 30.20 − 0.17 has shown no variability to date, whereas 30.22 − 0.18 shows clear variability.

30.70 − 0.07, 30.76 − 0.05 and 30.82 − 0.05. Note from the three aligned spectra that 30.76 − 0.05 confuses, and is confused by, the two others. There are two OH masers in this region: OH 30.70 − 0.07 with a velocity range of 86 to 105 km s^{-1}; and OH 30.79 − 0.06 with position (poor) between the other two methanol masers but with a velocity range of 103 to 113 km s^{-1}, suggesting that it corresponds to 30.82 − 0.05.

30.78 + 0.23. This source was discovered while searching near 30.82 + 0.27; it has no detectable OH counterpart.

30.79 + 0.20. This source was discovered while searching near 30.82 + 0.27; an OH counterpart was discovered in 1993 October.

30.82 + 0.27. The OH counterpart's velocity range extends from 100 to 105 km s^{-1}.

31.28 + 0.06. This source is one of the few methanol masers in which the peak flux density on the 12.GHz transition exceeds that on the 6.6-GHz transition.

31.40 − 0.26. From this direction (an OH maser reported by Cohen et al. 1988) we detected weak (0.4 Jy) emission in 1993 September. We have not yet measured an accurate position and we have therefore not listed the methanol emission in Table 1, nor shown a spectrum.

31.41 + 0.31. The corresponding continuum source has a diffuse (6 arcsec) halo and a 5-mJy peak at RA $18^h44^m59\overset{s}{.}2$, Dec. −01°16′08″ (Wood & Churchwell 1989).

33.09 − 0.07. This source was discovered while investigating 33.13 − 0.09; there is no detectable OH maser here.

34.24 + 0.13 and 34.26 + 0.15. The aligned spectra indicate confusion between the sources at some velocities. 34.24 + 0.13 is the slightly weaker methanol maser and has no known OH counterpart. 34.26 + 0.15 corresponds with a strong OH maser, which in turn coincides with a 43-mJy H II region with diameter less than 1 arcsec (Wood & Churchwell 1989).

35.20 − 0.74. The OH maser counterpart has been accurately positioned (Forster & Caswell 1989) and coincides with a continuum source of 1.9 mJy at 15 GHz (Heaton & Little 1988) which is an ultracompact H II region, optically thick at 5 GHz. Extensive studies of other molecules in the region reveal large-scale outflows (Heaton & Little 1988; Brebner et al. 1987).

35.20 − 1.74. This source is variable at 6.6 GHz and also at 12 GHz (Caswell et al. 1993). In the continuum, Wood & Churchwell (1989) have studied a strong compact nearby H II region, but its coordinates, RA $18^h59^m14\overset{s}{.}1$, Dec. 01°09′02″, are offset from the OH maser and probably the methanol maser as well.

40.62 − 0.14. The feature at velocity +36 km s^{-1} is offset in right ascension and declination by +15 and +7 arcsec respectively, and is variable, with intensity decreasing in 1992.

W49N. This well-known molecular complex contains a number of H II regions and OH masers as tabulated by Gaume & Mutel (1987). From our single-dish measurements, we are able to distinguish at least four methanol centres of activity, and these are shown on two spectra. There is no marked variability, but it is difficult to set limits due to blending.

43.15 + 0.02 is the 23-Jy methanol peak at velocity +13 km s^{-1}. A 1665-MHz OH maser has a peak of 5.6 Jy at velocity 13.8 km s^{-1}, RA $19^h07^m47\overset{s}{.}4$, Dec. 09°00′23″. 43.16 + 0.02 includes emission at velocities +8.4, +9.3 (23 Jy), +18.3 and +19.6 km s^{-1}; a 1665-MHz OH maser, with peak intensity of 99 Jy at velocity 17 km s^{-1}, is at RA $19^h07^m49\overset{s}{.}6$, Dec. 09°01′16″ and may correspond with the methanol site. 43.17 + 0.01 has velocity +20.3 km s^{-1} (10 Jy); it may be the counterpart of a 1665-MHz OH maser with a peak of 9 Jy at velocity 16 km s^{-1}, and RA $19^h07^m51\overset{s}{.}0$, Dec. 09°00′57″. For velocities near +19 km s^{-1}, there appears to be a blend of emission from 43.16 + 0.02 and 43.17 + 0.01, and indeed the Gaume & Mutel OH observations show several other centres of activity. 43.17 − 0.00 is a weak source with velocity −1 km s^{-1} which is clearly distinct from the other features.

45.07 + 0.13. The weak feature at velocity 59.6 km s^{-1} is real. The methanol position agrees with that of both OH and H_2O masers and a strong, very compact (790 mJy and 1-arcsec diameter) H II region (Forster & Caswell 1989; see also Wood & Churchwell 1989).

45.47 + 0.05 and 45.44 + 0.07. Although close together, the two sources are not confused, as can be seen from the aligned spectra. Both methanol masers were discovered while searching at the position of OH 45.47 + 0.05 (Forster & Caswell 1989), but the methanol positional errors make it uncertain whether either coincides precisely with the OH and H_2O masers. Furthermore, the entire velocity range of the OH emission, +62 to +70 km s^{-1}, is at higher velocity than any of the methanol emission, so the association must be regarded as dubious. Wood & Churchwell (1989) reported a compact H II region (80 mJy, 2-arcsec diameter) which does coincide with the OH and H_2O masers.

45.47 + 0.13 and 45.49 + 0.13. These closely spaced methanol masers are quite distinct (see aligned spectra), and 45.47 + 0.13 is the counterpart of the OH maser that prompted the search.

W51. This well-known complex of H II regions and molecular clouds contains several methanol masers. We distinguish three sites that can be satisfactorily differentiated by single-dish observations, and show three aligned spectra. No marked variability was seen, but small variations would be difficult to discern because of the blending of features.

49.47 − 0.37 has a major peak of 12 Jy at velocity +64.1 km s^{-1}, but its range extends at least from +75 km s^{-1} down to 61.8 km s^{-1}. Gaume & Mutel (1987) found a nearby 1665-MHz OH maser with 0.6-Jy peak and total velocity range +74 to +66 km s^{-1}.

49.49 − 0.39 refers to the strongest emission, nearly 900 Jy, which probably coincides with the OH position of Forster & Caswell (1989). The precise velocity range of methanol is uncertain because of blending, but extends from 60 km s^{-1} down to at least 51 km s^{-1}. Note that the OH velocity range of emission is about 63 to 50 km s^{-1}, but absorption extends over a larger range, from 50 to 70 km s^{-1}; some OH is from a site 5 arcsec north where there is also H_2O (quoted as the reference H_2O position by Forster & Caswell; see also Gaume & Mutel 1987). This is the fifth strongest methanol maser in our sample, but is the most luminous of the five since it is at a significantly larger (well-determined) distance of 7.7 kpc (see Section 4.4).

49.49 − 0.37 probably coincides with the 12-GHz methanol maser (Caswell et al. 1993). Because of confusion, only the single bright feature can be confidently assigned to this position. From approximately this position, Gaume & Mutel (1987) reported a 1.6-Jy OH maser, slightly offset from the H II region W51d (flux density 5 Jy, angular size 4 arcsec).

59.78 + 0.06. This source shows clear variability, with some features stable, some increasing and some decreasing monotonically from 1992 June to December. OH was first reported by Braz & Sivagnanam (1987); our 1993 July data shown a peak OH flux density of 1.7 Jy in the velocity range 19 to 22 km s^{-1}. An H_2O maser was reported by Lada et al. (1981) at RA 19^{h}41^{m}04^s.23, Dec. +23°36′42″.4. Note that the listing of this source as V645 Cyg by Menten (1991b) and others is incorrect. In this direction, Kurtz, Churchwell & Wood (1994) reported that there is no ultracompact H II region, with an upper limit of 0.3 mJy as observed with a 0.9-arcsec beam at 8.4 GHz.

4 DISCUSSION

4.1 General

First, we briefly compare our data with other observations of the 6.6-GHz methanol transition. We observed the 73 masers reported by Menten (1991b) that are accessible to the Parkes telescope and, for most of these, detected the maser with an intensity similar to that reported by Menten, e.g. 345.50 + 0.35 as shown in Fig. 1. In a few cases, however, the peak changed by a factor of 2 or more, with the most extreme variations occurring in 345.00 − 0.22 which increased three-fold and 10.47 + 0.03 which decreased ten-fold. Towards W33 (12.80 − 0.19), we detected the absorption reported by Menten but found the emission in this direction to be merely from nearby sources at the edge of the beam (confirmed by Menten, private communication).

During the compilation of our southern observations, the brighter ones have been reported as a result of several searches by the Hartebeesthoek radio telescope over a similar period of time (MacLeod, Gaylard & Nicolson 1992; MacLeod & Gaylard 1992; Gaylard & MacLeod 1993). In total, our list of 245 masers includes 146 previously reported by Menten or from Hartebeesthoek. The masers listed previously, however, show no direct correspondence with ours in the vicinity of clusters of masers, because no positional measurements were made in the earlier work and confusion was exacerbated by the larger beamwidth used. Our list does not include observations of 33 masers recently reported by Schutte et al. (1993) in the directions of *IRAS* sources. Only 13 masers have so far been reported north of the region that we have studied.

4.2 C omparison with 1665-MHz OH masers

Most of the sources have been found as a result of searching at the positions of 1665-MHz OH masers already catalogued. In Fig. 1 we showed a typical comparison of OH and methanol spectra. The positions are in agreement to within 1 arcsec, and the velocity ranges are similar. There is, however, no detailed similarity of the spectra for the two species, and the 6.6-GHz methanol intensity is an order of magnitude higher than the OH intensity, as is common for the whole sample.

4.2.1 *Positional coincidence of methanol and OH masers*

We are concerned here not with detailed coincidence of maser spots and velocities, but with whether both species are excited by the same activity centre or compact H II region.

Published observations allow precise positional comparisons of five methanol masers (Norris et al. 1993) with their OH counterparts (measured with the VLA by Forster & Caswell 1989). In four of the five associations (345.01 + 1.79, 351.42 + 0.64, 351.77 − 0.54 and 9.62 + 0.20), the separation of major features in the two species is no more than 2 arcsec, and is comparable with the expected errors or the size of the region showing maser emission; the offset is slightly larger for 339.88 − 1.26.

Our new data allow comparisons for a further 62 associations for which accurate OH positions are available, mainly from Forster & Caswell. Most of the methanol/OH apparent separations are less than 15 arcsec; this is compatible with spatial coincidence in view of the uncertainties in our Parkes methanol positions. Notable exceptions are 350.10 + 0.09 and 45.47 + 0.05; two others are of less significance (since the methanol is weak and may have a larger positional error): 348.89 − 0.19 (separation 27 arcsec) and 19.61 − 0.23 (separation 39 arcsec). Overall, we believe that at least 90 per cent of the apparent counterparts are intimate associations.

For the more southerly sources, for which we have not yet determined precise OH positions, we would expect similar statistics. We are conducting more measurements with the ATCA (with an east–west baseline of 6 km) to investigate this further; these unpublished observations confirm, for example, that 345.50 + 0.35 (the source selected for display in Fig. 1 as typical of our results) has methanol and OH masers coincident to within 1 arcsec.

4.2.2 *Comparison of methanol and OH intensities*

For this comparison we use the peak flux density of each source, since this is the essential property that determines detectability above noise. For the 1665-MHz OH data, we use measurements from Parkes, both published and unpublished, and, although not corresponding to the same epoch as the methanol data, the intensity variation of the OH over many years is usually less than a factor of 2. Comparison of Fig. 1 with earlier OH spectra provides an example of the typical slow OH variability over nearly 20 years, as discussed in the notes on 345.50+0.35 in Section 3. As we show below, 345.50+0.35 is also typical of the whole sample, in so far as its 6.6-GHz methanol emission is an order of magnitude more intense than its OH emission.

While investigating the methanol masers in the direction of the OH masers, we discovered many additional methanol masers nearby but at locations with no previously known OH masers. Some represent other centres of activity within a cluster, while a few are unrelated, at greatly different radial velocity. In some cases, we have made new OH measurements at the position of a pair of methanol masers, which have revealed a previously unknown second OH maser; examples include 328.24−0.55 and 328.25−0.53 and the pair 316.36−0.36 and 316.41−0.31. In other cases, nearby extra OH components are already known from VLA studies. However, where there are no targeted OH observations at the position of a new methanol maser, we have, for statistical purposes, generally adopted an upper limit to the OH flux density of 1 Jy, since this is about the level at which previous observations (slightly offset from this position) would have failed to detect a counterpart. In a few instances, where the separation of methanol sources is small, an OH maser almost as intense as the presently catalogued one may have been missed. For any source where the assumed OH/methanol coincidence is incorrect, then of course the more appropriate methanol-to-OH intensity ratio comprises two limits, one higher and one lower than the adopted value. Sgr B2 has been omitted from these statistics, since the clusters of OH and methanol masers are too complex to assess coincidence with our single-dish methanol data.

We found no methanol at 24 of 208 OH maser sites, and these are listed in Table 2; we did, however, detect methanol at 56 additional sites with no known OH maser. In view of the dependence of the statistics on the sample selection criteria, we will summarize results of several different samples.

The median ratio of intensities of methanol and OH is 5.9 for the 184 sources with good measurements of both species. The quartiles are at 18.7 and 1.0, i.e. 25 per cent have methanol intensity more than 18.7 times greater than the OH intensity, and 25 per cent have methanol intensity less than the OH peak. If we consider the whole sample of 208 OH masers and thus include those with no detectable methanol, the median is 3.65, with the quartiles at 17.6 and 0.66. Ten per cent of OH masers have a methanol intensity more than 50 times greater than the OH intensity, and 10 per cent have methanol weaker than 0.075 times the OH intensity. These are the statistics applicable to the detection probability for methanol from a sample of OH masers.

The corresponding statistics for detection of OH from a sample of methanol masers are less readily estimated, since we do not have a reasonably complete sample of methanol masers. If we consider our whole methanol sample (including those with no OH detection), however, the median methanol-to-OH intensity ratio is 7. The methanol sources in the sample of Schutte et al. (1993) have a much higher ratio, ~60 (using our unpublished OH measurements, in which we detected OH from approximately two-thirds of the sources). This is a high ratio because it applies to a biased sample from which previously known strong OH sources were intentionally excluded. More appropriately, these 33 sources should be added to our list (with the total becoming 273 methanol masers), resulting in a median ratio of 9. Finally, we note that, on using the full sample of 297 sources (with either OH or methanol, or both), the median ratio is 7.

For all of the above samples, the distribution of the intensity ratio is smooth and shows no evidence of being bimodal.

For the sample with both OH and methanol detected, the extreme ratios of methanol-to-OH intensity are 3575 for 323.74−0.26 and 707 for 188.95+0.89 in the case of strong methanol with weak OH; and 0.072 for 327.29−0.58 and 0.003 for 330.88−0.37 in the case of weak methanol with strong OH. Extreme limits to the ratio where no OH is found are 535 (291.28−0.71) and 340 (30.76−0.05). Extreme limits to the ratio where no methanol is found are 0.003 (343.13−0.06) and 0.005 (43.16−0.03).

In other words, the non-detections have limits wholly within the range of the intensity ratios measured for sources with both species detected. There is thus no reason to believe that the non-detections represent a distinct population of preferentially OH or preferentially methanol masers (although there exists another class of OH maser that we have intentionally omitted from this investigation: the class of late-type stars).

The general correspondence of the methanol and OH species of maser suggests that they require similar conditions and have similar lifetimes. Future investigation of sources with especially high or low ratios of methanol-to-OH intensity may, however, give some indication of differences.

Overall, the study of methanol masers as probes of star-forming regions has advantages compared with the study of OH masers, for several reasons.

(i) Methanol masers are stronger, on average.

(ii) Methanol masers are less often confused by strong absorption. Indeed, in the directions of some methanol masers where we find only OH absorption, there may none the less be OH masers that we are unable to detect because of foreground absorption.

(iii) Methanol masers are at a higher frequency where it is easier to carry out studies with high angular resolution.

(iv) Furthermore, if continuum studies are carried out in conjunction with spectral-line studies, it is easier to detect an H II region near 6 GHz than at 1.6 GHz where it is likely to be optically thick and weak. The relationship with any compact H II region therefore will be more easily studied in the case of methanol masers.

None the less, there remain maser sites that are detectable only (or more readily) as OH masers, and, where possible, comparison of the two species will be most profitable.

The majority of the masers lie in the directions of infrared sources listed in the *IRAS* Point Source Catalog and prominent at 60 and 100 μm; *IRAS* sources have also proved to be a useful means of finding some of the methanol masers (Schutte et al. 1993). Due to confusion in the *IRAS* catalogue, however, an apparent *IRAS* counterpart often refers to an extended H II region in which the more compact

H II regions are embedded; the masers pinpoint most precisely the ultracompact regions.

4.3 The association of masers with compact H II regions

Ultracompact H II regions have been detected towards many OH masers. The H II regions are most readily detected at radio frequencies above 5 GHz, since they are optically thick and weaker at low frequencies. They represent one of the earliest manifestations of star formation, when the star's optical emission is still obscured by dust.

In so far as the methanol masers are closely associated with the OH masers, they, too, pinpoint the sites of ultracompact H II regions. Further studies at the positions of all methanol masers to discover the associated H II region at each site will establish the relationship more clearly. Existing studies of H II regions associated with methanol masers reveal a variety of properties, ranging from large H II regions of several Jy in the directions of W3(OH) and 351.42 + 0.64 (NGC 6334Af), to weaker objects such as the 19-mJy source associated with 9.62 + 0.20, the 3-mJy source associated with 351.77 − 0.54, and the current upper limit of 0.3 mJy towards 59.78 + 0.06. In the source notes of Section 3.1, we drew attention to masers for which there are existing continuum measurements, mostly taken from Forster & Caswell (1989) and Wood & Churchwell (1989). Towards our 'typical' maser 345.50 + 0.35, no H II region has yet been detected, with an upper limit of 20 mJy (Forster & Caswell 1989).

The identification of an H II region towards each maser would be expected if submillimetre photons were needed to pump both the 6.6- and 12-GHz masers, as suggested by Cragg et al. (1992). The structure of the H II regions may provide evidence of outflows, as in 35.20 − 0.74 (Heaton & Little 1988), and the existence of discs. Thus further investigation of the H II regions is relevant to the study of the pumping scheme and the evolutionary states of the individual star-forming regions.

4.4 The luminosity function for methanol masers and the Galactic distribution of star-forming regions

First, we note that the highest flux density in our sample of 245 masers is 5090 Jy (9.62 + 0.20), the lowest is 0.2 Jy (264.29 + 1.46), the median flux density is 19 Jy and the quartile values are 70 and 5.8 Jy.

There are twenty 6.6-GHz methanol masers with peak flux density greater than 380 Jy (including three northern ones outside the range of our sample and reported only by Menten 1991b). The five strongest are 9.62 + 0.20, W3(OH), 351.42 + 0.64, 323.74 − 0.26 and 339.88 − 1.26. In considering luminosities, we make the usual assumption that the emission beamed in our direction is representative of the intensity in other directions, and thus can be regarded as pseudo-isotropic. We define a 'peak luminosity' as Sd^2, where S(Jy) is the peak flux density and d(kpc) is the distance. We generally use kinematic distances based on systemic velocities in conjunction with the Galactic rotation model described by Caswell & Haynes (1987b). In this model, and in many earlier papers citing kinematic distances, a Galactic Centre distance of 10 kpc is assumed; relative to the currently favoured Galactic Centre distance of 8.5 kpc, our distances are overestimated by a factor of 10/8.5 and our luminosities by a factor $(10/8.5)^2$, as is also the case for the luminosities of 1665-MHz OH masers studied by Caswell & Haynes (1987a). Of the five strongest methanol masers, the most distant is probably 323.74 − 0.26 with a near kinematic distance of 3.6 kpc and hence a luminosity of 37 000 Jy kpc^2. A slightly higher luminosity (50 000 Jy kpc^2) is found for 49.49 − 0.39 which is weaker but at larger distance (7.7 kpc).

For some of the 20 brightest sources there is a kinematic distance ambiguity, with no reliable means yet of distinguishing between near and far alternatives. If any of these are at the far distance, they may be the most luminous sources of all. As we discussed in the notes to individual sources, likely candidates are 318.95 − 0.20 (134 000 Jy kpc^2 if at 13.1 kpc), 328.25 − 0.53 (83 000 Jy kpc^2 if at 13.9 kpc), 328.24 − 0.55 (77 000 Jy kpc^2 if at 13.9 kpc), 23.01 − 0.41 (66 000 Jy kpc^2 if at 12.8 kpc) and 328.81 + 0.63 (74 000 Jy kpc^2 if at 14 kpc). It will be especially valuable, therefore, to distinguish between near- and far-distance alternatives for these sources; 1420-MHz H I absorption spectra of the associated radio continuum H II regions will be valuable for this purpose, as they have been for many other sources (Caswell et al. 1975).

9.62 + 0.20 has the highest flux density of the presently known methanol masers and, at about 2 kpc (if we adopt the distance suggested by Forster & Caswell), its luminosity would be 20 000 Jy kpc^2. Garay et al. (1993a) suggest that it is at 16.1 kpc, and it would then have a peak luminosity of 1 000 000 Jy kpc^2, larger than that of its nearest possible rival by a factor of nearly 6, and so not likely on current evidence. To resolve this problem, we suggested in Section 3.1 that it might lie at a distance of 6 kpc, where its luminosity would be 180 000 Jy kpc^2, which would make it the most luminous maser, but not by very much.

The luminosity function and Galactic distribution of OH masers have been investigated by Caswell & Haynes (1983a, 1987a), using extensive OH surveys of the Galactic plane. In the absence of such a methanol survey, we are not yet able to apply their method to methanol masers. In particular, we emphasize that the distribution of currently known methanol masers necessarily mimics the distribution of the OH search list, especially in view of the high detection rate. Given the apparent close correspondence between the methanol and OH, however, we might expect the true distributions to be similar, and thus the OH maser distribution will remain the best estimate of the methanol maser distribution until there is fresh evidence from an unbiased methanol survey.

The luminosity function for the OH masers (Caswell & Haynes 1987a) has three sources with luminosity greater than 10 000 Jy kpc^2 in the Galactic disc out to the distance of the solar circle. For comparison, our consideration of the most luminous methanol masers suggests that there may be three methanol masers with luminosity exceeding 70 000 Jy kpc^2. This fact would be compatible with a luminosity distribution for methanol that is similar in form to the OH but shifted to values of luminosity that are several times higher, just as the median flux density ratio is larger (by a factor of between 3.65 and 9 depending on the sample selection criteria). Note that the individual high-luminosity OH masers do not correspond to the individual high-luminosity methanol masers. As a yardstick for comparison with future estimates, we suggest that the luminosity function for the 6.6-

GHz methanol masers is similar to that for OH, but shifted to luminosities that are seven times higher. The maximum luminosities found are clearly of special interest in assessing the sensitivity needed to discover similar masers in other galaxies, and in assessing the significance of non-detections. With regard to lower luminosity masers, Caswell & Haynes (1987a) suggested that in the whole Galactic disc there are nearly 1000 OH masers with luminosity >3 Jy kpc^2, and thus our present analysis implies that there are 1000 methanol masers with luminosity >20 Jy kpc^2.

From a practical viewpoint, we have used the luminosity function to estimate that a comprehensive methanol survey over the whole Galactic disc, with a flux density limit of 1 Jy, would yield more than 500 masers (a factor of at least 2 higher than the number of 1665-MHz OH sources to this flux density limit), and would thus indeed provide the most complete inventory of regions where massive stars are forming in our Galaxy.

4.5 Velocities and velocity ranges

Many of the spectra show a large number of individual peaks, with a few representing features sufficiently isolated to allow a measurement of their widths. Typical narrow features are seen in 189.03 + 0.78 and 336.36 − 0.14, and these have widths at half-intensity of 0.25 km s^{-1}. Features with width significantly larger than 0.5 km s^{-1} are in many cases asymmetric, an indication that they comprise a blend of two or more components. The small linewidths of the components are similar to those found in the 12-GHz methanol masers (Caswell et al. 1993).

Strong sources observed with high sensitivity often show additional weak emission over quite large velocity ranges. The widest velocity range, after removing those cases that result from the obvious confusion of two adjacent sources, is 24 km s^{-1}. The masers with the widest range are 340.79 − 0.10, 338.08 + 0.01, 32.74 − 0.08, 339.68 − 1.21 and 0.67 − 0.03; all other sources have ranges less than 20 km s^{-1}.

For the 61 strongest sources (greater than 70 Jy), the median velocity range is 12 km s^{-1}. The source 345.50 + 0.35 shown in Fig. 1 is typical in this respect. For samples of lower flux density, the median velocity range steadily drops; for all of the 184 sources above 5.8 Jy, the extreme ranges are 1 and 24 km s^{-1}, the median 9 km s^{-1} and the quartile values 5 and 13 km s^{-1}. For the 61 sources weaker than 5.8 Jy, the extreme ranges are 1 and 17 km s^{-1}, the median 5 km s^{-1} and the quartiles 3 and 7 km s^{-1}. The generally smaller ranges for weaker sources are likely to be due to a bias, where the range is underestimated as a result of the undetectability of weak features when the signal-to-noise ratio is lower.

In summary, many spectra show emission that is continuous over a wide velocity range, but with many peaks at intervals of about 1 km s^{-1}, as seen for example in 336.36 − 0.14. Thus, for a source with the typical value of velocity range of 10 km s^{-1}, there will be typically at least 10 features, and probably more that are, due to overlap, not distinguishable. In the cases of several examples of the closely associated 12-GHz methanol masers, high-resolution interferometer data clearly indicate the presence of many overlapping features (McCutcheon et al. 1988; Norris et al. 1988).

In addition to sources showing emission of comparable intensity over the whole range, there are some sources with their strongest emission near the centre of the range, and with decreasing intensity towards the extremities. Of course, the occurrence of weak features at the extreme velocities need not imply that they occur only there; it is possible that weak features occur over the whole velocity range but are not recognizable in the central regions where they are dwarfed by the stronger features. There is also a group of sources that have double velocity ranges (even after rejecting those arising from nearby, but separate, sources). They are insufficient in number to cause a subsidiary peak in the histogram of the velocity distribution, and must be recognized on a case-by-case basis. They may represent separate sites but with separation too small to distinguish with our beamsize. In some instances, however, they may represent outflows (or inflows) spatially coincident with emission at the systemic velocity. In the notes to individual sources, we have drawn attention to several possible examples of outflow emission; eight promising candidates deserving further investigation are 300.51 − 0.18, 320.23 − 0.29, 322.16 + 0.64, 327.29 − 0.58, 339.68 − 1.21, 340.79 − 0.10, 341.21 − 0.21 and 20.23 + 0.07.

4.6 Variability

Again we use the example of Fig. 1 to show the typical properties of our sample. The second and third panels show that the intensity of 6.6-GHz methanol emission varies by about 10 per cent in several features over a 3-month period.

The principal purpose of our observations was to detect new sources and to measure their positions, but the resulting data set has proved to be valuable for initial variability investigations on several different time-scales. When measuring positions of strong sources with many spectral features, we obtained six spectra within 20 min and found no variability. When system performance checks were made on strong sources at intervals of 1 or 2 d, no perceptible changes were seen above the noise level. Changes were commonly seen, however, on the time-scale of the 3-month interval between observing sessions.

Within sources possessing complex spectra, if there are variations in the intensities of only some features, we can readily recognize this even at a level of a few per cent, since relative variability does not rely on the accuracy of the absolute calibration. Indeed, amongst sources with at least 10 velocity components, we usually find at least one component displaying variability on a time-scale of 3 months. Where a source shows almost continuous emission over several km s^{-1} and only slight variability, this can result from much blending so that, on the average, the variations partially cancel if they are not varying synchronously. Even for apparently isolated features, however, the variability is rarely large and is often oscillatory, with an increase or decrease and then a return to the original value. The generally low amplitude of the variation suggests that the maser gain is linearly, rather than exponentially, dependent on path-length, usually (but not always – see Reid & Moran 1988) argued to be the signature of saturated masers. A detailed investigation of individual strongly varying methanol masers will be presented elsewhere (Caswell et al. 1994); overall, we note that, since the variability has some characteristics in common with that of H_2O masers, the possible explanations may be similar. An extensive summary of H_2O variability is given by Peng (1989a,b), and we suggest that his conclusions may be applicable to methanol masers. The study of OH variability by Clegg & Cordes (1991) also provides useful comparisons in interpretation.

To explore the statistics of the methanol variability, for each source we estimated the number of individual peaks that showed variability in our observations, and the total number of distinguishable peaks suitable for a variability investigation. The number of variable peaks is necessarily a lower limit in view of (1) our limited number of observing epochs, (2) the signal-to-noise ratio limitation, and (3) the calibration uncertainty which allows us to recognize with confidence only relative variations (whole-source variations are significant only if larger than ~10 per cent). Averaged over all sources, the fraction of variable features is 0.28. We also subdivided the sources into four equal groups, ranked by flux density. The number of individually recognizable features decreased with flux density, as would be expected on account of the poorer signal-to-noise ratio. The fraction of variable features, however, dropped by an insignificant amount, from 0.33 for the strongest sources to 0.27 for the weakest.

We have also summarized the variability with a classification in column 10 of Table 1: 'nv' (where no variations have yet been seen), 'sv' (variable in at least one feature but with only slight variations to date, of <10 per cent), or 'v' (at least one feature shows variability of >10 per cent).

The variability of 12-GHz masers was investigated by Caswell et al. (1993). A few sources showed strong variability, and most showed some variability. Although we find the majority of 6.6-GHz masers to be variable, overall they are less variable than the 12-GHz masers (see also Section 4.7).

Are there velocity changes? We have seen no obvious examples of features that retain their appearance but change velocity. We do, however, occasionally see changes of shape, as would be expected when two blended features vary by different amounts.

4.7 Comparisons of 6.6- and 12-GHz masers

Fig. 1 shows a typical comparison of spectra of the 6.6- and 12-GHz methanol transitions. The 12-GHz intensity is much lower than the 6.6-GHz intensity, but its peak coincides in velocity with a major 6.6-GHz peak. There are, however, some strong 6.6-GHz peaks with no detectable counterparts.

For seven of our 245 6.6-GHz masers we have no 12-GHz measurement. We have detected a 12-GHz counterpart to 131 of the remaining 238, with flux densities ranging from 1100 Jy (351.42+0.64) to 0.4 Jy (33.09−0.07), and a median flux density of 7 Jy; for the remainder, we have upper limits or uncertain detections of typically 0.5 Jy. The detection rate of 12-GHz masers is lower than that of the weaker 6.6-GHz masers. For the 6.6-GHz masers stronger than 19 Jy, we detected 95 of the 121 sources searched, and the median ratio of 12- and 6.6-GHz intensities is 0.11 (where we include the 26 masers with upper limits to the 12-GHz flux density, so that the ratio is applicable to a complete sample of 6.6-GHz masers). If this ratio is applicable to the weaker 6.6-GHz masers, it is not surprising that, in many cases, any 12-GHz emission falls below the level of detectability.

For nearly half of the 12-GHz masers, the strongest 12-GHz peak coincides with the strongest 6.6-GHz peak. For the remainder of the 12-GHz masers, the peak usually coincides with a less prominent 6.6-GHz peak and thus the ratio of 12- and 6.6-GHz intensities in a one-to-one comparison of individual peaks has a larger scatter.

We will discuss these comparisons more extensively in a further paper, where the 12-GHz results will be given in detail. One result from the 12- and 6.6-GHz comparisons should be mentioned briefly here, however, since it is especially relevant to the 6.6-GHz observations. The clear correspondence between features seen at both 12 and 6.6 GHz was noted by Menten (1991b) in his initial discovery of 6.6-GHz masers. No precise laboratory measurement of the rest frequency for the 6.6-GHz transition has been made, and so Menten used the comparison of source spectra to derive the currently accepted value, 6668.518 MHz, relative to the value of 12 178.595 MHz for the other transition. In our large sample of sources we find that, with this choice of rest frequencies, there is a very slight offset of 0.07 km s^{-1} between corresponding features from the two transitions. This would be eliminated if the adopted rest frequency near 6.6 GHz were increased by 1.5 kHz to 6668.519 MHz (or if the rest frequency near 12 GHz were decreased by 3 kHz). Since the laboratory value for the 12-GHz transition has an uncertainty of 3 kHz, it would seem best to defer any change in the adopted values until at least one of the frequencies is measured to higher accuracy. However, the slight discrepancy should be allowed for in any detailed comparison of spectra.

Finally, we note that in a few sources the peak 12-GHz intensity exceeds the peak 6.6-GHz intensity. Sources with a ratio exceeding or approaching unity are 31.28+0.06, 24.33+0.14, 345.01+1.80, its nearby companion 345.01+1.79, 338.08+0.01, 335.79+0.17 and 331.28−0.19. Intensive investigation of these might elucidate the conditions favouring this high ratio of 12- to 6.6-GHz emission.

4.8 Absorption at 6.6 GHz

Absorption is evident in 11 of the 6.6-GHz spectra that we show in Fig. 2. Individual examples are discussed in the notes. In all cases, we see corresponding absorption on our 12-GHz spectra (not shown). In general, the absorption is more prominent and more easily studied at 12 GHz, and is less confused by maser emission. We therefore defer detailed discussion of absorption until the 12-GHz observations are published in full. Note that a 12-GHz absorption study of strong continuum sources has already been made by Peng & Whiteoak (1992).

From a practical viewpoint, the absorption present at 6.6 GHz rarely obscures any maser emission, whereas absorption often creates problems in recognizing weak masers on the OH 1665-MHz transition if studied with a single dish with large beamsize.

5 CONCLUSIONS

The present results constitute a comprehensive search for 6.6-GHz methanol towards OH masers readily accessible to the Parkes telescope (south of declination 24°) along the Galactic plane, especially in the longitude range 270°

through 360° to 50°. It provides a current catalogue of well-studied southern methanol 6.6-GHz masers with positions adequate to eliminate confusion. The sensitivity and velocity resolution are sufficient to make our data suitable as early-epoch measurements against which to measure future long-term variability. We have shown that variability of 6.6 GHz masers is very common on a time-scale as short as months, as is also true for the closely related 12-GHz masers (Caswell et al. 1993). We have also singled out some masers showing marked variability which deserves more extensive investigation. More precise positions will be obtained in future studies to allow detailed comparison with OH and H_2O masers, and with compact H II regions. The chance detection of methanol masers offset from the target OH positions points to the existence of many more methanol masers. As discussed in Section 4.4, surveying of the Galactic plane for 6.6-GHz methanol masers appears to be a most practical means of increasing our inventory of Galactic sites of massive star formation.

ACKNOWLEDGMENTS

We are grateful to Rafik Kandalian and Marc Elmouttie for their valued assistance with some of the observing, to Rick Forster for the many useful routines embodied in his spectral-line reduction program, and to Henrietta May for adding several new features to the reduction program.

REFERENCES

Bachiller R., Menten K. M., Gomez-Gonzalez J., Barcia A., 1990, A&A, 240, 116
Benson J. M., Johnston K. J., 1984, ApJ, 277, 181
Braz M. A., Sivagnanam P., 1987, A&A, 181, 19
Brebner G. C., Heaton B., Cohen R. J., Davies S. R., 1987, MNRAS, 229, 679
Caswell J. L., Haynes R. F., 1983a, Aust. J. Phys., 36, 361
Caswell J. L., Haynes R. F., 1983b, Aust. J. Phys., 36, 417
Caswell J. L., Haynes R. F., 1987a, Aust. J. Phys., 40, 215
Caswell J. L., Haynes R. F., 1987b, A&A, 171, 261
Caswell J. L., Murray J. D., Roger R. S., Cole D. J., Cooke D. J., 1975, A&A, 45, 239
Caswell J. L., Haynes R. F., Goss W. M., 1980, Aust. J. Phys., 33, 639
Caswell J. L., Gardner F. F., Norris R. P., Wellington K. J., McCutcheon W. H., Peng R. S., 1993, MNRAS, 260, 425
Caswell J. L., Vaile R. A., Ellingsen S. P., Norris R. P., 1994, Proc. Astron. Soc. Aust., in press
Churchwell E., 1993, in Cassinelli J. P., Churchwell E. B., eds, ASP Conf. Ser. Vol. 35, Massive Stars: Their Lives in the Interstellar Medium. Astron. Soc. Pac., San Francisco, p. 35
Clegg A. W., Cordes J. M., 1991, ApJ, 374, 150
Cohen R. J., Baart E. E., Jonas J. L., 1988, MNRAS, 231, 205
Cragg D. M., Johns K. P., Godfrey P. D., Brown R. D., 1992, MNRAS, 259, 203
Fix J. D., Mutel R. L., Gaume R. A., Claussen M. J., 1982, ApJ, 259, 657
Forster J. R., Caswell J. L., 1989, A&A, 213, 339
Forster J. R., Caswell J. L., Okumura S. K., Hasegawa T., Ishiguro M., 1990, A&A, 231, 473
Gaines L., Casleton K. H., Kukolich S. G., 1974, ApJ, 191, L99
Garay G., Rodriguez L. F., Moran J. M., Churchwell E., 1993a, ApJ, 418, 368
Garay G., Rodriguez L. F., Moran J. M., 1993b, in Cassinelli J. P., Churchwell E. B., eds, ASP Conf. Ser. Vol. 35, Massive Stars: Their Lives in the Interstellar Medium. Astron Soc. Pac., San Francisco, p. 114
Gardner F. F., Whiteoak J. B., Forster J. R., Pankonin V., 1986, MNRAS, 218, 385
Gaume R. A., Mutel R. L., 1987, ApJS, 65, 193
Gaylard M. J., MacLeod G. C., 1993, MNRAS, 262, 43
Heaton B. D., Little L. T., 1988, A&A, 195, 193
IRAS Point Source Catalog, 1985, *IRAS* Science Working Group, US Government Printing Office, Washington DC
Kurtz S., Churchwell E. B., Wood D. O. S., 1994, ApJS, 91, 659
Lada C. J., Blitz L., Reid M. J., Moran J. M., 1981, ApJ, 243, 769
McCutcheon W. H., Wellington K. J., Norris R. P., Caswell J. L., Kesteven M. J., Reynolds J. E., Peng R. S., 1988, ApJ, 333, L79
MacLeod G. C., 1991, MNRAS, 252, 36P
MacLeod G. C., Gaylard M. J., 1992, MNRAS, 256, 519
MacLeod G.C., Gaylard M. J., Nicolson G. D., 1992, MNRAS, 254, 1P
Menten K. M., 1991a, in Haschick A. D., Ho P. T., eds, ASP Conf. Ser. Vol. 16, Skylines: Proc. 3rd Haystack Obs. Meeting. Astron. Soc. Pac., San Francisco, p. 119
Menten K. M., 1991b. ApJ, 380, L75
Mirabel I. F., Rodriguez L. F., Ruiz A., 1989, ApJ, 346, 180
Norris R. P., McCutcheon W. H., Caswell J. L., Wellington K. J., Reynolds J. E., Peng R.-S. Kesteven M. J., 1988, Nat, 335, 149
Norris R. P., Whiteoak J. B., Caswell J. L., Wieringa M. H., Gough R. G., 1993, ApJ, 412, 222
Peng R. S., 1989a, A&A, 216, 165
Peng R. S., 1989b, A&A, 216, 173
Peng R. S., Whiteoak J. B., 1992, MNRAS, 254, 301
Reid M. J., Moran J. M., 1988, in Verschuur G. L., Kellermann K. I., eds, Galactic and Extragalactic Radio Astronomy, 2nd edn. Springer, New York, p. 255
Robinson B. J., Caswell J. L., Goss W. M., 1974, Aust. J. Phys., 27, 575
Schutte A. J., van der Walt D. J., Gaylard M. J., MacLeod G. C., 1993, MNRAS, 261, 783
Wood D. O. S., Churchwell E. B., 1989, ApJS, 69, 831
Zijlstra A. A., Pottasch S. R., Engels D., Roelfsma P. R., te Lintel Hekkert P., Umana G., 1990, MNRAS, 246, 217